

PERIODIC TENSION DISTURBANCE ATTENUATION
IN WEB PROCESS LINES USING
ACTIVE DANCERS

By

Fu Pei Yuet

Bachelor of Science
Oklahoma State University
Stillwater, Oklahoma
1999

Submitted to the Faculty of the
Graduate College of the
Oklahoma State University
in partial fulfillment of
the requirements for
the Degree of
MASTER OF SCIENCE
August, 2002

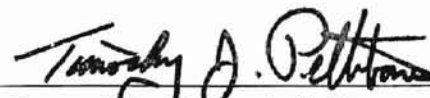
PERIODIC TENSION DISTURBANCE ATTENUATION
IN WEB PROCESS LINES USING
ACTIVE DAMPERS

Thesis Approved:


Thesis Adviser






Dean of the Graduate College

ACKNOWLEDGMENTS

I wish to express my sincerest appreciation to my major advisor, Dr. Prabhakar R. Pagilla for his intelligent supervision, constructive guidance, inspiration, and friendship.

I would like to extend my warmest thanks to my masters committee members: Dr. Eduardo A. Misawa and Dr. Gary E. Young for their support and suggestions in completion of this research. Their guidance and understanding made the development of this thesis a positive learning experience.

I would also like to thank my colleagues at Oklahoma State University Ramamurthy V. Dwivedula, Yongliang Zhu and Gimkhuan Ng, K. I. Hopcus and his colleagues at FIFE Corporation, and Ron Markum and the staff at the Web Handling Research Center.

TABLE OF CONTENTS

Chapter	Page
1 INTRODUCTION	1
1.1 Background	1
1.2 Previous Studies	2
1.3 Thesis Contributions	5
1.4 Thesis Outline	5
2 DYNAMIC MODELING	6
2.1 Active Dancer System	6
2.2 Unwind/Rewind System	8
3 EXPERIMENTAL WEB PLATFORM	12
3.1 Experimental Platform at FIFE Corporation	12
3.2 Data Acquisition and Software	15
4 CONTROLLER DESIGNS	24
4.1 Proportional-Integral (PI) Controller	25
4.2 Internal Model Based Controller (IMC)	25
4.3 Self-Tuning Controller (STC)	26
4.4 Proportional-Integral-Derivative Controller with Linearly Time Varying Gains	31
5 EXPERIMENTAL RESULTS	33
5.1 Experimental Results	34
5.2 Experimental Results Using Upstream Load Cell as Feedback Signal	35

Chapter	Page
5.3 Experimental Results on Back Propagation	35
5.4 Experimental Results with Linearly Varying PID Controller for Unwind Roll	47
6 CONCLUSIONS AND FUTURE RESEARCH	51
6.1 Future Research	53
BIBLIOGRAPHY	54
A ACTIVE DANCER MODELS AND ANALYSIS	58
A.1 State Space Model	58
A.2 Input/Output Model	59
A.3 Structural Restrictions Based on the Upstream and Downstream Lengths . .	60
B SENSOR CALIBRATION	63
C	66
C.1 Real-Time Parameter Estimation	66
C.2 Derivation for Linearly Varying PID Controller	67
D EXPERIMENTAL DATA	71
D.1 Tension Attenuation Downstream Load Cell Signal	71
D.2 Tension Attenuation Using Upstream Load Cell Signal	75
D.3 Back Propagation	79

LIST OF TABLES

Table		Page
3.1	A/D and D/A channels	15
5.1	Tension disturbance attenuation with the downstream load cell as the feed-back signal.	36
5.2	Tension disturbance attenuation using upstream load cell as the feedback signal.	36

LIST OF FIGURES

Figure	Page
2.1 Active dancer system.	11
2.2 Unwind and Rewind system.	11
3.1 Schematic of web line at FIFE Corporation.	18
3.2 Experimental web line with active dancer.	19
3.3 Web line at FIFE Corporation.	20
3.4 Endless web line.	21
3.5 Active dancer module.	21
3.6 Schematic of the Versatec and Digitrac controller system.	22
3.7 The eccentricity of the roller are used to generate tension disturbance.	22
3.8 A/D Channel Configuration	23
4.1 Active dancer tension control system with inner and outer loop.	25
4.2 Active dancer tension control system.	27
4.3 Block diagram of a self-tuning controller.	28
4.4 Two degrees of freedom direct self-tuning controller.	29
5.1 The frequencies of the tension disturbances corresponding to different speeds.	34
5.2 Tension disturbance attenuation with downstream load cell as feedback.	37
5.3 Tension disturbance attenuation with upstream load cell as feedback.	38
5.4 Tension disturbance attenuation with downstream load cell as feedback.	39
5.5 Tension disturbance attenuation with downstream load cell as feedback.	40
5.6 Tension disturbance attenuation with downstream load cell as feedback.	41

Figure	Page
5.7 Tension disturbance attenuation with downstream load cell as feedback.	42
5.8 Tension disturbance attenuation with upstream load cell as feedback.	43
5.9 Tension disturbance attenuation with upstream load cell as feedback.	44
5.10 Tension disturbance attenuation with upstream load cell as feedback.	45
5.11 Tension disturbance attenuation with upstream load cell as feedback.	46
5.12 FIFE controller: Torque applied to the brake with reference tension 20 lbs and 600 feet per minute speed.	48
5.13 FIFE controller: Torque applied to the brake with reference tension 20 lbs and 400 feet per minute speed.	48
5.14 Constant gain PID controller with reference tension 20 lbs and 600 feet per minute speed.	49
5.15 Linearly varying PID controller with reference tension 20 lbs and 600 feet per minute speed. The variation of the gains are experimentally determined.	49
5.16 Linearly varying PID controller.	50
5.17 Linearly varying PID controller	50
A.1 Root locus plot for $L_1 > L_2$	61
A.2 Root locus plot for $L_1 = L_2$	61
A.3 Root locus plot for $L_1 < L_2/2$	62
B.1 Upstream load cell(near the brake) calibration.	64
B.2 Downstream load cell(near the dancer) calibration.	64
B.3 The torque of the clutch in relationship to the current supplied with rated torque at 26 lb-ft.	65
B.4 The torque of the brake in relationship to the current supplied with rated torque at 11 lb-ft.	65

Figure	Page
5.7 Tension disturbance attenuation with downstream load cell as feedback. . .	42
5.8 Tension disturbance attenuation with upstream load cell as feedback.	43
5.9 Tension disturbance attenuation with upstream load cell as feedback.	44
5.10 Tension disturbance attenuation with upstream load cell as feedback.	45
5.11 Tension disturbance attenuation with upstream load cell as feedback.	46
5.12 FIFE controller: Torque applied to the brake with reference tension 20 lbs and 600 feet per minute speed.	48
5.13 FIFE controller: Torque applied to the brake with reference tension 20 lbs and 400 feet per minute speed.	48
5.14 Constant gain PID controller with reference tension 20 lbs and 600 feet per minute speed.	49
5.15 Linearly varying PID controller with reference tension 20 lbs and 600 feet per minute speed. The variation of the gains are experimentally determined.	49
5.16 Linearly varying PID controller.	50
5.17 Linearly varying PID controller	50
A.1 Root locus plot for $L_1 > L_2$	61
A.2 Root locus plot for $L_1 = L_2$	61
A.3 Root locus plot for $L_1 < L_2/2$	62
B.1 Upstream load cell(near the brake) calibration.	64
B.2 Downstream load cell(near the dancer) calibration.	64
B.3 The torque of the clutch in relationship to the current supplied with rated torque at 26 lb-ft.	65
B.4 The torque of the brake in relationship to the current supplied with rated torque at 11 lb-ft.	65

D.1	Tension disturbance attenuation with downstream load cell as feedback. . .	71
D.2	Tension disturbance attenuation with downstream load cell as feedback. . .	72
D.3	Tension disturbance attenuation with downstream load cell as feedback. . .	72
D.4	Tension disturbance attenuation with downstream load cell as feedback. . .	73
D.5	Tension disturbance attenuation with downstream load cell as feedback. . .	73
D.6	Tension disturbance attenuation with downstream load cell as feedback. . .	74
D.7	Tension disturbance attenuation with upstream load cell as feedback.	75
D.8	Tension disturbance attenuation with upstream load cell as feedback.	76
D.9	Tension disturbance attenuation with upstream load cell as feedback.	76
D.10	Tension disturbance attenuation with upstream load cell as feedback.	77
D.11	Tension disturbance attenuation with upstream load cell as feedback.	77
D.12	Tension disturbance attenuation with upstream load cell as feedback.	78
D.13	Back propagation of tension disturbances.	79
D.14	Back propagation of tension disturbances.	80
D.15	Back propagation of tension disturbances.	80
D.16	Back propagation of tension disturbances.	81
D.17	Back propagation of tension disturbances.	81
D.18	Back propagation of tension disturbances.	82
D.19	Back propagation of tension disturbances.	82
D.20	Back propagation of tension disturbances.	83
D.21	Back propagation of tension disturbances.	83
D.22	Back propagation of tension disturbances.	84

NOMENCLATURE

- A = Area of cross section of the web
- B_{fi} = Bearing friction coefficient in the i^{th} roller
- E = Young's Modulus of the web material
- h = Thickness of the web
- J_i = Polar moment of inertia of the i^{th} roller about its axis of rotation
- L_i = Length of the i^{th} web span
- M_i = Mass of the i^{th} Roller
- R_i = Radius of the i^{th} roller
- R_{i0} = Initial radius of the unwind/rewind roller
- t_i = Tension in the i^{th} web span
- t_r = Reference tension of the web
- T_i = Deviation of tension in the i^{th} span from the reference tension ($= t_i - t_r$)
- u = Active dancer velocity input
- u_i = Drive torque on the i^{th} roller
- u_u = Unwind roller braking torque input
- u_w = Rewind roller torque input
- v_i = Velocity of the web on the i^{th} roller
- v_r = Reference velocity of the web
- V_i = Deviation of velocity of the web on the i^{th} roller from reference velocity
- x_i = Dancer displacement at the i^{th} roller
- X_i = Deviation of the dancer displacement from its reference
- θ_i = Angle of wrap on the i^{th} roller
- τ_b = Braking torque
- τ_i = Time constant of the i^{th} web span ($= L_i/v_r$)
- ω_i = Angular velocity of the i^{th} roller

CHAPTER 1

INTRODUCTION

1.1 Background

Any continuous material whose width is significantly less than its length and whose thickness is significantly less than its width can be described as a web. Plastic wrap, paper, photographic film, and aluminum strips are examples of webs. It is very important that the tension in a web span be maintained within a close tolerance band during processing of a web. For example, if the tension in the web changes during printing/perforating processes, the print (perforation) gets skewed. Further, excessive tension variations may cause wrinkles or may even tear the web. Thus, a tension control system is an important requirement in a web handling system since any disturbance such as an uneven roller and variations in web speed or roll size affect the tension.

As the demand for higher productivity and better performance from the web processing industry increases, better models and more accurate control algorithm for the processes have to be developed. Longitudinal control algorithms involve maintaining the tension and velocity at desired values in the direction parallel to the web travel. Tension control plays a key role in improving the quality of the finished web. It is essential to keep the web in the process at a preset tension, which could change throughout the process by many conditions. Poor tension control leads to dishing, coning, and telescoping of the the rewind roll, which are undesirable.

A typical dancer mechanism consists of a roller that is free to move on linear guides and is either connected to a fixed support by passive elements such as springs and dampers or has an actuator that can move the roller and thus change web tension. Dancer devices are

commonly used to attenuate periodic tension disturbances caused by uneven wound rolls, eccentric rolls, mis-alignment of idle rollers, inertia changes of the unwind and rewind roll, and slacks in webs. A dancer mechanism is also used as a feedback element in a number of web tension control systems by measuring the displacement of the roller from a reference point. The tension control system attenuates disturbance by moving the dancer roller to different position on the linear guides to compensate for the tension variation.

Dancer systems can be used to reject tension disturbances, to create tension disturbance, or to measure tension. Dancer systems can be broadly classified as passive and active. Passive dancers can be divided into two categories, namely dancer rollers with passive elements such as springs and dampers and inertia compensated dancer rollers. Passive dancers have known to act as good tension feedback elements and/or tension disturbance attenuators for low speed web lines; they have been known to have limitations in dealing with a wide range of dynamic conditions and cause resonance problems. In inertia compensated passive dancers, the resonant frequency of the dancer roller is mainly determined by its mass. Thus to increase the tension disturbance frequency range that can be attenuated, the dancer roller mass must be reduced. However, the weight of the dancer roller is twice the reference web tension, which limits any changes to the dancer roller mass to increase the resonant frequency. It is expected that by introducing an active element into a dancer mechanism gives a control engineer more flexibility in attenuating periodic tension disturbances of a wide range of frequencies and also to maintain lower tension fluctuations. The focus of this work is on modelling of an active dancer, controller design, and the implementation of the active dancer control algorithms in a web process line for better tension regulation in the presence of periodic disturbance.

1.2 Previous Studies

Early development of the longitudinal dynamics was given in [28]. A mathematical model was developed for a web span between two pinch rolls using Hooke's Law. The model does

not reflect the tension entering the span nor does it predict tension transfer. Development by [30] included the tension from the entering span in the model. The moving web is assumed to be equivalent to a moving continuum in [29] and the general methods of continuum mechanics such as conservation of mass and conservation of momentum were used in the development of a model. [29] discussed the steady state and transient behavior of stress, strain, and tensile force as a function of variables such angle of wrap, position and speed of the driven rolls, density, cross-sectional area, modulus of elasticity and temperature.

A large web process consists of many rollers that are controlled by electrical motors (DC/AC) with various different operations being performed on the web. The entire system is interconnected through the web. In [8], the authors proposed a decentralized method to decouple an interconnected system. The decentralized decoupling is able to successfully separate the coupling factors between the subsystems, which consists of the roller and the span upstream of the roller. A non-interacting model for subsystems within the web process system is proposed in [15]. The subsystem consists of the span and its immediate downstream roller. The new model involves redefining a new variable as the difference of the tangential velocities of the rollers next to the span. Simulations show that the web tension is regulated properly since the velocity variations in the upstream web span are reflected in the new model. The authors noted one disadvantage namely that the velocities have to be measured very accurately.

In [7], a passive dancer is used as a feedback element. Comparison on whether a load cell or a dancer is a better feedback element is investigated in [21]. It is deduced in this work that there is no decisive advantage of one method as compared to the other. The load cell worked better for lower frequencies and the dancer performed better for the mid range frequencies. The dancer also has an extra natural frequency (occurring at low frequency) due to the dancer's translational dynamics. In [1], the paper discusses the optimum positions that sensors should be placed within the web process to yield the best feedback for control. In particular the sensors for tension as well as lateral control should be attached to

the rewind stand and the unwind sensor should be stationary relative to unwind platform. The active dancer dynamics are studied in [9, 27] and treated as a subsystem within the entire web handling process.

The performance of a fixed PID controller is compared to a variable gain controller for tension control before the rewind roll in [6]. The variable gain controller compensated for the time-varying parameters due to the changes in the rewind roll size. A self-tuning control is proposed in [13]. The matrix interpolation self-tuning controller showed significant improvement in the responsiveness as compared to the standard PI design when simulations were conducted on subsystems consisting of a span and the two rollers adjacent to it. The authors noted that implementation may cause problems because the self-tuning controllers take 30 seconds to obtain a meaningful FFT. [20] proposes the use of estimators as feedback elements. The tension can be estimated based on motor torque. [9] performed simulations to study the dynamic behavior of passive dancers in attenuating tension disturbances. Three cases were investigated with an example web system: (1) without a dancer, (2) with a dancer with passive elements, (3) with an inertia compensated dancer. [9] concluded that better tension attenuation could be achieved with a dancer rather than a web line without a dancer. [22] employed an adaptive controller to control the dancer arm. The control of the tension is an indirect result of controlling the dancer arm.

The role of electro-mechanical active dancers in attenuation of tension disturbance was investigated in [27]. The term endless web line refers to a web line that is in a continuous closed loop, without unwind and rewind rolls. An input/output and a state space model of an active dancer were derived and analysis revealed that the ratio of downstream to upstream span length must be less than two for effective tension attenuation using an active dancer. Experiments were conducted on an endless web platform. Experimental results on the endless web line with the three controllers, the PID controller, internal model based controller, and the linear quadratic optimal controller, showed that the active dancer was able to attenuate periodic tension disturbances.

1.3 Thesis Contributions

The following are the thesis contributions.

- Development of an active dancer system containing an hydraulic actuator.
- Development of the necessary hardware and software for use of the active dancer system in an unwind/rewind web line.
- Design and investigation of a direct self-tuning controller (STC) for the active dancer system and its comparison with a PI controller and an internal model based controller.
- Experimental evaluation of the active dancer system by incorporating it in an unwind/rewind web line at FIFE Corporation.
- Design and experimental evaluation of a PID controller with linearly time varying gains for control of unwind brake to compensate for changing inertia of the unwind roll.

1.4 Thesis Outline

The rest of the report is organized as follows. Chapter 2 discusses the modeling of the active dancer and the unwind/rewind systems. Chapter 3 describes the experimental platform and how periodic tension disturbances are generated in the web line. Chapter 4 explains the controller designs for the active dancer and the unwind system. Chapter 5 presents and discusses a number of representative experimental results. Chapter 6 gives conclusions of this research and gives future directions.

CHAPTER 2

DYNAMIC MODELING

This chapter presents the dynamics of the active dancer system, the unwind/rewind systems, and the web span dynamics within these systems. The dancer system is modeled as a subsystem independent of the rest of the web process. The active dancer subsystem can be placed upstream of any section of the process where accurate tension control is required. Mathematical models for dancer subsystems have been derived in numerous works. The precise tension control at unwind and rewind rolls are essential to producing high quality finished web products. Tension regulation can also be accomplished with the unwind and rewind systems. In a typical web process, the unwind and rewind rolls are under torque control implemented through a brake on the unwind roll and a clutch on the rewind roll.

The chapter is organized as follows. Section 2.1 presents the equations of the active dancer system while Section 2.2 gives the equations that compose the unwind and rewind systems.

2.1 Active Dancer System

The dancer subsystem shown in figure 2.1 has an incoming span with tension T_0 , an upstream span with tension T_1 and length L_1 , a downstream span with tension T_2 and length L_2 , and an outgoing span with tension T_3 . The tensions T_0 and T_3 are considered as a disturbance tension entering the active dancer subsystem.

The dynamics of the free span were derived using the law of conservation of mass for the control volume of the spans. In the case of the span adjacent to the active dancer, the dancer's translational velocity influences the tension dynamics of the span. Balancing the

torque on the rollers yields the dynamic equation for a free roller. The variables stated in the nomenclature are used for the dancer systems dynamics. Given below are the equations that were derived in [27] for a general free span, the dancer roller and upstream and downstream spans. (2.6)

- General free span:

$$L_i \dot{t}_i = EA(v_i - v_{i-1}) + v_{i-1}t_{i-1} - v_i t_i \quad (2.1)$$

- Upstream span of the dancer:

$$\begin{aligned} L_i \dot{t}_i &= EA(v_i - v_{i-1}) + v_{i-1}t_{i-1} - v_i t_i \\ &+ \frac{EA}{L_i} v_i x_i \sin\left(\frac{\theta_i}{2}\right) + EA \dot{x}_i \sin\left(\frac{\theta_i}{2}\right) \end{aligned} \quad (2.2)$$

- Downstream span of the dancer:

$$\begin{aligned} L_i \dot{t}_i &= EA(v_i - v_{i-1}) + v_{i-1}t_{i-1} - v_i t_i \\ &+ EA x_i \left[\frac{v_i}{L_i} - \frac{v_{i-1}}{L_{i-1}} \right] \sin\left(\frac{\theta_i}{2}\right) + EA \dot{x}_i \sin\left(\frac{\theta_i}{2}\right) \end{aligned} \quad (2.3)$$

- Free roller:

$$J_i \dot{v}_i = -B_{fi} v_i + R_i^2 (t_{i+1} - t_i) \quad (2.4)$$

The above equations can be linearized using the definitions,

$$\begin{aligned} v_i &= V_i + v_r, \\ t_i &= T_i + t_r, \\ x_i &= X_i + x_r, \end{aligned} \quad (2.5)$$

where V_i, T_i, X_i are deviations of i^{th} velocity, tension and dancer displacement from the reference point. The linearized equations are given below,

- General free span:

$$L_i \dot{T}_i = EA(V_i - V_{i-1}) + v_r T_{i-1} + t_r V_{i-1} - v_r T_i - t_r V_i \quad (2.6)$$

- Upstream span of the dancer:

$$L_i \dot{T}_i = EA(V_i - V_{i-1}) + v_r T_{i-1} + t_r V_{i-1} - v_r T_i - t_r V_i + \frac{EA}{L_i} v_r X_i \sin\left(\frac{\theta_i}{2}\right) + EA \dot{X}_i \sin\left(\frac{\theta_i}{2}\right) \quad (2.7)$$

- Downstream span of dancer:

$$L_i \dot{T}_i = EA(V_i - V_{i-1}) + v_r T_{i-1} + t_r V_{i-1} - v_r T_i - t_r V_i + EAX_i v_r \left[\frac{L_{i-1} - L_i}{L_i L_{i-1}} \right] \sin\left(\frac{\theta_i}{2}\right) + EA \dot{X}_i \sin\left(\frac{\theta_i}{2}\right) \quad (2.8)$$

- Free roller:

$$J_i \dot{V}_i = -B_{fi} V_i + R_i^2 (T_{i+1} - T_i) \quad (2.9)$$

The above linearized equations are used in analyzing the dancer subsystem and designing control algorithms. In the active dancer subsystem, the angle of wrap (θ) is 180° . It is interesting to note a structural constraint in terms of the lengths L_1 and L_2 as derived in [27]. These constraints are given in Appendix A.3. The state space and input-output models were derived in detail in [27] and are presented in Appendix A.1 and A.2, respectively.

2.2 Unwind/Rewind System

The model of the unwind system consists of the unwind roll, the immediately downstream span, and the adjacent free roller as shown in figure 2.2. Similarly, the rewind system consists of the rewind roll, the upstream span, and the adjacent roller. The following equations compose the unwind/rewind system with the bearing friction assumed to be negligible.

Unwind Roll

$$J_u(\tau) \dot{V}_u = -R_u(\tau) U_u + R_u^2(\tau) T_1 \quad (2.10)$$

where

$$R_u(\tau) = \sqrt{R_{u0}^2 - \frac{v_r h \tau}{\pi}} \quad (2.14)$$

and

$$J_u(\tau) = m R_u(\tau)^2$$

where h is the thickness of the web, τ is time, R_u is the radius of the unwind roll, and R_{u0} is the initial radius of the unwind roll. Because of the change in the radius, the inertia is changing.

Span 1

$$L_1 \dot{T}_1 = v_r T_u + t_r T_u - v_r T_1 - t_r T_1 + EA(V_1 - V_u) \quad (2.11)$$

Because the general span tension depends on the tension of the current span and the tension of the previous span, the tension in the unwind roll is needed for the span downstream of the unwind roll. To find the tension in the unwind roll, static condition is assumed in equation 2.10, which gives the following equation for tension in the span immediately downstream of the unwind roll.

$$T_1 = \frac{U_u}{R_u} \quad (2.12)$$

To stop the movement of the unwind roller, we assume that the tension of the web of the unwind roll is equal to that stated in equation 2.12.

$$T_u = \frac{U_u}{R_u} \quad (2.13)$$

Equation 2.13 is substituted into equation 2.11 to get the following equation for span one tension dynamics.

$$L_1 \dot{T}_1 = v_r \frac{U_u}{R_u} + t_r U_u - v_r T_1 - t_r V_1 + EA(V_1 - V_u) \quad (2.14)$$

Roller 1

$$J \dot{V}_1 = R_1^2 (T_2 - T_1) \quad (2.15)$$

Figure 2.2 also shows a rewind system, which consists of the rewind roll, the web span immediately before it, and the upstream roller. The mathematical model of the rewind system is described by equations of a free span and roller, which are given by equations 2.1 and 2.4, respectively. The rotational dynamics for rewind roll can be written as

$$J_n(\tau) \dot{v}_n = R_n(\tau) u_n - R_n^2(\tau) T_n \quad (2.16)$$

R_n is the radius of the unwind roller, and R_{n0} is the initial radius of the rewind roll. The radius of the rewind roller increases as the web is wound onto the roller. The radius of rewind roller at time τ can be obtained from the following equation

$$R_n(\tau) = \sqrt{R_{n0}^2 + \frac{v_r h \tau}{\pi}} \quad (2.17)$$

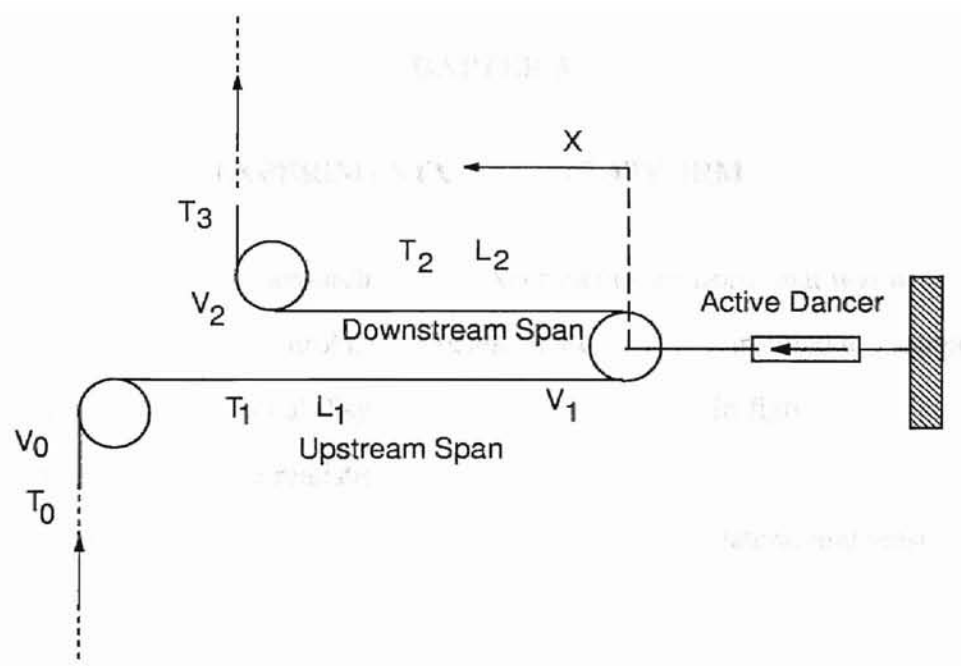


Figure 2.1: Active dancer system.

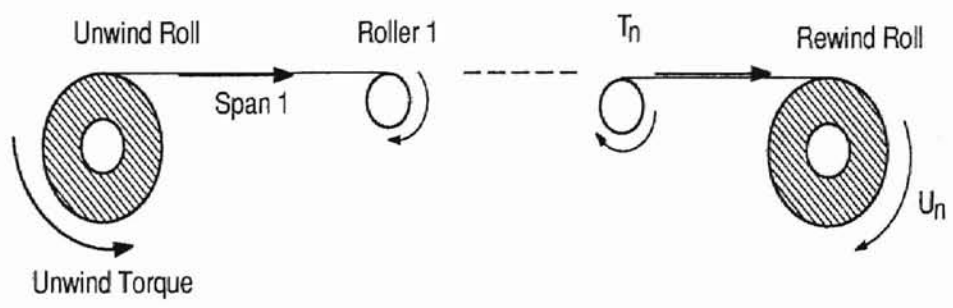


Figure 2.2: Unwind and Rewind system.

CHAPTER 3

EXPERIMENTAL WEB PLATFORM

This chapter describes the open-architecture experimental platform that was used for conducting lateral and tension control experiments. A web line is retrofitted to incorporate an active dancer and an additional displacement guide as shown in figure 3.1. This experimental platform represents a realistic web process line with unwind and rewind capability and thus reveals the validity of the controllers designed for the lateral and tension control of the web.

The remaining parts of this chapter are organized as follows: Section 3.1 describes the web line and the module added to the web line that includes the displacement guide and the active dancer mechanism with an hydraulic actuator and Section 3.2 discusses the data acquisition system and the software used to implement the control algorithms.

3.1 Experimental Platform at FIFE Corporation

A picture of the FIFE Corporation web line is shown in figure 3.3. This machine has seventeen rollers including the guide rollers. The unwind and rewind rolls on the machine are controlled by a brake and a clutch, respectively. Lateral sensors next to the unwind and rewind stands measure the lateral position of the web coming out of the unwind roll and going into the rewind roll. Based on these measurements, the unwind and rewind stands have the capability to displace laterally to provide lateral correction to the web. The unwind roll is braked based on feedback from the load cell located immediately downstream of it. This maintains the web reference tension in the web line. An ultrasonic sensor (Magpower US-2) measures the radius of the rewind roll; the machine stops when the radius of the

rewind roll exceeds a preset range. A steering guide and a displacement guide within the web line provide lateral correction to the web; edge sensors downstream of the guides measure the lateral position for feedback to the guide motor. Because the width of the rollers on the active dancer system is 8 inches and is smaller than that of the rollers on the FIFE line, the width of the web that is used in the line is limited to less than 8 inches. The web used in all the experiments was a polyester film of width 6 inches.

Figure 3.1 shows the schematic of the FIFE web line along with the OSU addition. It also shows the location and the types of sensors and actuators used on the web line. Particular attention should be given to the location of the hydraulic actuator, which is labeled as M6 in the figure. To evaluate the performance of the active dancer system for tension disturbance attenuation, periodic tension disturbances were created by an eccentric roller upstream of the dancer roller. Referring to figure 3.1, the roller located above and to the right of the label M2 is the eccentric roller.

Discussion on generating tension disturbance whose frequency is independent of the web speed is given in the next two paragraphs. In previous studies as well as on the web line with unwind/rewind system in this investigation, the tension disturbance was created by making one of the free roller surface uneven. Since there was not external power source apply to it, this uneven roller's speed is the same as the web process speed.

Periodic disturbances can be created by offsetting the shaft through the roller. Figure 3.7 shows how this is accomplished. The end plate of the roller has three possible positions. There is no disturbance generation when the roller shaft is running through the center of the roller as shown in part (a). Part (b) and (c) show the shaft set off center by different distance to create different disturbance amplitudes. A Baldor three phase motor is used to control the speed of the disturbance through a MC3000 Series motor driver available from AC Tech resulting in a disturbance frequency that is independent of the web process velocity.

Referring to figure 3.1, the upstream load cell labeled B can also be used as a feedback

element. In this case, the eccentric roller is located immediately upstream of this load cell. Lateral disturbance was created by the steering guide and is rejected using the displacement guide on the OSU module. Notice also that the upstream span of the actuator is longer than the downstream span as required for effective tension disturbance attenuation. The load cell labeled G is used as the feedback element for the dancer while the load cell B is used as a feedback element for the controller on the unwind roll. Calibrations for these sensors are given in appendix B.

The guide motors are controlled by FIFE CDP-01 controllers. The brake and clutch are controlled by Magpower Digitrac and Versatec controllers, respectively. The magnetic brake model BGG90 from Magpower attached to the unwind roll is controlled by the Digitrac 2 (Digital Tension Readout and Control). The Versatec (Tension Control) controls magnetic clutch model GCC90 on the rewind roller. Versatec and Digitrac includes the power amplifier PS-90, which has an output of 0 to 10 voltages to the clutch and brake, respectively. The torque-current relationships are shown in figures B.3 and B.4 in appendix B. Figure 3.6 shows schematic of the Versatec and Digitrac controller system with US-2 ultrasonic sensor and load cell sensor as the feedback elements, respectively.

The module added to the FIFE web line consists of the active dancer mechanism and a lateral displacement guide. A picture of the additional module is shown in figure 3.5. The translational velocity of the active dancer roller is controlled using an electro-hydraulic actuator with a servo-valve. The displacement guide for this module was received as an in-kind donation from FIFE Corporation. Also located in this module is a linear displacement transducer (LDT) from MTS Corporation that is used as the feedback element for inner loop, which maintains the ram position of the hydraulic actuator at a reference value. The sensor consists of a steel rod with a circular magnet sliding on it. The position of the magnet gives an output voltage in the range of ± 15 Volts for a maximum displacement of 2.5 feet.

Figure 3.2 shows a picture of the entire web line used to conduct lateral and tension

Table 3.1: A/D and D/A channels

Channel Number	Description	Variable used
ADCH4	Load cell C (FIFE)	loadcell_C
ADCH7	Dancer Load Cell (OSU)	dancer_loadcell
ADCH10	Brake Control Signal	brake_monitor
ADCH11	US-2 Ultrasonic sensor for diameter	sensor_A
ADCH12	Clutch Control signal monitored	clutch_monitor
DACH1	Control Signal to Dancer	dancer_control
DACH5	Control Signal to Brake	brake_control

control experiments. The data collection station is shown on the left side of the figure, which is given in more detail in the next section.

3.2 Data Acquisition and Software

The computer system consists of a Pentium 1 GHz processor with a digital data acquisition board, a top of the line industrial type from dSPACE. A dSPACE DS1103 PPC controller is used for real-time data acquisition. The DS1103 PPC controller is a complete real-time system based on Motorola PowerPC640e processor. DS1103 PPC controller Board is a standard PC/AT card that can be plugged into a PC using ISA Bus as a backplane. The board contains 20 A/D channels and 8 D/A channels. All the 20 A/D channels were used for collecting signals for feedback and also for web line monitoring purposes. Table 3.1 shows the channel assignments with their variable names for all the A/D and D/A signals for tension control while figure 3.8 shows the channel configurations, which are grouped into four modules with each module consisting of 5 channels. Besides, it has a slave DSP subsystem based on Texas Instruments TMS320F240 microcontroller. Because the DS1103 PPC controller is a dedicated data acquisition system, the sampling periods are accurately maintained to achieve faster sampling rates.

The software environment for the PPC controller includes a Control Desk, a GUI for managing dSPACE boards, a source code editor and a Microtec PowerPC C Compiler. This software environment offers very user-friendly environment through which data acquisition and data visualization can be done very conveniently without having to write separate codes for these tasks. Optional software packages include the following:

- Real-Time Interface which is an interface between Simulink and dSPACE hardware.
- Control Desk Standard which offers Virtual Instruments.
- Multiprocessor Extension.
- Test Automation.
- MLIB/MTRACE offers interface between MATLAB and dSPACE.

The algorithms for real-time control are written in C programming language (C file). The C program file consists of three main modules:

- A module to initialize the dSPACE board.
- Functions for executing various tasks (these are invoked in the interrupt service routine).
- Interrupt routine which calls the following functions after each sampling period.
 - A/D conversion.
 - Digital I/O.
 - The control algorithm.
 - D/A conversion.

On-line data display and data storage can be done very conveniently in the Control Desk environment. Data analysis and visual display are performed through Layout files.

This file serves as a graphical user interface to display data on the host computer. Besides these features, a host of “Virtual instruments” and “Data acquisition controls” are provided in Control Desk environment. These offer ease of changing the parameters of the controller while the controller is running. Multiple Layout files could be open for one experiment. Thus, this file serves as a communication device between the dSPACE Board and the host computer. A trace file keeps track of input and output signals (.trc file). This file contains definitions describing the variables used in the C-program so that these can be accessed in the Layout file. A major part of this file contains a list of the variables used in the C program file. Thus, this file stands as a link between the C program file and the Layout file. The three files compose an experiment. An experiment allows the user to implement the codes, displays the data, send and receive data, thus, allowing conceptually simple way of implementing control algorithms.

Off-line analysis of the data was done using MATLAB/SIMULINK.

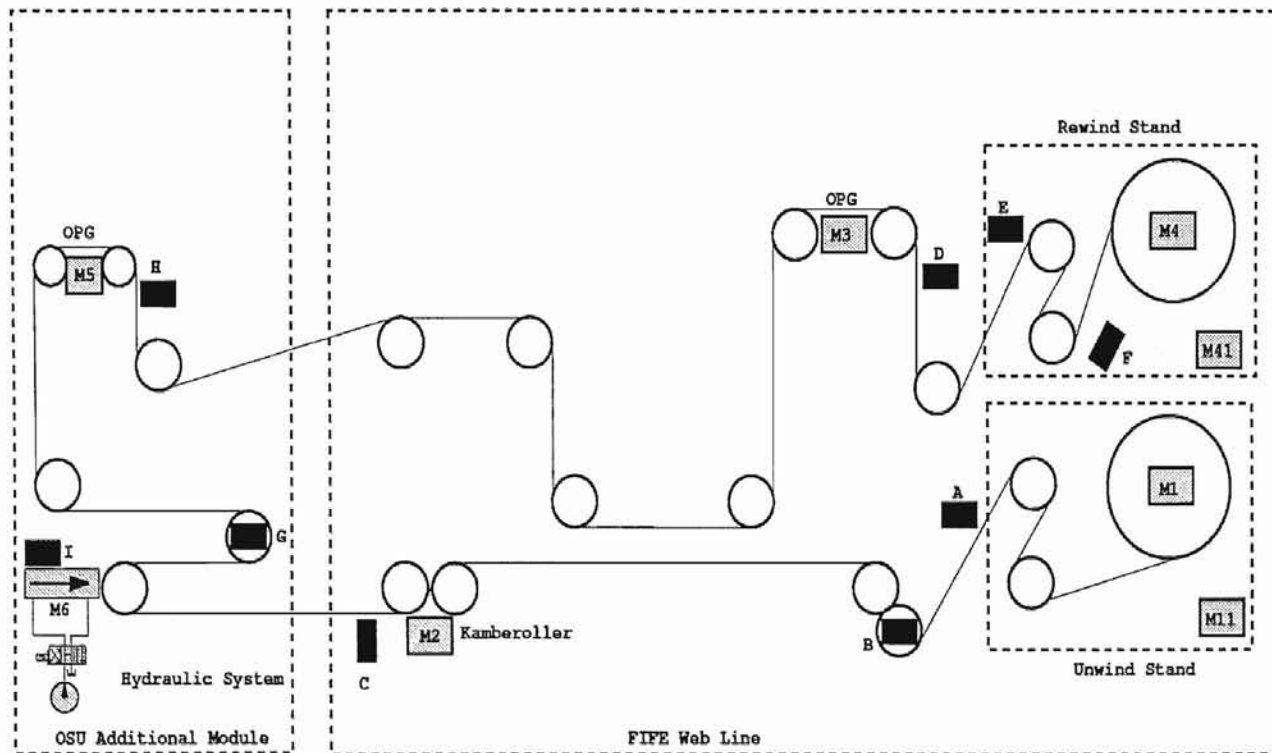


Figure 3.1: Schematic of web line at FIFE Corporation.



 Motors/Drive	 Sensors
M1 - Unwind Roll Motor	A - Fife SE-31 Ultrasonic Edges Sensor
M11 - Lateral Motor For Unwind Roll	B - Magpowr TS-150 FC Load Cell
M2 - Steering Guide Motor	C - Fife SE-17 Infrared Edge Sensor
M3 - OPG Motor	D - Fife SE-34 Infrared Edge Sensor
M4 - Rewind Roll Motor	E - Fife SE-26 Optical Edge Sensor
M41 - Lateral Motor For Rewind Roll	F - Magpowr US-2 Ultrasonic Radius Sensor
M5 - OPG Motor	G - Cleveland-Kidder Tensi-Master Load Cell
M6 - Parker Hydraulic Cylinder	H - Fife SE-31 Ultrasonic Edge Sensor
	I - MTS LDT Sensor



Figure 3.2: Experimental web line with active dancer.

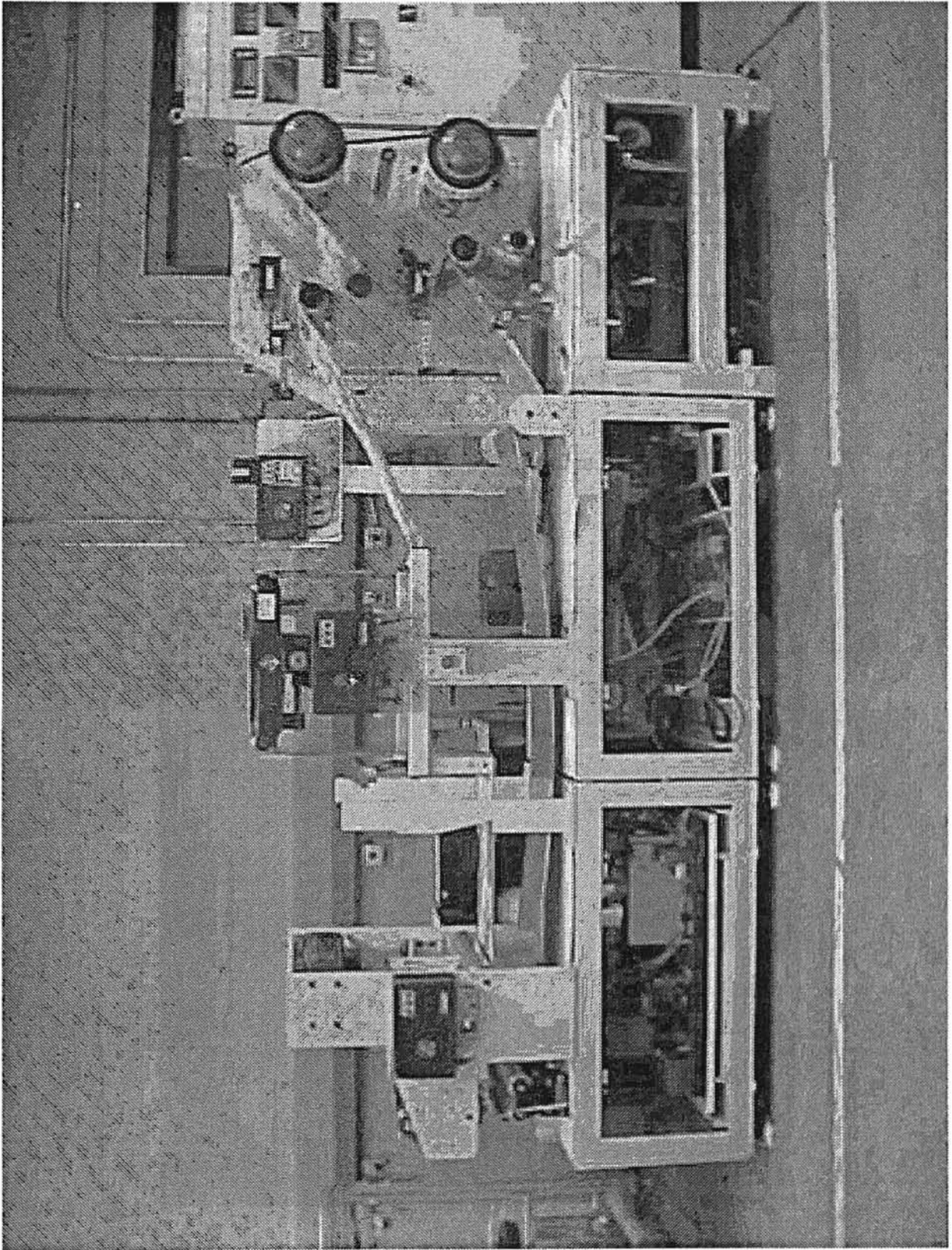


Figure 3.3: Web line at FIFE Corporation.

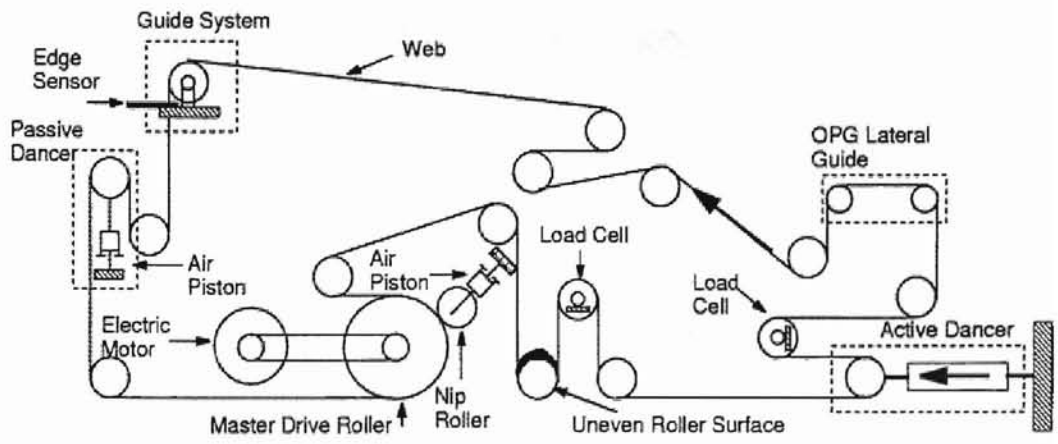


Figure 3.4: Endless web line.

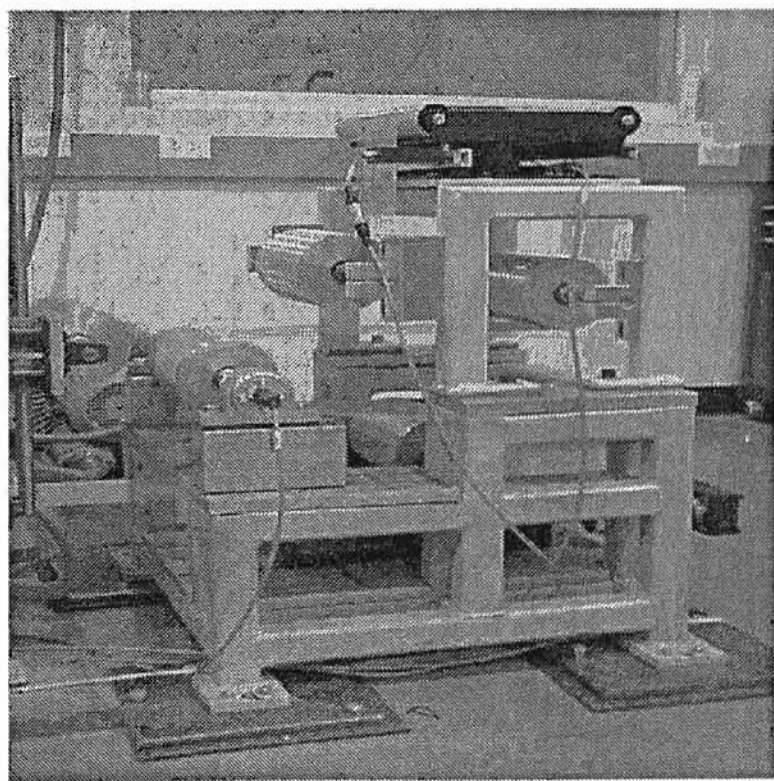


Figure 3.5: Active dancer module.

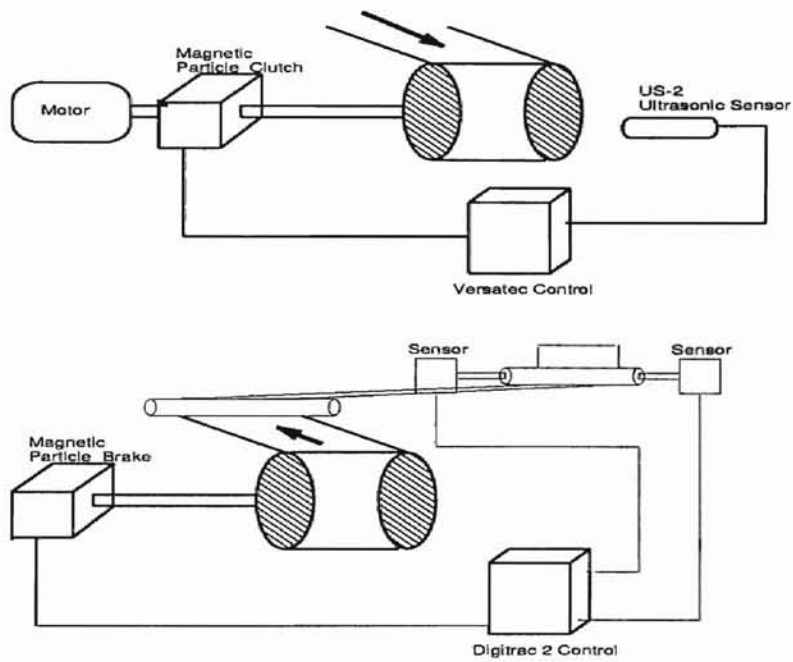
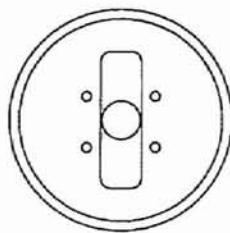
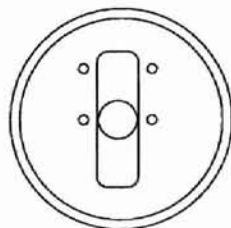


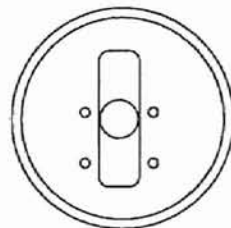
Figure 3.6: Schematic of the Versatec and Digitrac controller system.



a) The roller shaft is running through the center of the roller. There is no tension disturbance.



b) The roller shaft is positioned 0.5 inches off the center.



c) The roller shaft is positioned 0.375 inches off the center.

Figure 3.7: The eccentricity of the roller are used to generate tension disturbance.

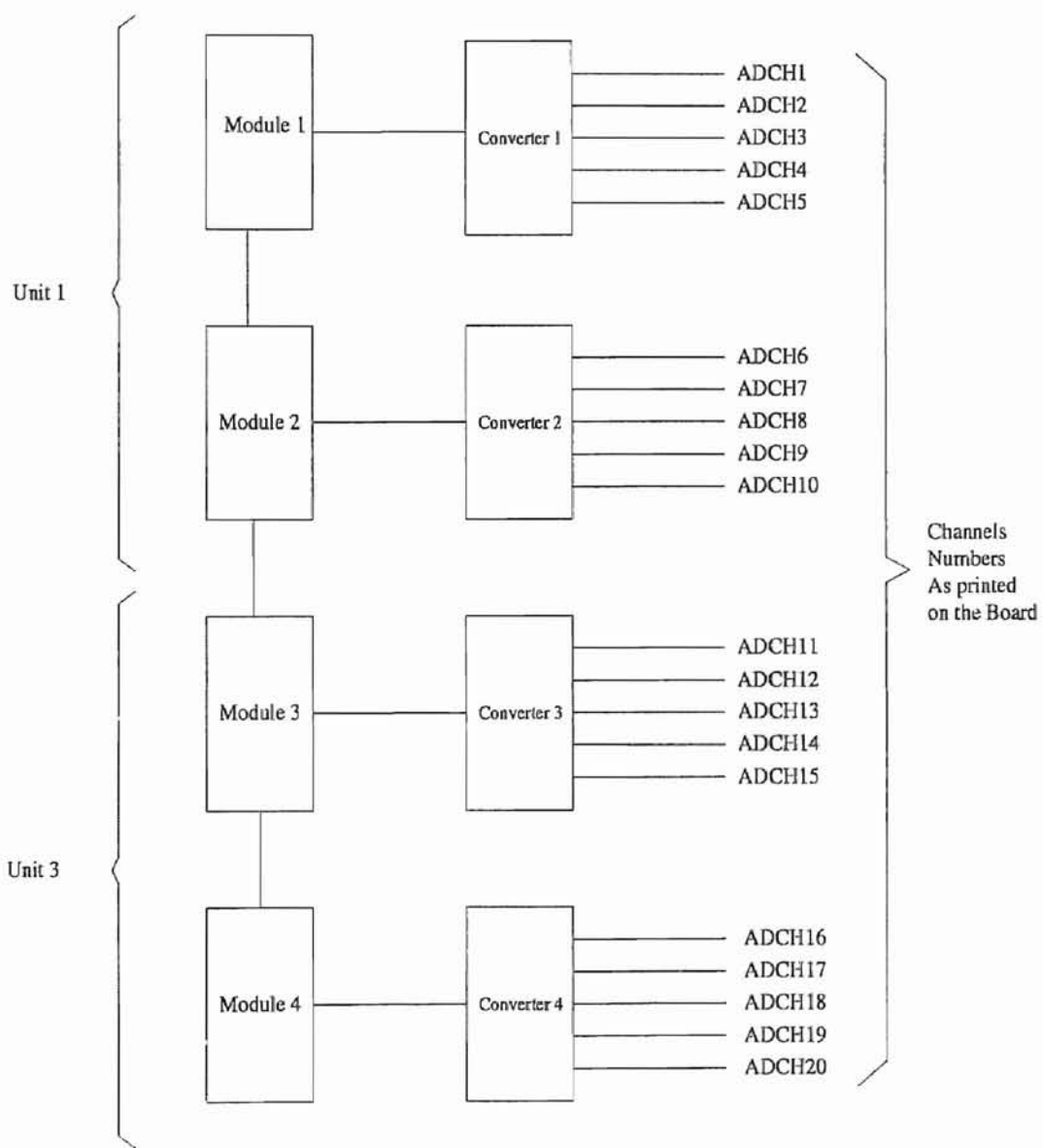


Figure 3.8: A/D Channel Configuration

CHAPTER 4

CONTROLLER DESIGNS

Three control designs were considered for the active dancer system. The controllers are a Proportional-Integral (PI) Controller, Internal Model Controller (IMC), and Self-tuning Controller (STC). Each one of these controllers have their own advantages. The PI controller is an industrial standard. Many industries use this controller because of its simplicity. Because the tension disturbances are often periodic, the IMC works well when the frequency of the disturbances is known. Self-tuning controllers find their place in situations where the process or its environment are changing continuously or at times. These systems are difficult to control if there are no mechanisms to detect these changes and adjust the controller parameters to achieve the control goal. The advantages of the STC are the automation of the tuning of the controller gains and its versatility.

The hydraulic active dancer control system has an inner and an outer loop. The inner loop is to center the ram or piston of the hydraulic actuator in the middle of the cylinder. This helps in utilizing the entire ram stroke in the cylinder. Figure 4.1 shows the inner loop and the outer loop. The inner loop employs a PI controller while the controller for the outer loop employs one of the PI, IMC, and STC.

Each of the controllers are discussed in the following sections. Section 4.1 discusses the PI controller. Section 4.2 discusses the IMC controller while Section 4.3 describes the design of the STC controller. Section 4.4 discusses the development of a linearly varying PID controller for braking control of the unwind roller based on load cell feedback.

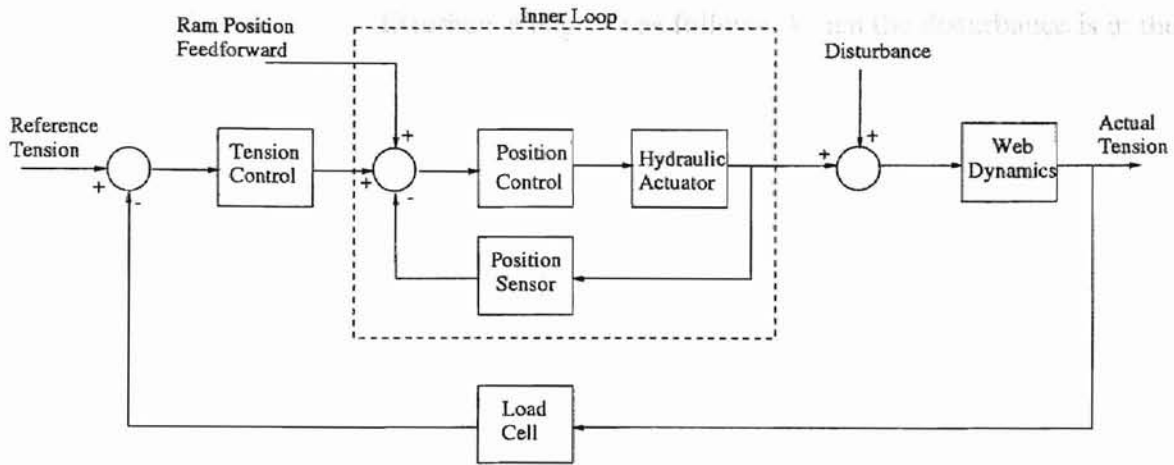


Figure 4.1: Active dancer tension control system with inner and outer loop.

4.1 Proportional-Integral (PI) Controller

One of the extensively used controllers in industry is the PID controller and variations of it. The continuous time equation of the PI controller is given below.

$$U(t) = K_p E(t) + K_i \int_0^t E(t) dt \quad (4.1)$$

where $U(t)$ is the control input and $E(t)$ (the difference between the reference tension and the measured tension) is the feedback error signal. The discrete-time version of the PI controller is

$$U(k) = K_p E(k) + K_i T_s \sum_{j=1}^k E(j) \quad (4.2)$$

where T_s is the sampling period, $U(k)$ is the control input and $E(k)$ is the error signal. The gains K_p and K_i can be tuned appropriately to obtain the desired performance.

4.2 Internal Model Based Controller (IMC)

Internal model controller is most effective when some properties about the disturbance are partially or completely known. Typically, this controller can be used to reject periodic disturbances whose frequency is known to the designer. Referring to figure 4.2, the derivation

of the internal model of the disturbance is given as follows. When the disturbance is in the form,

$$d(t) = A_d \sin(\theta t + \phi) \quad (4.3)$$

where A_d and ϕ are unknown, but θ is known approximately. The control objective is to select $G_c(s)$, the controller, to eliminate the disturbances, $d(t)$, from the output. Equation 4.4 gives the closed-loop transfer function from $D(s)$ to $E(s)$.

$$\frac{E(s)}{D(s)} = -\frac{G_p(s)}{1 + G_c(s)G_p(s)} \quad (4.4)$$

Substituting $s = j\omega$ gives the following results

$$E(j\omega) = -\frac{G_p(j\omega)}{1 + G_c(j\omega)G_p(j\omega)}D(j\omega) \quad (4.5)$$

To reject the disturbance at a particular frequency $\omega = \theta$, we should have $E(j\theta) = 0$. Therefore, the choice of the controller is such that $G_c(j\theta) = \infty$, i.e., $G_c(s)$ has a pair of poles at $s = \pm j\theta$. The following controller is the discretized version of the IMC controller that is used; it contains a proportional controller augmented with the discretized version of the disturbance model equation 4.3.

$$G_c(z) = \frac{K_p + z^{-1}K_{imc} \sin(\theta T_s)}{1 - 2z^{-1} \cos(\theta T_s) + z^{-2}} \quad (4.6)$$

where K_p is the proportional gain and K_{imc} is used to compensate for the unknown amplitude of the periodic disturbance. With the choice of $G_c(z)$ as given in (4.6), $G_c(z) = \infty$ when $z = \cos(\theta T_s) + j \sin(\theta T_s)$. The control algorithm for real-time implementation is

$$U(k) = [2\cos(\theta T_s)]U(k-1) - U(k-2) + K_{imc}[\sin(\theta T_s)]E(k-1) + K_p E(k) \quad (4.7)$$

4.3 Self-Tuning Controller (STC)

Development of a control system involves many tasks such as modeling, design of a control law, implementation, and validation. The self-tuning controller attempts to automate

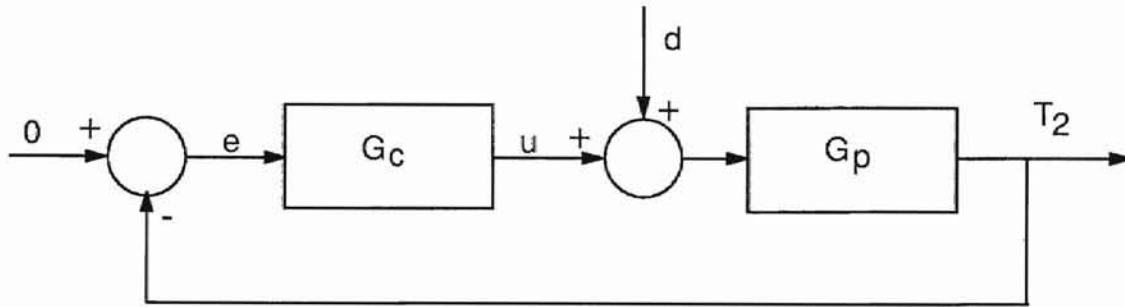


Figure 4.2: Active dancer tension control system.

several of these [31]. The term “self-tuning” is used to express the property that the controller parameters converge to the controller that is designed if the process is known. The estimated parameters are usually treated as if they are “true” in designing the controller. Figure 4.3 shows a block diagram of a process with a self-tuning controller.

Usually, the structure of the process model is assumed to be known. This is the case for Indirect Adaptive Control where the parameters are estimated first. The block labeled “Estimation” in figure 4.3 gives the estimates of the process parameters. This block typically implements a recursive estimator as discussed in appendix C.1. The block labeled “Controller Design” performs the computations needed for implementing a control law and the block labeled “Controller” implements the control law designed.

In the indirect adaptive algorithm, the parameters of the transfer function are estimated and the controller parameters are updated based on the current parameters. The term direct refers to the controller parameters being estimated rather than updated based on estimates of the plant parameters. Quite often in the case of direct self-tuning controllers, the model can be reparametrized such that the controller parameters can be estimated directly, still the relative degree of the plant transfer function has to be known.

The design calculations for the Minimum Degree Pole Placement algorithm [31] for the indirect self-tuning controller are time-consuming and may be poorly conditioned for some parameter values. Thus, it is desirable to reparametrize the model in terms of the

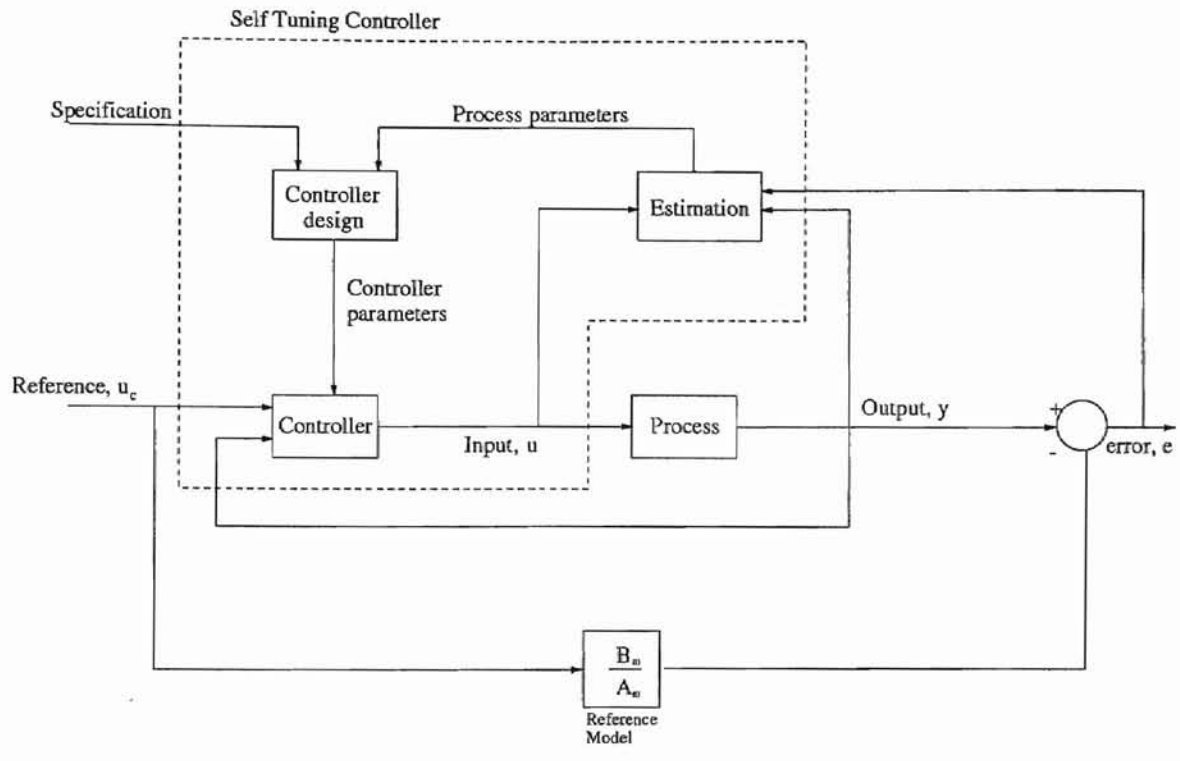


Figure 4.3: Block diagram of a self-tuning controller.

parameters of the controller. Consider the process shown in figure 4.4 with $v = 0$. Further, consider the control law given by

$$Ru = Tu_c - Sy \tag{4.8}$$

where R , S , and T are polynomials in the forward shift operator z . The idea is to find the coefficients in these polynomials such that the closed loop system shown in figure 4.4 follows a prescribed reference model. Let us denote this reference model in terms of the polynomials A_m and B_m where

$$A_m y = B_m u_c \tag{4.9}$$

To reparametrize the process dynamics in terms of the controller parameters, multiply equation (4.8) by B_m on both sides and rearrange the terms to get

$$B_m T u_c = B_m R u + B_m S y$$

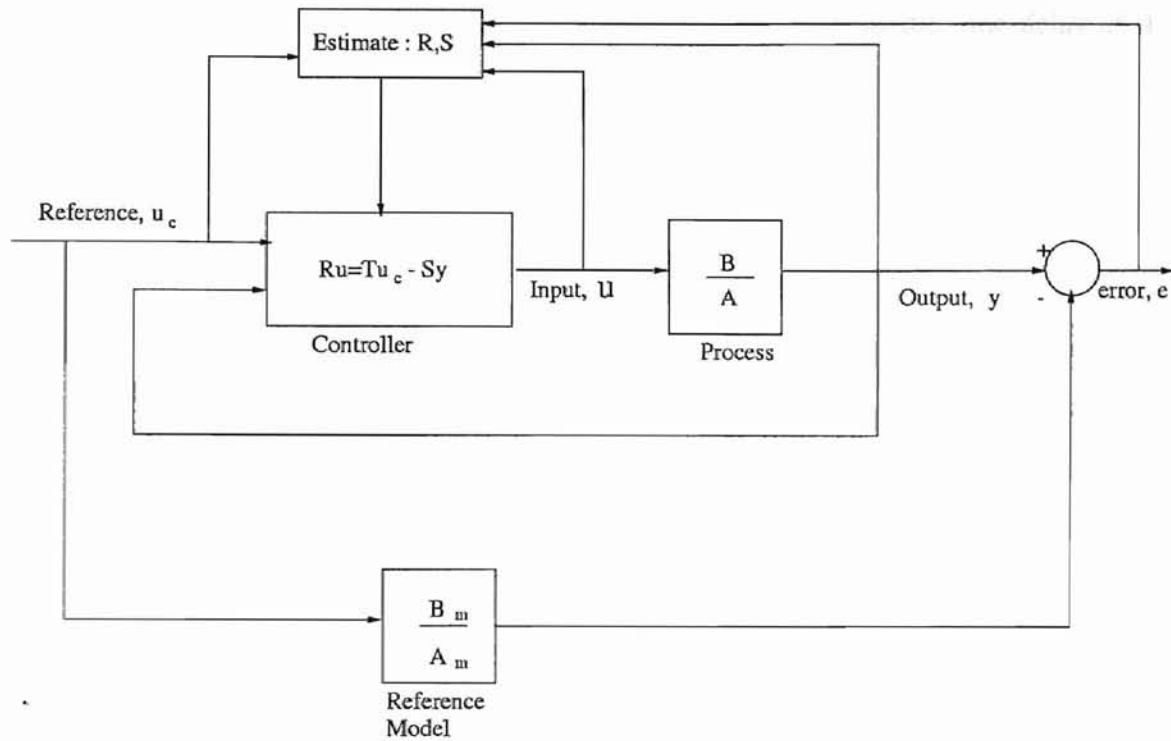


Figure 4.4: Two degrees of freedom direct self-tuning controller.

If the closed-loop system follows the reference model as given in equation (4.9), $B_m u_c = A_m y$. Therefore, the above equation can be written as

$$y = \frac{B_m}{A_m T} (Ru + Sy) \quad (4.10)$$

Equation (4.10) represents the dynamics of the process reparametrized in terms of the controller parameters R , S , and T . This indicates that if the parameters in R , S , and T are chosen such that the input to the plant (u) and the output from the plant (y) satisfy the equation (4.10), then the closed loop system with the control law given in equation (4.8) makes the closed loop system follow the reference model given in equation (4.9).

The recursive least squares estimation algorithm given in Appendix C.1 can be used to estimate the parameters in R , S and T to satisfy the equation (4.10). However, we need to know the relative degree $d_0 = \deg(A) - \deg(B)$ of the plant in order to satisfy the compatibility condition given by [31]

$$\deg(A_m) - \deg(B_m) \geq \deg(A) - \deg(B) \quad (4.11)$$

This means that the time delay of the model be at least as large as the time delay of the process. The polynomials A_m and B_m must be chosen such that the compatibility equation (4.11) is satisfied. As an example, consider a plant with $\deg(A) = 4$ and $\deg(B) = 3$ and so $d_0 = 1$. For this plant, we can conveniently choose

$$A_m = z^3 + a_{m2}z^2 + a_{m1}z + a_{m0} \quad (4.12)$$

$$B_m = kz^{d_0} = kz \quad \text{where } k = A_m(1) \quad (4.13)$$

$$T = kz \quad (4.14)$$

$$R = r_2z^2 + r_1z + r_0 \quad (4.15)$$

$$S = s_2z^2 + s_1z + s_0 \quad (4.16)$$

The choice of B_m given in (4.13) shows the response of the system with minimal delay and unit static gain. Equation (4.10) is rewritten with the parameters given in equations (4.12)-(4.16) as follows

$$y(t) = \frac{r_2z^2 + r_1z + r_0}{z^3 + a_{m2}z^2 + a_{m1}z + a_{m0}}u(t) + \frac{s_2z^2 + s_1z + s_0}{z^3 + a_{m2}z^2 + a_{m1}z + a_{m0}}y(t) \quad (4.17)$$

The above equation can be rewritten in the form of a regression model given by (C.2). With the following terms given below

$$R^* = r_2z^{-1} + r_1z^{-2} + r_0z^{-3}$$

$$S^* = s_2z^{-1} + s_1z^{-2} + s_0z^{-3}$$

$$T^* = kz^{-2}$$

$$A_m^* = 1 + a_{m2}z^{-1} + a_{m1}z^{-2} + a_{m0}z^{-3}$$

$$u_f(t) = \frac{1}{A_m^*}u(t)$$

$$y_f(t) = \frac{1}{A_m^*}y(t)$$

This means that the time delay of the model be at least as large as the time delay of the process. The polynomials A_m and B_m must be chosen such that the compatibility equation (4.11) is satisfied. As an example, consider a plant with $\deg(A) = 4$ and $\deg(B) = 3$ and so $d_0 = 1$. For this plant, we can conveniently choose

$$A_m = z^3 + a_{m2}z^2 + a_{m1}z + a_{m0} \quad (4.12)$$

$$B_m = kz^{d_0} = kz \quad \text{where } k = A_m(1) \quad (4.13)$$

$$T = kz \quad (4.14)$$

$$R = r_2z^2 + r_1z + r_0 \quad (4.15)$$

$$S = s_2z^2 + s_1z + s_0 \quad (4.16)$$

The choice of B_m given in (4.13) shows the response of the system with minimal delay and unit static gain. Equation (4.10) is rewritten with the parameters given in equations (4.12)-(4.16) as follows

$$y(t) = \frac{r_2z^2 + r_1z + r_0}{z^3 + a_{m2}z^2 + a_{m1}z + a_{m0}}u(t) + \frac{s_2z^2 + s_1z + s_0}{z^3 + a_{m2}z^2 + a_{m1}z + a_{m0}}y(t) \quad (4.17)$$

The above equation can be rewritten in the form of a regression model given by (C.2). With the following terms given below

$$R^* = r_2z^{-1} + r_1z^{-2} + r_0z^{-3}$$

$$S^* = s_2z^{-1} + s_1z^{-2} + s_0z^{-3}$$

$$T^* = kz^{-2}$$

$$A_m^* = 1 + a_{m2}z^{-1} + a_{m1}z^{-2} + a_{m0}z^{-3}$$

$$u_f(t) = \frac{1}{A_m^*}u(t)$$

$$y_f(t) = \frac{1}{A_m^*}y(t)$$

equation (4.17) can be written as

$$y(t) = R^*u_f(t) + S^*y_f(t) = \theta^T \phi(t)$$

where

$$\theta^T = [r_2 \quad r_1 \quad r_0 \quad s_2 \quad s_1 \quad s_0] \tag{4.18}$$

$$\phi^T(t) = [u_f(t-1) \quad u_f(t-2) \quad u_f(t-3) \quad y_f(t-1) \quad y_f(t-2) \quad y_f(t-3)]$$

Algorithm for Simple Direct Self-Tuner:

Data: Specifications in terms of A_m, B_m , and d_0 .

Step 1: Estimate the coefficients of polynomials R and S in equation (4.18) using the least squares estimation.

Step 2: Compute the control signal from

$$R^*u(t) = T^*u_c(t) - S^*y(t)$$

where R and S are obtained from the estimates in Step 1. Repeat Step 1 and Step 2 at each sampling period.

Note, however, that the relative degree of the transfer function of the process has to be known *a priori* to implement the Direct Self-Tuner Algorithm specified above.

4.4 Proportional-Integral-Derivative Controller with Linearly Time Varying Gains

A proportional-integral-derivative controller with constant gains for the unwind and rewind roll will make the system unstable. The gains have to be adjusted during the process to compensate for the change in masses of the unwind and rewind rolls. In order to compensate for the changes in the mass, a linear relationship was derived based on systematic calculated gains when the unwind is at full roll and when it is at empty along with the velocity of the process.

The characteristic equation in equation C.15 is a third order equation. The three desired poles will be design based on the percentage overshoot and the settling time. To reduce the third order system to a second order system, one pole is designed to be at least ten times greater than the other two poles. Complete derivation of the transfer function and the PID gains are given in appendix C.2.

$$\begin{aligned}
 K_d &= \frac{\gamma - \frac{z}{\beta} + \beta x - y - \theta\beta}{\alpha y + \alpha\beta^2 - \frac{z\alpha}{\beta} - \alpha\beta x} \\
 K_p &= \frac{x + x\alpha K_d - \theta - \alpha\beta K_d}{\alpha} \\
 K_i &= \frac{z + z\alpha K_d}{\alpha\beta}
 \end{aligned} \tag{4.19}$$

where $\alpha = \frac{v_r}{R_u L_1}$, $\beta = \frac{C}{J_u v_r}$, $\theta = \frac{v_r}{L_1}$, $\gamma = \frac{B}{L_1 J_1 J_u}$, $x = 2\zeta\omega_n + 10\zeta\omega_n$, $y = 21\zeta^2\omega_n^2 + \omega_n^2(1 - \zeta^2)$, and $z = 10\zeta\omega_n(\zeta^2\omega_n^2 + \omega_n^2(1 - \zeta^2))$. ζ and ω_n are determined from percentage overshoot and settling time.

With the gains known at full and empty unwind rolls, a linear equation can be obtain for the decrease of the PID gains. Given a reference velocity, the time between the full and empty roll can be calculated by rearranging equation 2.2.

$$t = \frac{\pi(R_{full}^2 - R_{empty}^2)}{v_r h} \tag{4.20}$$

Equation 4.21 shows how the gains will decrease.

$$y = -\frac{K_{empty} - K_{full}}{\frac{t}{T_s}} T_i + K_{full} \tag{4.21}$$

where K_{empty} and K_{full} could be K_p , K_i , or K_d gains at empty and full roll. T_s is the sampling time and T_i is the time increment. y is the computed linearly varying gains K_p , K_i , or K_d .

CHAPTER 5

EXPERIMENTAL RESULTS

Each of the controllers discussed previously were implemented on the web line discussed in chapter 3. Implementation of the PI and IMC require properly tuned gains. Taking the initial gains given in [27], the gains were then tuned for the PI and IMC to maximize the tension attenuation. The process of tuning the controller gains typical required between 5 to 10 minutes.

Periodic tension disturbance was generated upstream of the dancer roller by making one of the rollers eccentric. Because the disturbance is created by making a roller eccentric, the frequency of the disturbance is dependent on the speed of the web process. Estimate of this frequency is obtained by running the process for a specific amount of time and counting the number of cycles during that time. Figure 5.1 shows the relationship between the speed and the frequency of the disturbance. The frequency thus computed is used in the Internal Model Controller.

The web speed can be changed on the Fife control panel which indicates the speed as a number ranging from 0 to 10¹. The experiments are conducted at different speeds and different reference tensions. For each (speed,reference tension) combination, tension in the web line is collected without the controller running and then with the controller running so that percentage tension disturbance rejection can be computed.

All these experiments were conducted with a sampling period of 5 milliseconds. At each sampling instant, data on the load cell and the position of the dancer roller are collected and the computed control input is sent to the actuator. For experiments with the self-tuning

¹The actual speed is roughly the dial reading multiplied by 100 feet/min.

controllers, the gains of the controllers are also collected.

5.1 Experimental Results

This section discusses experimental results obtained using different controllers for the active dancer system. For ease of comparison, the performance of each of the controller at a given speed and a given reference tension are displayed on the same graph. Though the experiments are run at various speeds and reference tensions, only representative samples of the experimental results are presented.

Figures 5.4 and 5.5 show the performance of the three controllers at a reference tension of 15 lbs and speed setting ranging from 3 and 7. Similarly figures 5.6 and 5.7 show the performance of the controllers at a reference tension of 20 lbs and the same speeds. These figures indicate that the active dancer is able to reject the tension disturbances by around 30–60%. These results are summarized in Table. 5.3. The results of the controllers for the reference tension of 15 and 20 lbs are compared in figure 5.2.

Appendix D.1 gives additional experimental results for different web speeds.

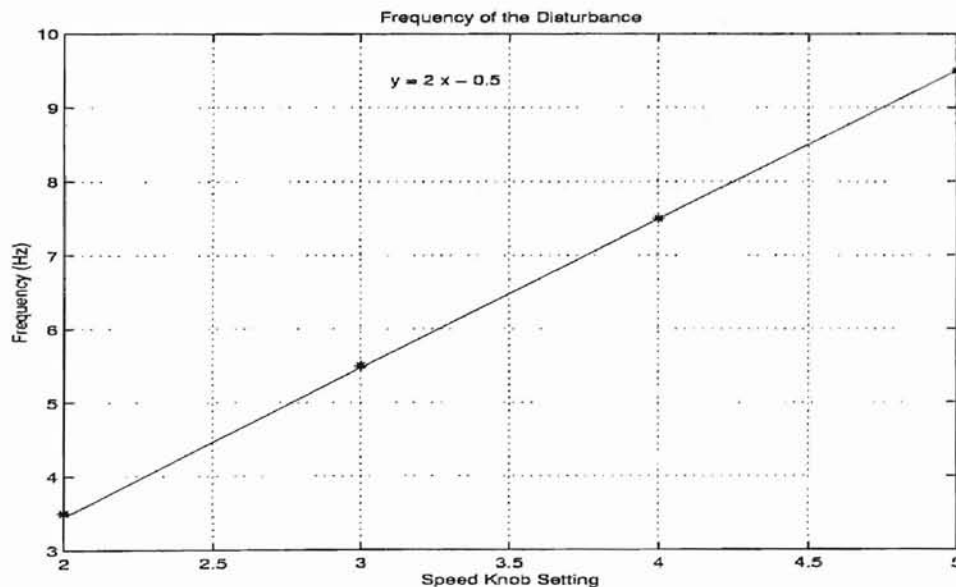


Figure 5.1: The frequencies of the tension disturbances corresponding to different speeds.

5.2 Experimental Results Using Upstream Load Cell as Feedback Signal

Preview controller was investigated in [26] on automobiles. In the preview controller, sensor measurements for the front wheel of the vehicle are used as the feedback signal of controller for the back wheel. The signal from the front wheel sensor informs the back wheel that it is about to encounter a disturbance in the road. The advanced information about the upcoming road profile allows the back wheel controller attenuated the disturbances creating a smoother ride. With increase in preview time, the acceleration curves becomes smoother indicating a more comfortable ride.

Figure 5.3 and table 5.3 lists the percentage of tension disturbance attenuation by the active dancer using the upstream load cell signals instead of the downstream load cell. By using the upstream load cell signal, the active dancer received information about the disturbance before the disturbance reaches the active dancer. Figures 5.8 to 5.11 shows the tension attenuation using the upstream load cell signal with the three controllers. Appendix D.2 gives additional experimental results for different web speeds.

5.3 Experimental Results on Back Propagation

The mathematical model of the web span includes the upstream tension and the tension of the current span. The tension from the downstream span is not included in the model. [27] stated “it is uncertain as to how much of the tension reflected by the load cell downstream of the active dancer is due to back propagation of the tension.” To determine the presence of back propagation, experimental data were collected using the upstream load cell.

Back propagation can be seen in figures D.13 to D.22 in appendix D.3. Data was collected with upstream load cell. Initially, the graphs show the active dancer turned off displaying the effect of the disturbances. Then the dancer is turned on. The movement of the dancer changes the tension in the web. This change in the tension as detected by the upstream load cell indicates back propagation.

Speed	Tension 15 lb			Tension 20 lbs		
	PI	IMC	STR	PI	IMC	STR
2	29	40	39	33	36	31
3	54	63	38	65	67	63
4	36	36	35	31	38	34
7	32	53	29	36	50	38
8	34	39	29	44	46	30

Table 5.1: Tension disturbance attenuation with the downstream load cell as the feedback signal.

Speed	Tension 15 lb			Tension 20 lbs		
	PI	IMC	STR	PI	IMC	STR
2	30	36	25	21	23	26
3	32	38	28	28	33	27
4	39	40	39	40	29	34
7	48	38	38	41	38	38
8	33	43	25	27	45	32

Table 5.2: Tension disturbance attenuation using upstream load cell as the feedback signal.

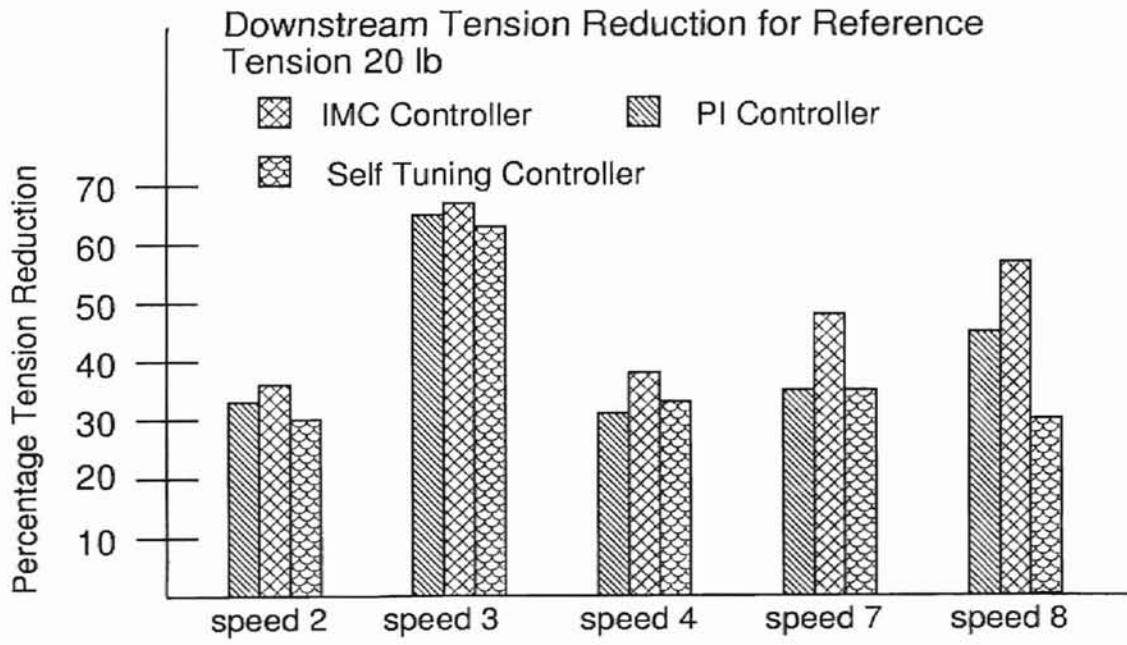
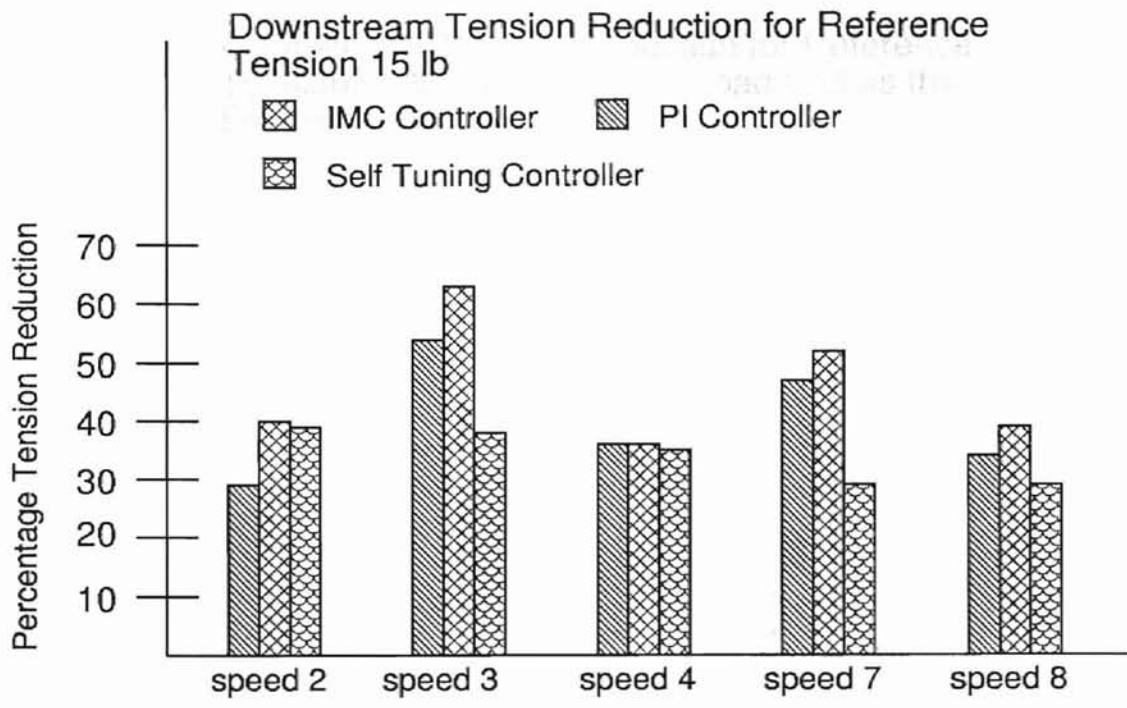


Figure 5.2: Tension disturbance attenuation with downstream load cell as feedback.

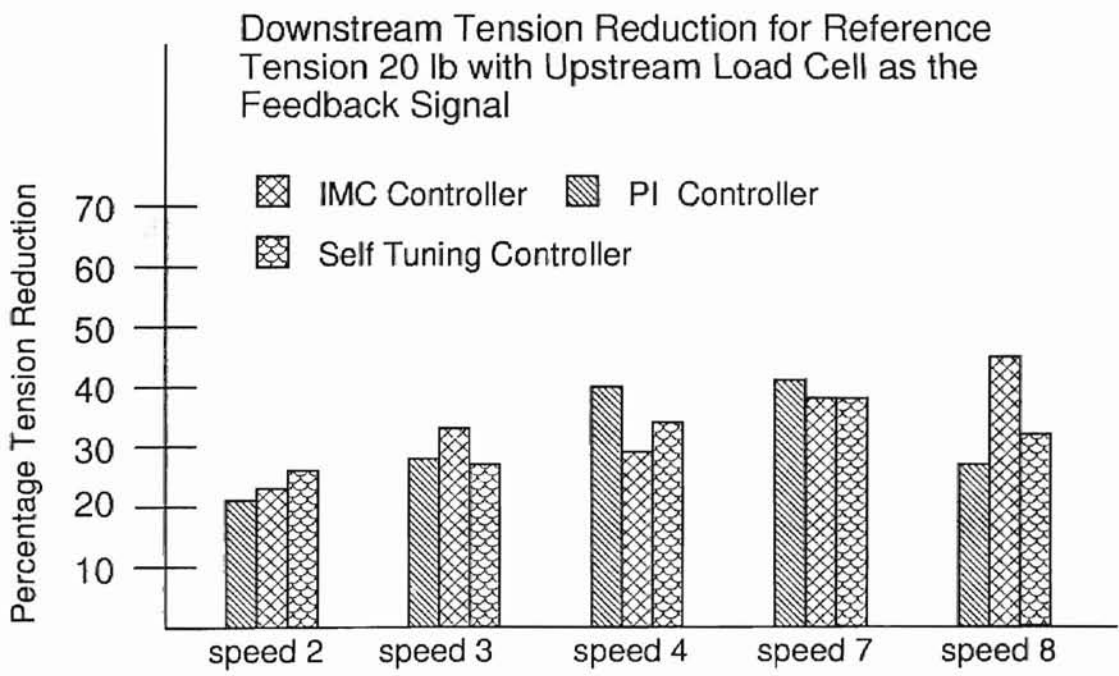
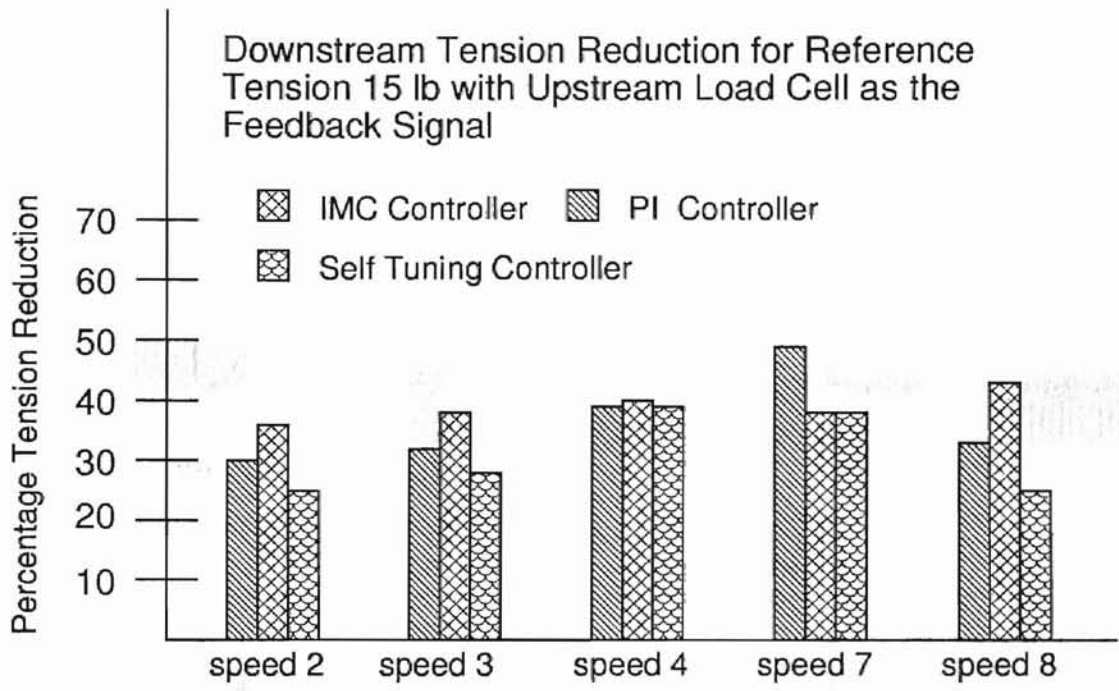


Figure 5.3: Tension disturbance attenuation with upstream load cell as feedback.

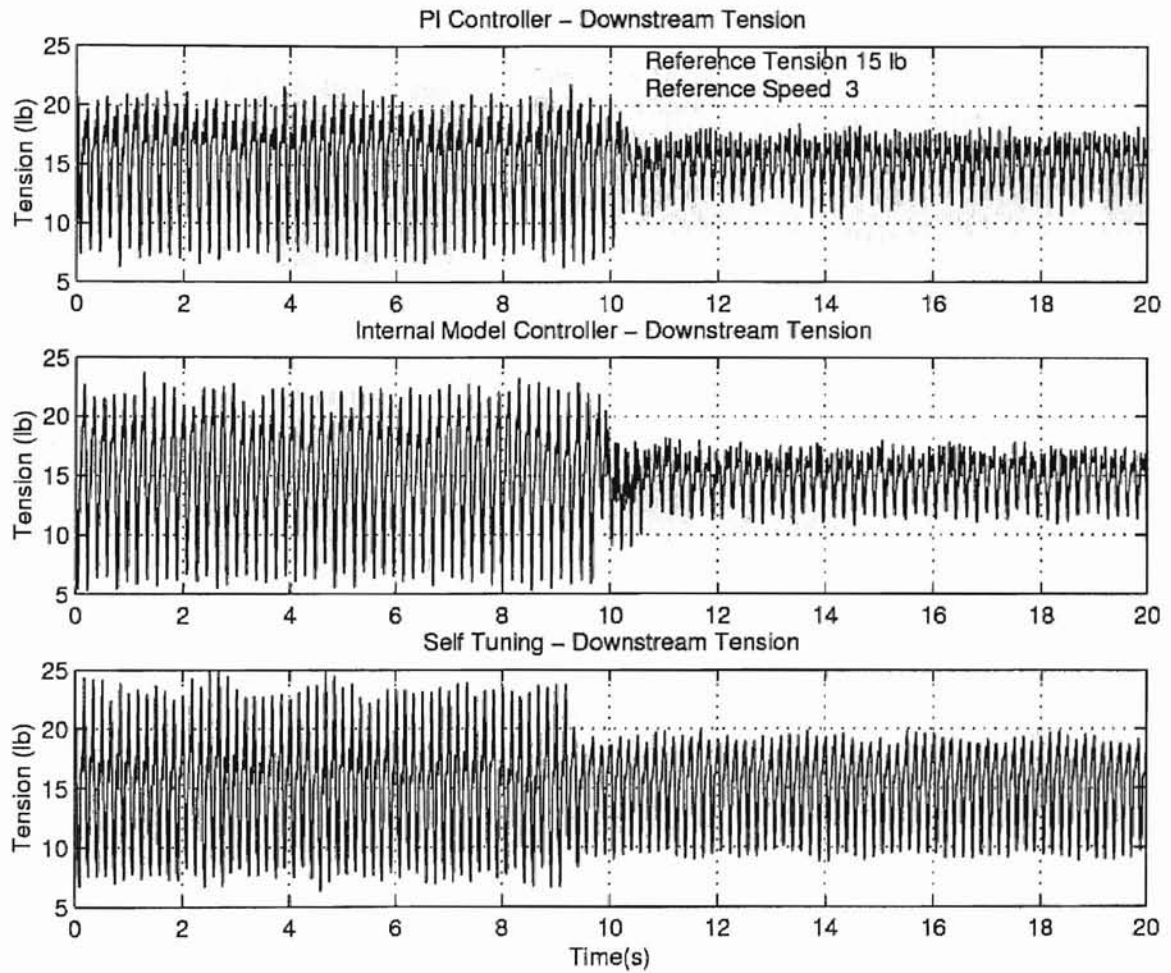


Figure 5.4: Tension disturbance attenuation with downstream load cell as feedback.

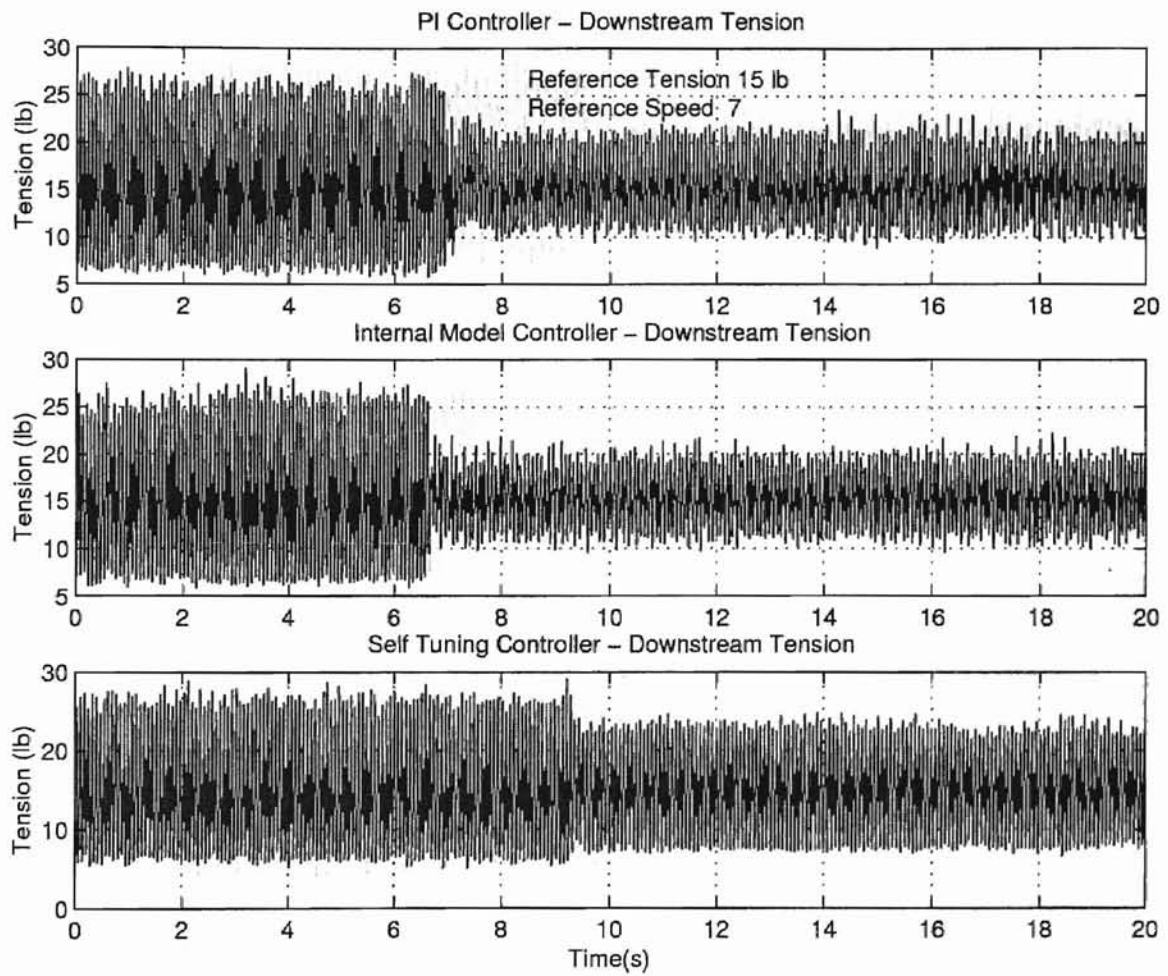


Figure 5.5: Tension disturbance attenuation with downstream load cell as feedback.

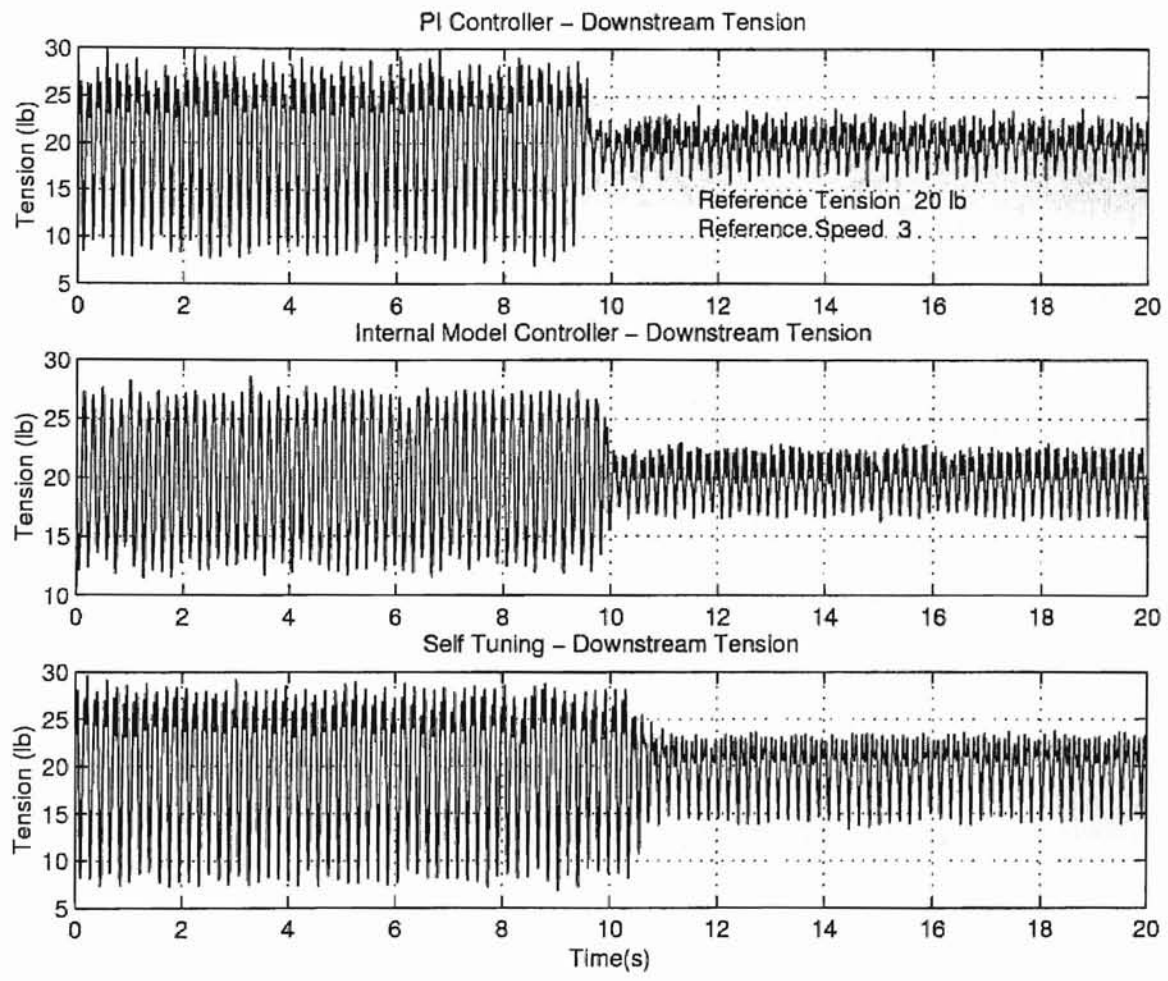


Figure 5.6: Tension disturbance attenuation with downstream load cell as feedback.

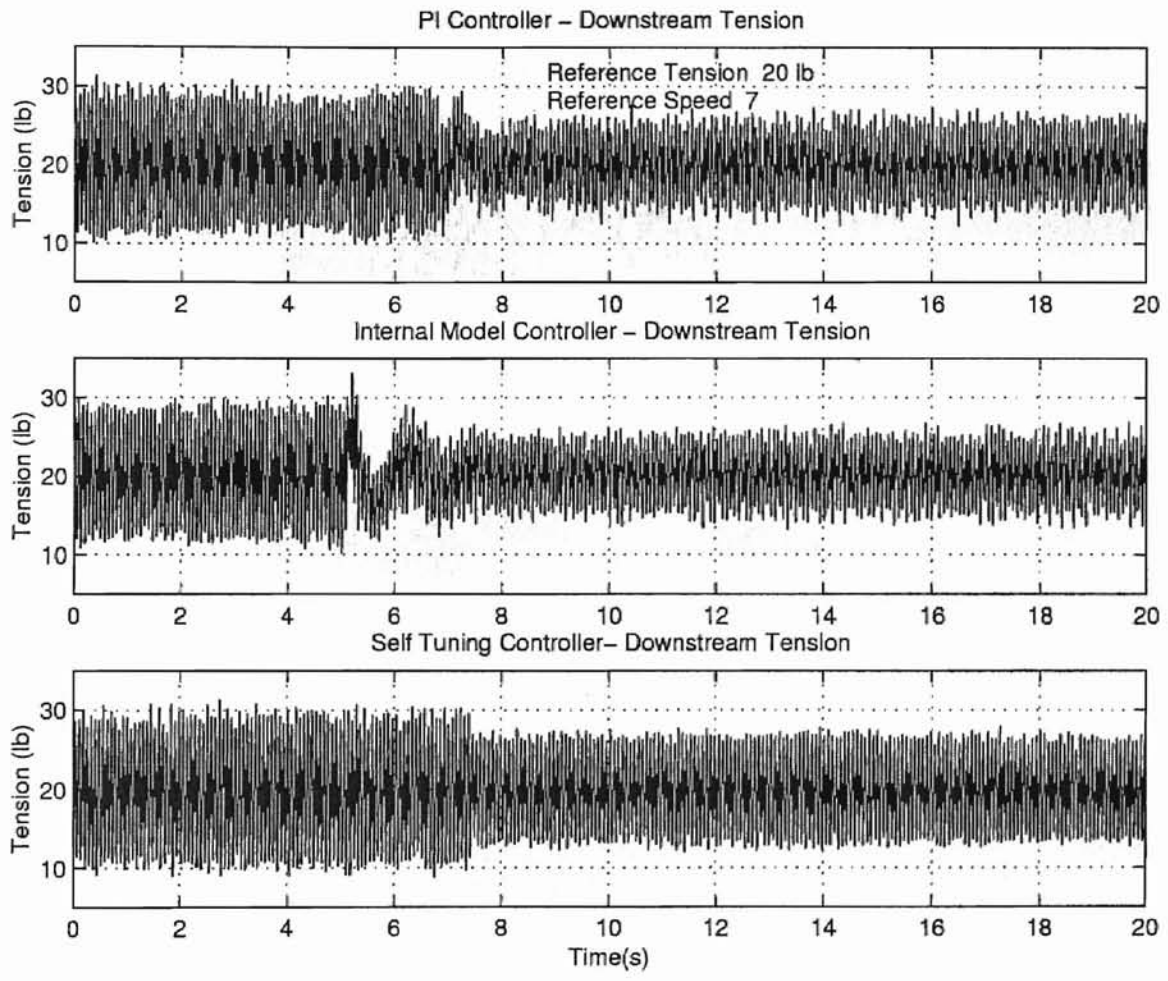


Figure 5.7: Tension disturbance attenuation with downstream load cell as feedback.

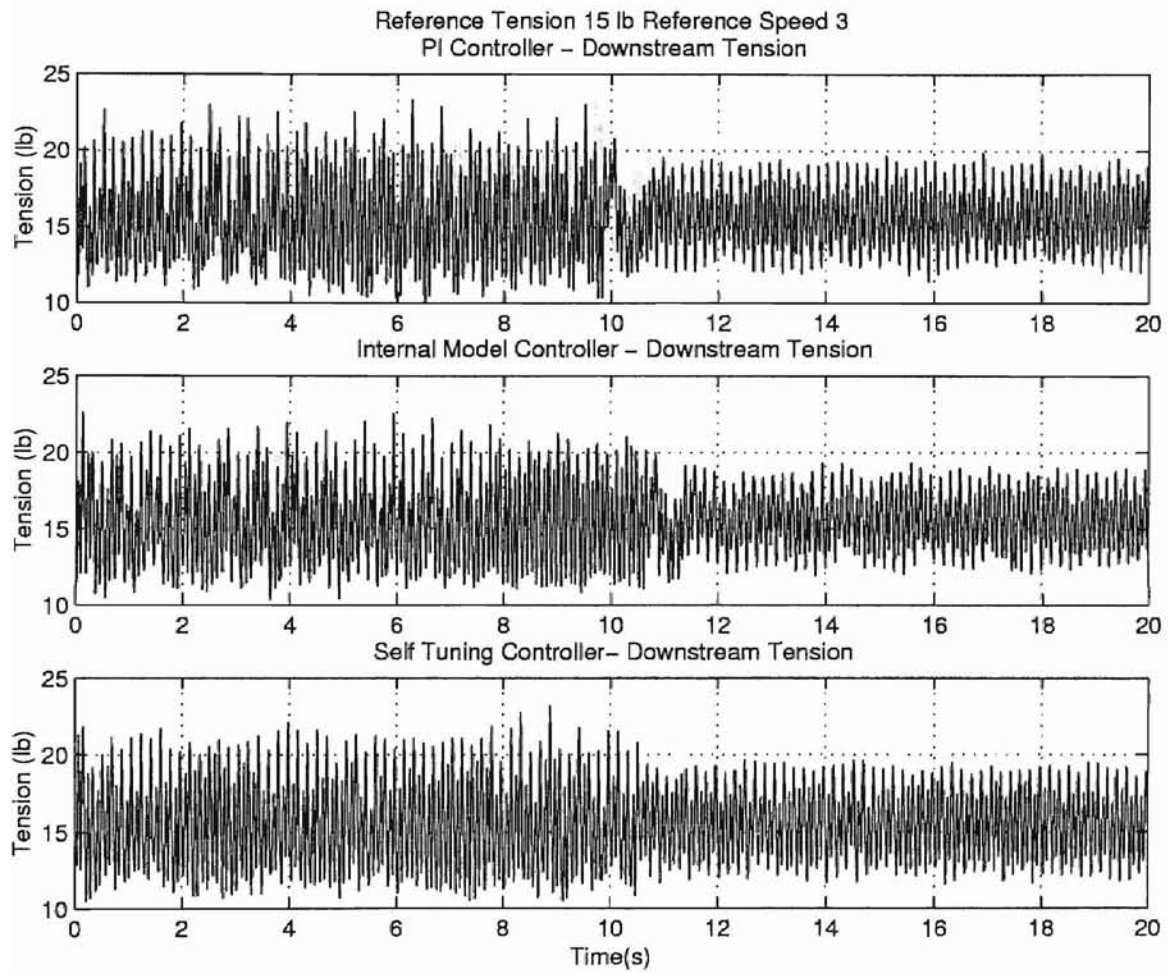


Figure 5.8: Tension disturbance attenuation with upstream load cell as feedback.

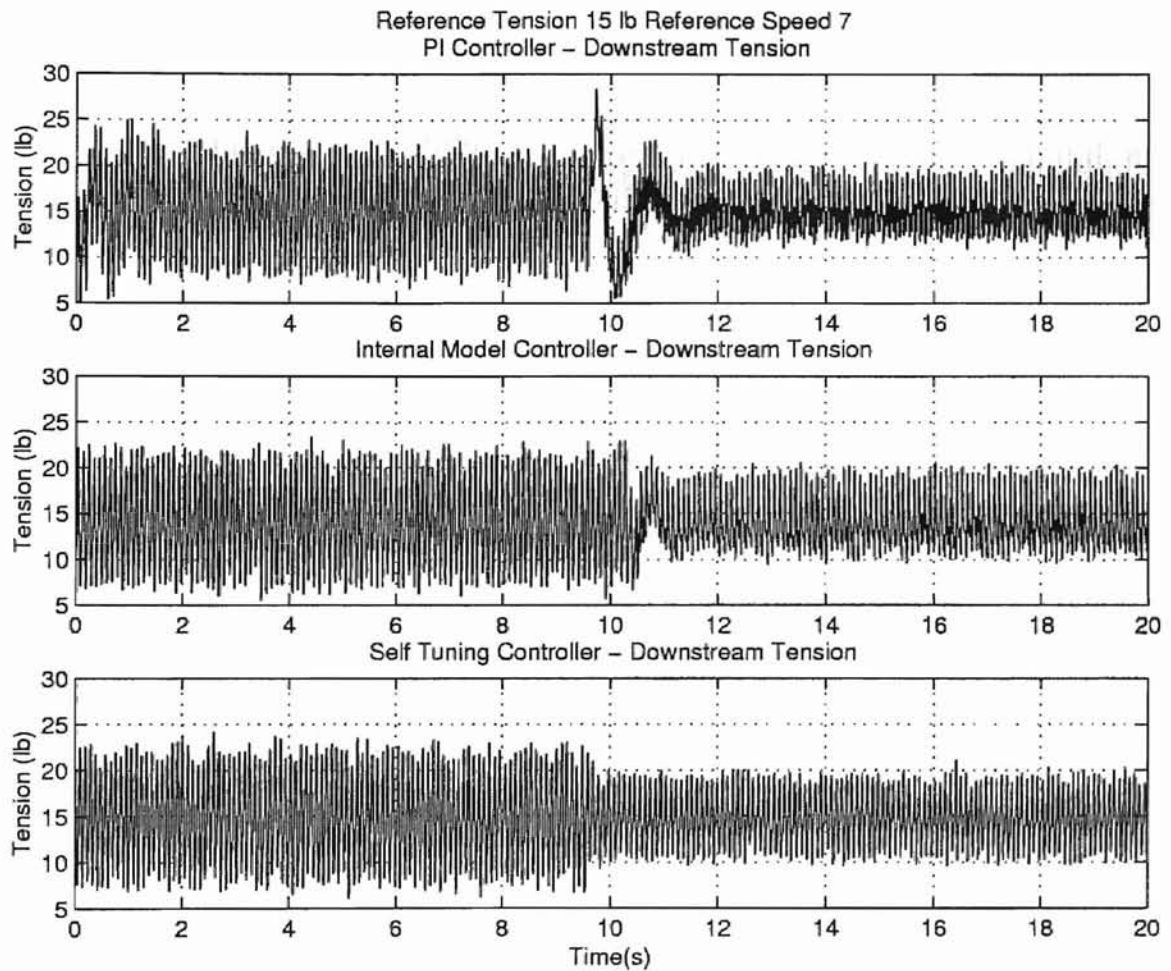


Figure 5.9: Tension disturbance attenuation with upstream load cell as feedback.

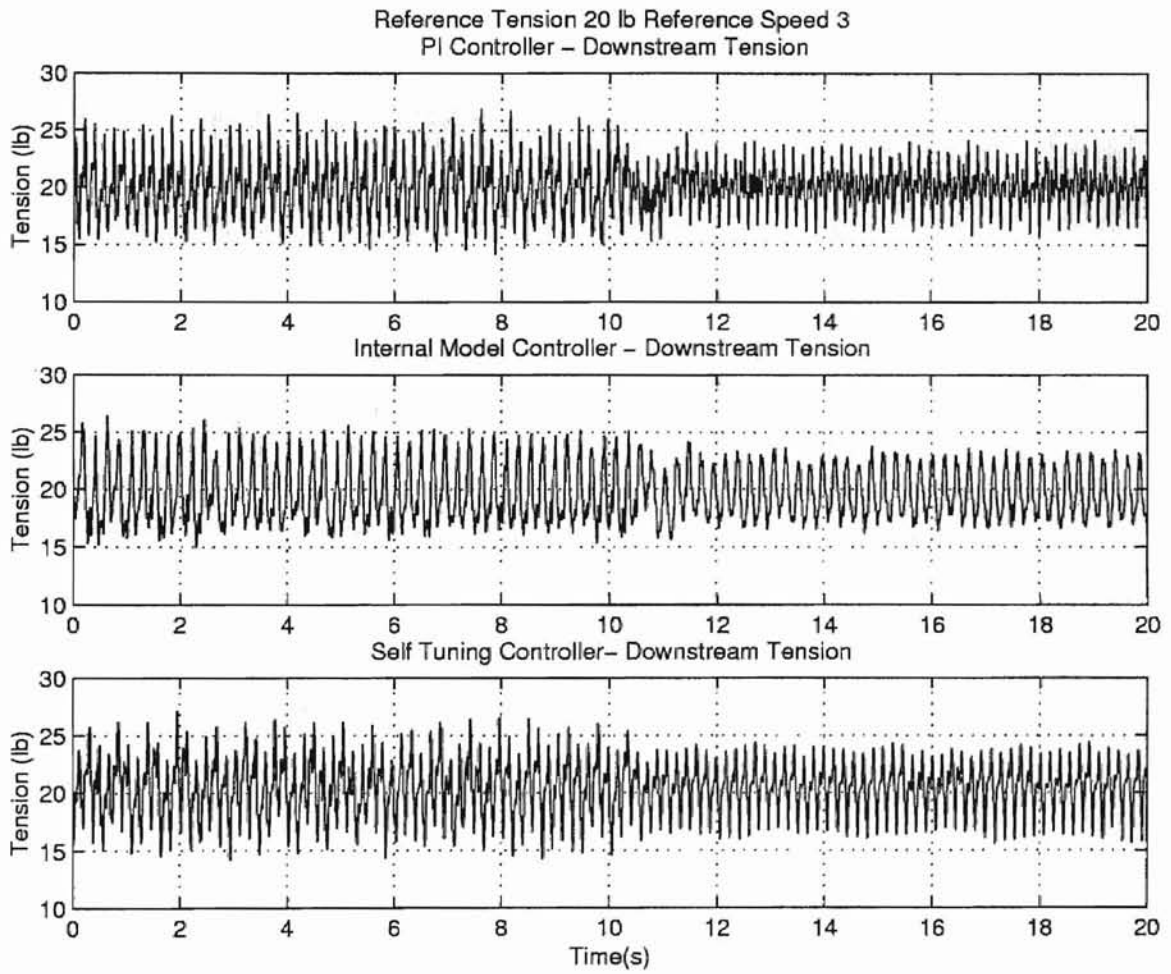


Figure 5.10: Tension disturbance attenuation with upstream load cell as feedback.

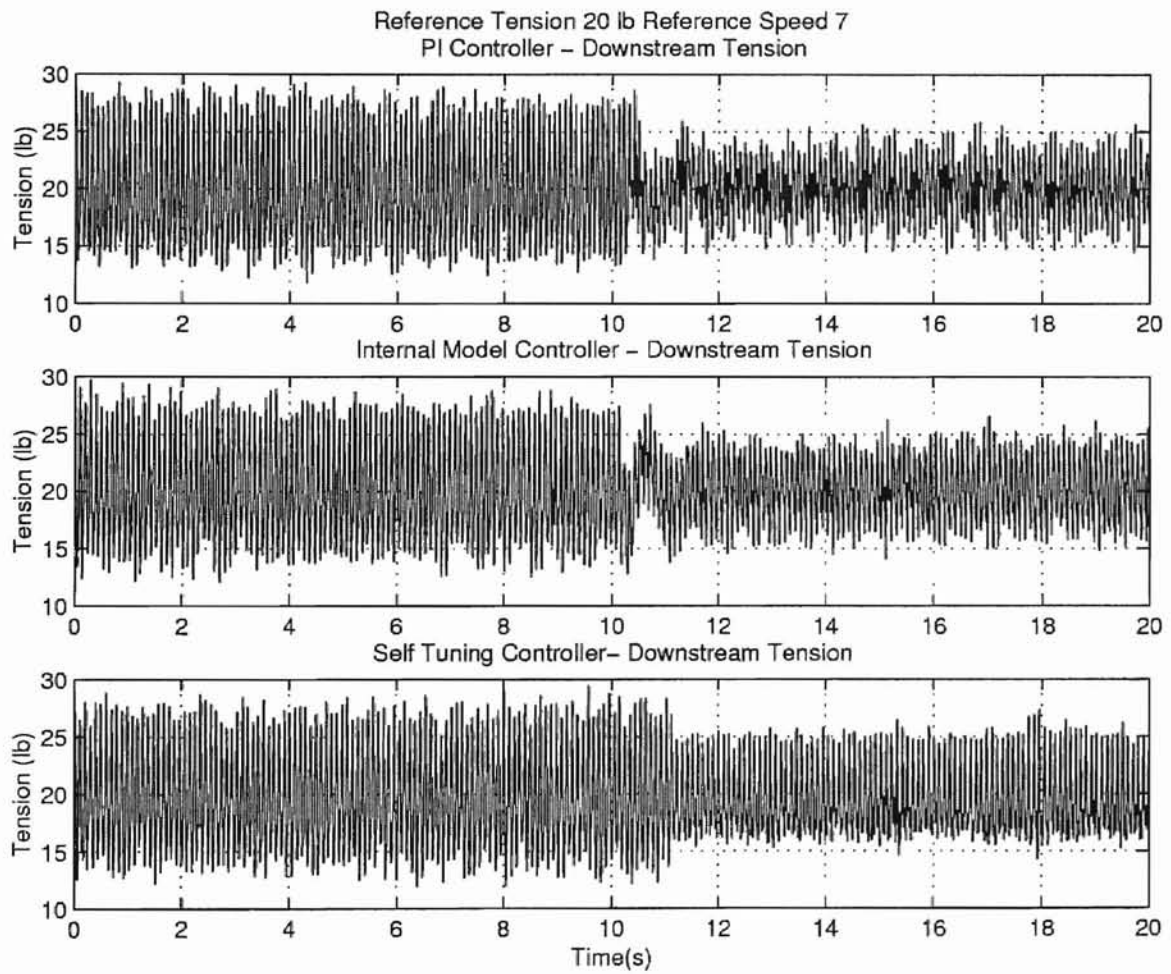


Figure 5.11: Tension disturbance attenuation with upstream load cell as feedback.

5.4 Experimental Results with Linearly Varying PID Controller for Unwind Roll

The mass of the unwind roll is constantly changing. A controller with constant gains will not be able to provide adequate performance as can be seen in figure 5.14. Data taken with the existing controller (the Digitrac 2, an industrial available controller) reveals the strategy to compensate for change in mass. To maintain constant tension in the web, figures 5.12 to 5.13 show the relation between the speed of the process and the decrease in the torques applied to the brake and the increase in the torque applied to the clutch. There are no disturbances injected into the web. As the speed on the process increases, the brake torque decreases more rapidly by comparing figures 5.13 and 5.12.

Figure 5.15 shows the results with a PID controller where the proportional gain is linearly decreasing. The slope of the proportional gain is experimentally obtain. A set of gains is obtained by tuning a PID controller to maintain a stable system at the time of start-up and ending of the process. A linear equation is calculated and the proportional gain decreases accordingly. From figure 5.15, the system no longer becomes unstable for duration of the process, but the brake torque is not decreasing and the tension takes nearly the entire process (160 seconds) to reach the reference tension.

A PID controller is designed by modeling the unwind subsystem, which is shown in figure 2.2. The system transfer function was obtained and the gains calculated at full and empty unwind roll. The time for the unwind roll to completely unwind together with the gains at full and empty unwind roll of the process, the linearly varying relationship was obtained. Figures 5.16 and 5.17 show the performance of the linearly varying PID controller to maintain the tension in the web by compensating for the changing inertia of the unwind roll.

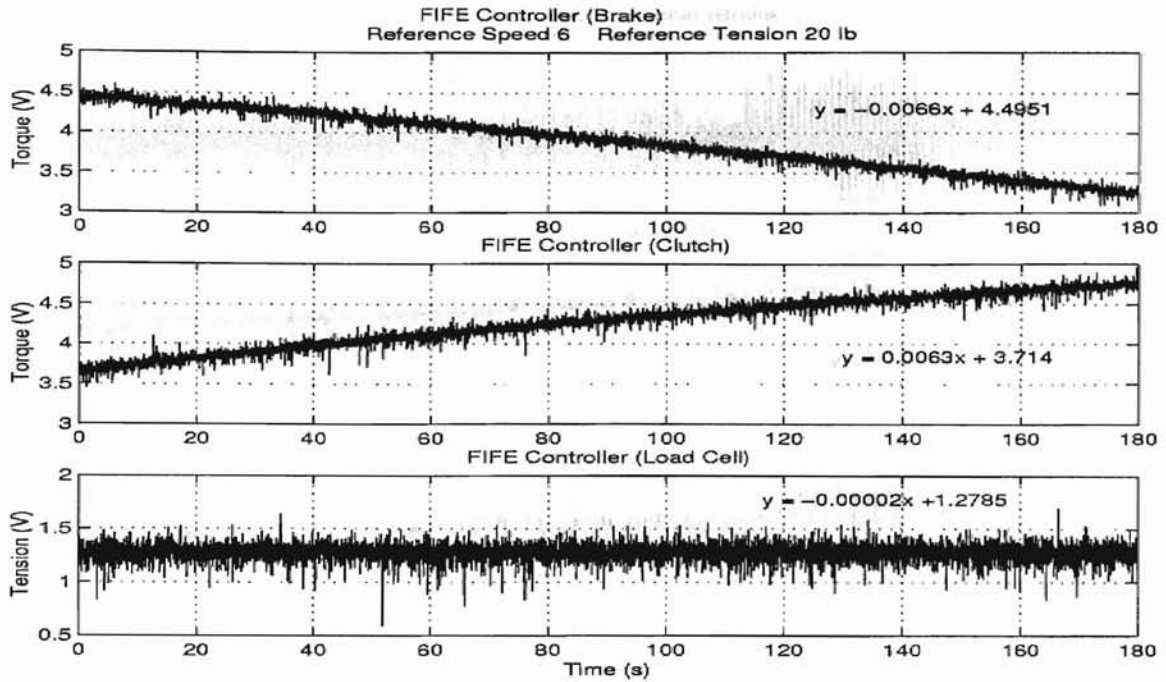


Figure 5.12: FIFE controller: Torque applied to the brake with reference tension 20 lbs and 600 feet per minute speed.

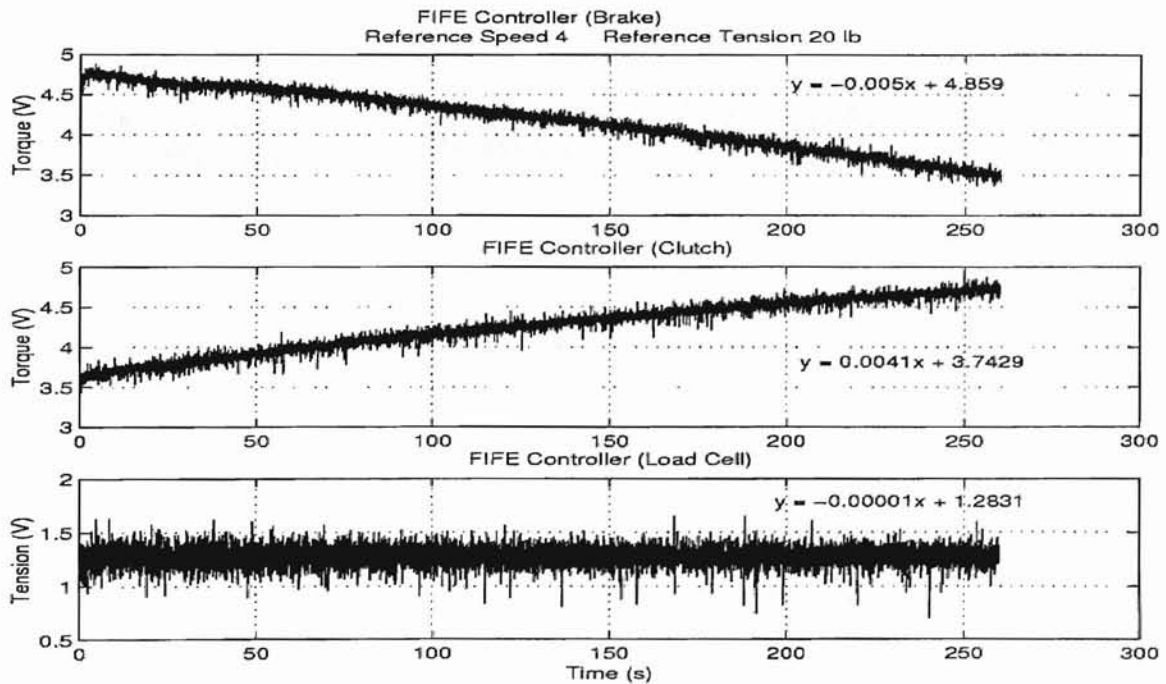


Figure 5.13: FIFE controller: Torque applied to the brake with reference tension 20 lbs and 400 feet per minute speed.

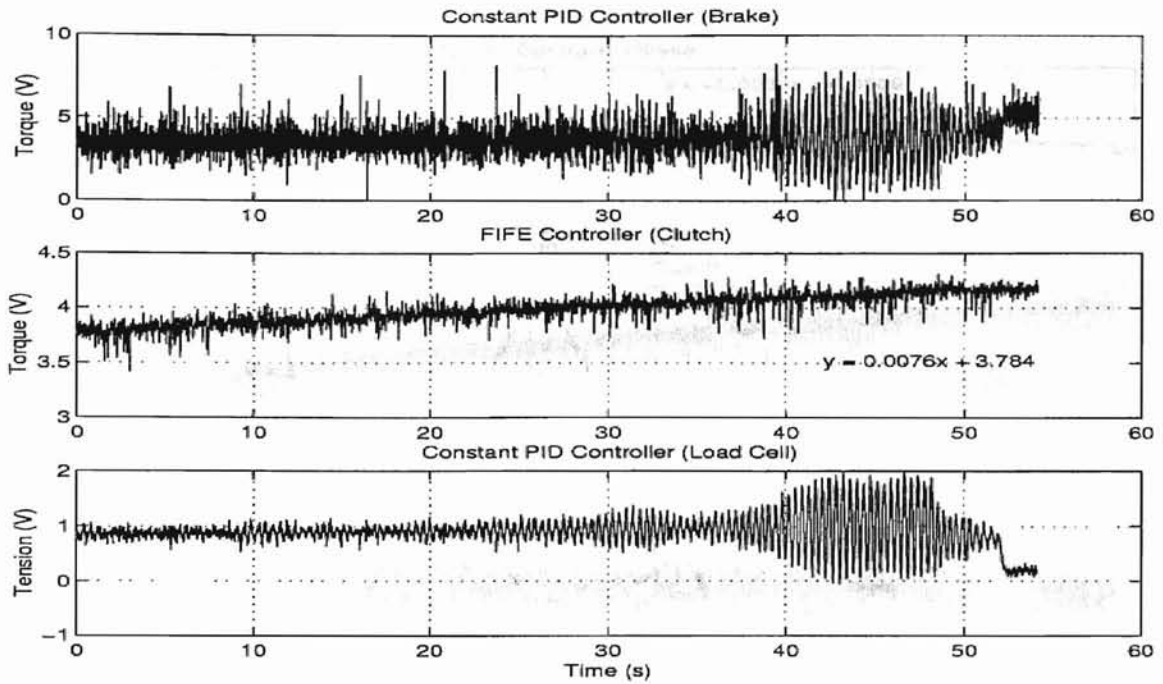


Figure 5.14: Constant gain PID controller with reference tension 20 lbs and 600 feet per minute speed.

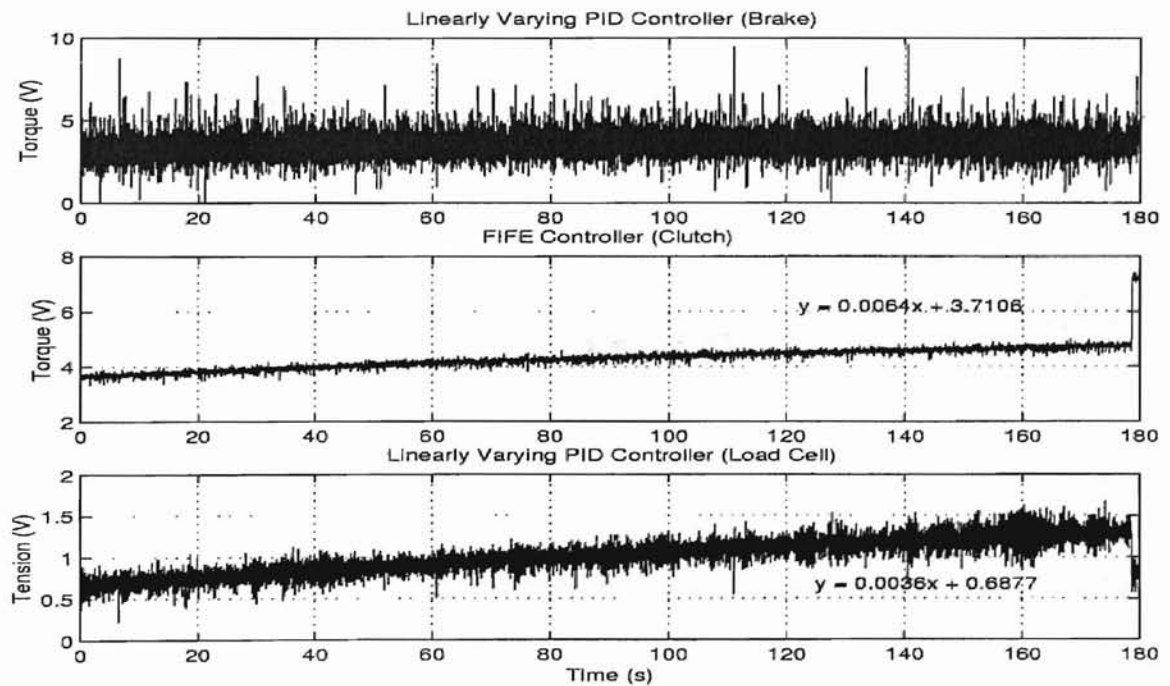


Figure 5.15: Linearly varying PID controller with reference tension 20 lbs and 600 feet per minute speed. The variation of the gains are experimentally determined.

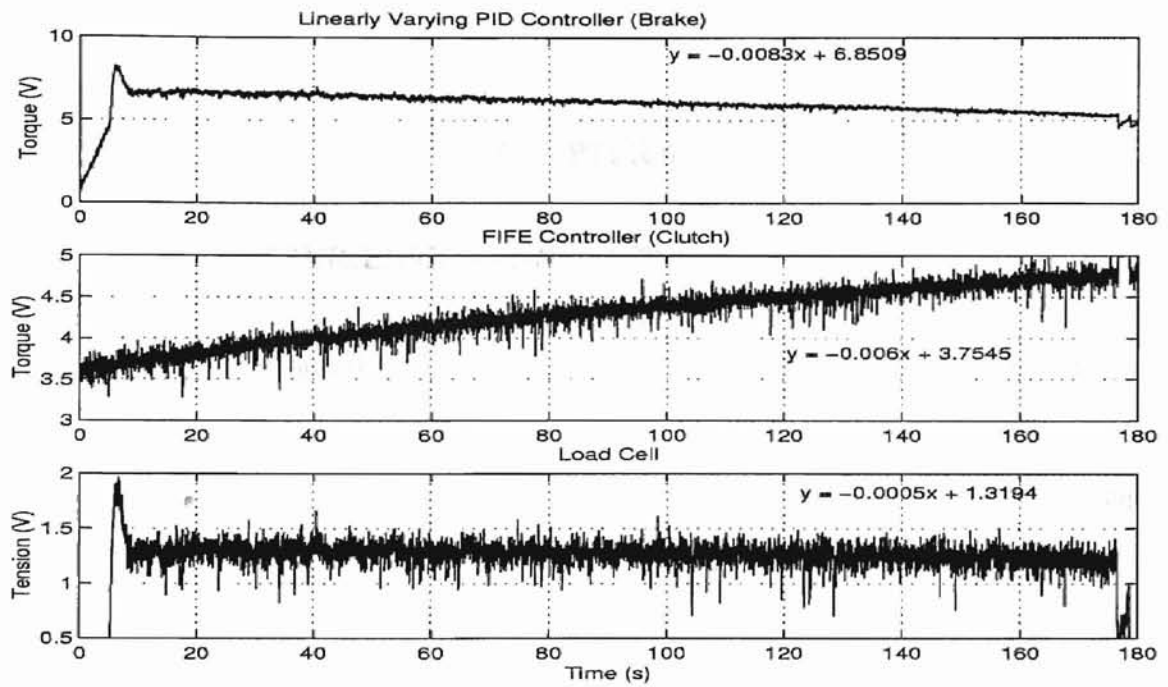


Figure 5.16: Linearly varying PID controller.

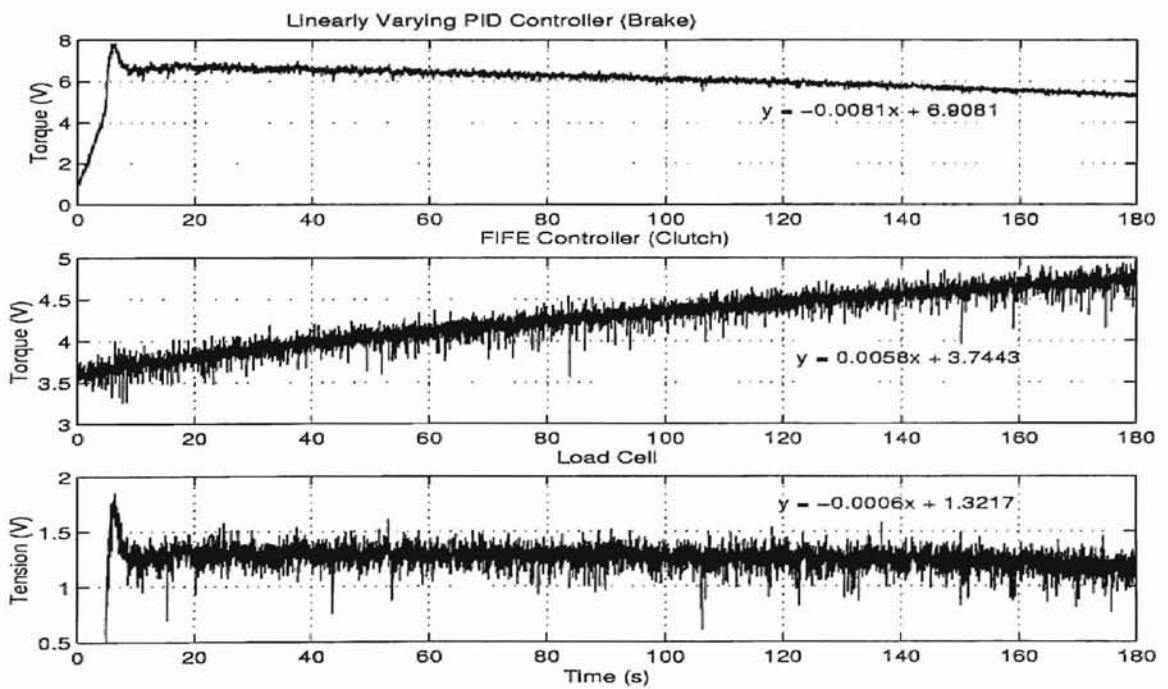


Figure 5.17: Linearly varying PID controller

CHAPTER 6

CONCLUSIONS AND FUTURE RESEARCH

Experimental results show that good downstream tension disturbance attenuation is achieved using the Proportional-Integral Controller, Internal Model Controller, and the Self-tuning Controller using feedback signals. The percentage of tension disturbance attenuation ranges from 30–60%. This type of controller is very easy to implement and can be applied to control tension at all speeds. This controller can be implemented in the least amount of time and yet is seen to give a minimum 30% of tension disturbance rejection.

The IMC is seen to perform better than the other two controllers considered. However, the IMC requires knowledge of the frequency of the tension disturbance that is to be attenuated. At very high speeds, estimating the frequency of the disturbance becomes very difficult. At high speeds, there could be more frequencies in the disturbance than what is estimated. This fact, then, makes implementation of IMC difficult.

Finding the gains for internal model based and PI controller is a laborious task. To alleviate this problem, a direct self-tuning controller was designed for the active dancer. In the direct self-tuning approach, the controller gains are tuned to make the system behave as closely as possible to a reference model. Though, the STC yields slightly poorer performance in rejecting the tension disturbance, it does not require the tuning process, which makes this controller an ideal technique in many cases where the process is continuously changing. Referring to Table. 5.3, the self-tuning controller did not perform as well as the two other controllers. This could be attributable to the fact that the development of the self-tuning controller is based on the assumption that the system dynamics is linear as given by one of the assumptions in [31]. Also, it may be noted from Table 5.3 that all

three controllers exhibited superior performance at a speed of 300 feet per minute which corresponds to a disturbance frequency of around 5.5 Hz.

Throughout all three sets of experiments with the active dancer, the PI and IMC controllers' performance were better than the STC in most instances. This could be attributable to the fact that the development of the self-tuning controller is based on the assumption that the system dynamics is linear as given by one of the assumptions in [31].

In an unwind and rewind process, the mass and inertia of the unwind and rewind rolls are changing. Controllers implemented on these systems must be able to compensate for these changes. Controllers with constant gains are not able to compensate for the changes and the system becomes unstable. The development of a PID controller whose gains decrease linearly was able to maintain the tension in the web by compensating for the changes in the unwind roll. There was an overshoot initially and the settling time was 10 seconds. This may be the result of the startup process and increasing desired speed to which the controller gains were design for. Once the desired speed has been reached, the controller signal gradually decreased to compensate for the decrease in the unwind roll mass and inertia to maintain the desired web tension.

Taking the idea from [26] whose study on a preview control for an active suspension improve the ride comfort for automobiles, the upstream load cell signal was used as the feedback element for the controllers implemented on the hydraulic active dancer. The tension signal from the load cell upstream of the dancer was used. Experimental results show that the upstream load cell signal acting as the feedback signal is able to attenuate the tension disturbance. The percentage of tension disturbance attenuation ranges from 21–48%.

In a previous study [27], the experiments were conducted on an endless web line. The prospect of back propagations may have skewed the results. The current mathematical model does not reflect the tension from downstream spans. With a web line that has a rewind and unwind roll, data was collected with the load cell upstream of the eccentric

roller to determine the presence of disturbance back propagation. With the uneven roller located between the active dancer and the upstream load cell, experimental results show that there is back propagation of tension disturbances in a web line. Initially, the data in appendix D.3 shows the active dancer turned off displaying the effect of the disturbances. Then the dancer is turned on. The change in the tension profile indicates the presence of back propagation.

6.1 Future Research

In this report, experimental investigation were performed on a web line with unwind/rewind. This experimental platform reflects more characteristics of an actual industrial web process. Future investigation should be done on a platform that incorporates more processes such as printing and coating on the web line. The results from such a platform would be more relevant to industrial application.

The linearly varying PID controller was applied to compensate for the mass and inertia change of the unwind roll. Future research should focus on developing the self-tuning controller for the unwind roll. The expectation would be for the self-tuning controller to identify the changing of the unwind roll mass and inertia and adjust the controller gains accordingly. Future investigation also should involve employing the controller to reject periodic disturbances as well as using the active dancer and the unwind roll together to reject tension disturbance.

BIBLIOGRAPHY

- [1] K. I. Hopcus, "Unwind and Rewind Guiding," *Proc. of the Second Intl. Conf. on Web Handling*, June 6-9, 1993.
- [2] Karl N. Reid and Ku-Chin Lin "Control of Longitudinal Tension in Multi-Span Web Transport Systems During Start Up," *Proc. of the Second Intl. Conf. on Web Handling*, June 6-9, 1993.
- [3] Charles B. Richardson "Advanced Winding Machine Development at Sandia National Laboratories," *Proc. of the Second Intl. Conf. on Web Handling*, June 6-9, 1993.
- [4] L.G. Eriksson, P. Hellentin and P. Johnson "Changes in Web Tension Profiles and Paper Properties During Repeated Rewinding," *Proc. of the Second Intl. Conf. on Web Handling*, June 6-9, 1993.
- [5] H. Linna, P. Moilanen and J. Koskimies "Web Tension Measurements In The Paper Mill," *Proc. of the First Intl. Conf. on Web Handling*, May 19-22, 1991.
- [6] K.N. Reid and K.H. Shin "Variable-Gain Control of Longitudinal Tension in a Web Transportation," *Proc. of the First Intl. Conf. on Web Handling*, May 19-22, 1991.
- [7] P. Lin and M.S. Lan "Effects of PID Gains for Controller with Dancer Mechanism on Web Tension ," *Proc. of the Second Intl. Conf. on Web Handling*, June 6-9, 1993.
- [8] W. Wolfermann and D. Schroder "New Decentralized Control in Processing Machines with Continuous Moving Webs," *Proc. of the Second Intl. Conf. on Web Handling*, June 6-9, 1993.

- [9] K.N. Karl and K.C. Lin "Dynamic Behavior of Dancer Subsystems in Web Transport Systems," *Proc. of the Second Intl. Conf. on Web Handling*, June 6-9, 1993.
- [10] C.A. Piper "A Nonlinear Model to Calculate the Stressed State of a Centered-Wound Roll," *Proc. of the Third Intl. Conf. on Web Handling*, June 18-21, 1995.
- [11] J.E. Olsen "The Effect of High Velocities, Startup, and Shutdown on Winding," *Proc. of the Third Intl. Conf. on Web Handling*, June 18-21, 1995.
- [12] J.P. Ries "Longitudinal Dynamics of a Winding Zone," *Proc. of the Third Intl. Conf. on Web Handling*, June 18-21, 1995.
- [13] B.T. Boulter and Z. Gao "Matrix Interpolation Based Self-Tuning Web Tension Regulation," *Proc. of the Third Intl. Conf. on Web Handling*, June 18-21, 1995.
- [14] H. Linna, P. Moilanen and A. Mahonen, M. Parola "Variation of the Web Tension at the Roll Change in the Printing Press," *Proc. of the Third Intl. Conf. on Web Handling*, June 18-21, 1995.
- [15] K.H. Shin, K.N. Reid and S.O. Kwon "Non-Interacting Tension Control in a Multi-Span Web Transport System," *Proc. of the Third Intl. Conf. on Web Handling*, June 18-21, 1995.
- [16] B.J. Becker "A System Approach to Reducing Winding Defects at Alcoa-Warrick Operations," *Proc. of the Fourth Intl. Conf. on Web Handling*, June 1-4, 1997.
- [17] L. Ericksson "Disturbances During Reel Change in Paper Machines," *Proc. of the Fourth Intl. Conf. on Web Handling*, June 1-4, 1997.
- [18] B. Walton and B.S. Rice "Web Longitudinal Dynamics," *Proc. of the Fourth Intl. Conf. on Web Handling*, June 1-4, 1997.
- [19] J.J. Shelton "Limitations to Sensing of Web Tension by Means of Roller Reaction Forces," *Proc. of the Fifth Intl. Conf. on Web Handling*, June 6-9, 1999.

- [20] M.R. Leonard "Tension Control With and Without Tension Sensors," *Proc. of the Fifth Intl. Conf. on Web Handling*, June 6-9, 1999.
- [21] J.P. Ries "Theoretical Comparison of Winding Tension Control Methods," *Proc. of the Fifth Intl. Conf. on Web Handling*, June 6-9, 1999.
- [22] B.C. McDow and C.D. Rahn "Adaptive Web-Tension Control Using a Dancer Arm," *Tappi Journal*, Vol. 81: No 10. page 197-205 October 1998
- [23] D. Hrovat "Applications of Optimal Control to Advanced Automotive Suspension Design," *Transaction of the ASME*, Vol. 115. page 328-342 June 1993
- [24] A. Hac, I. Youn and H.H. Chen "Control of Suspensions for Vehicles with Flexible Bodies - Part I: Active Suspensions," *Transaction of the ASME*, Vol. 118. page 508-517 September 1996
- [25] A. Hac, I. Youn and H.H. Chen "Control of Suspensions for Vehicles with Flexible Bodies - Part II: Semi-Active Suspensions," *Transaction of the ASME*, Vol. 118. page 588-525 September 1996
- [26] M. Tomizuka "Optimum Linear Preview Control with Application to Vehicle Suspension," *Transaction of the ASME Journal of Dynamics Systems, Measurements, and Control*, page 309-315 September 1976
- [27] Lokukaluge P. Perera "The Role of Active Dancers in Tension Control of Webs," *Thesis*, July 2001
- [28] D.P. Campbell, *Dynamic Behavior of the Production Process, Process Dynamics*. New York, John Wiley and Sone, Inc., 1st Edition, 1958.
- [29] G. Brandenburg, "New Mathematical Models for Web Tension and Register Error," *International IFAC Conference on Instrumentation and Automation in the Paper, Rubber, and Plastics Industry, 3rd Proc.*, Vol. 1, page. 411-438, 1977.

- [30] D. King, "The Mathematical Model of a Newspaper Press," page 3-7, December 1969.
- [31] Karl Johan Astrom, Bjorn Wittenmark, "*Adaptive Control*" 2nd Edition, 1995
- [32] P.R. Pagilla, R.V. Dwivedula, and L.P. Perera "Periodic Tension Disturbance Attenuation in Web Process Lines Using Active Dancers," submitted to *Transaction of the ASME Journal of Dynamics Systems, Measurements, and Control*

APPENDIX A

ACTIVE DANCER MODELS AND ANALYSIS

The derivation of the state-space and input/output models are based on the linearized equations given in Chapter 2.

A.1 State Space Model

Because the translational displacement is present in the equations, another state variable would have to be define. The problem is solved by changing the coordinates given in the variables $q_1 = V_0 - \gamma_1 x$ and $q_5 = V_2 + (\gamma_2 - \gamma_1) x$. The state-space model is derived by defining the following state variables.

$$\begin{aligned}
 q_1 &= V_0 - \gamma_1 x & (A.1) \\
 q_2 &= T_1 \\
 q_3 &= V_1 \\
 q_4 &= T_2 \\
 q_5 &= V_2 + (\gamma_2 - \gamma_1) x
 \end{aligned}$$

With the state variables defined above, the state space model becomes.

$$\begin{bmatrix} \dot{q}_1 \\ \dot{q}_2 \\ \dot{q}_3 \\ \dot{q}_4 \\ \dot{q}_5 \end{bmatrix} = \begin{bmatrix} 0 & \alpha & 0 & 0 & 0 \\ -\phi_2 & -\gamma_2 & \phi_2 & 0 & 0 \\ 0 & -\alpha & -\omega & \alpha & 0 \\ 0 & \gamma_3 & -\phi_3 & -\gamma_3 & \phi_3 \\ 0 & 0 & 0 & -\alpha & 0 \end{bmatrix} \begin{bmatrix} q_1 \\ q_2 \\ q_3 \\ q_4 \\ q_5 \end{bmatrix} + \begin{bmatrix} -\gamma_2 \\ \phi_2 \\ 0 \\ \phi_3 \\ (\gamma_3 - \gamma_2) \end{bmatrix} u + \begin{bmatrix} -\alpha & 0 \\ \gamma_2 & 0 \\ 0 & 0 \\ 0 & 0 \\ 0 & \alpha \end{bmatrix} \begin{bmatrix} T_0 \\ T_3 \end{bmatrix}$$

, where $\alpha = \frac{R^2}{J}$, $\gamma_i = \frac{v_r}{L_i}$, $\omega = \frac{B}{J}$, and $\phi_i = \frac{EA}{L_i}$.

The output equations is given as

$$\begin{bmatrix} y_t \end{bmatrix} = \begin{bmatrix} 0 & 0 & 0 & 1 & 0 \end{bmatrix} \begin{bmatrix} q_1 \\ q_2 \\ q_3 \\ q_4 \\ q_5 \end{bmatrix} + \begin{bmatrix} 0 \\ 0 \end{bmatrix} u + \begin{bmatrix} 0 & 1 \end{bmatrix} \begin{bmatrix} T_0 \\ T_2 \end{bmatrix} \quad (\text{A.2})$$

The above equation can be written in compact form as:

$$\dot{Q}(t) = \mathbf{A}Q(t) + \mathbf{B}_u U(t) + \mathbf{B}_w W(t) \quad (\text{A.3})$$

$$y(t) = \mathbf{C}Q(t) + \mathbf{D}_u U(t) + \mathbf{D}_w W(t) \quad (\text{A.4})$$

A.2 Input/Output Model

In the input/output model, the output is the downstream tension (T_2) and the control signal is the velocity of the hydraulic dancer roller (\dot{X}_1), i.e. $U(s) = sX(s)$. The disturbance is the variation in the tension of the upstream span.

$$T_2(s) = \frac{D_{ad}(s)}{C_{ad}(s)} U(s) + \frac{A_{ad}(s)}{C_{ad}(s)} T_0(s) + \frac{B_{ad}(s)}{C_{ad}(s)} T_3(s) \quad (\text{A.5})$$

$$A_{ad}(s) = (\eta s + 1)^2 \quad (\text{A.6})$$

$$B_{ad}(s) = (\eta s(\tau_1 s + 1) + 2)$$

$$C_{ad}(s) = ((\eta s(\tau_1 s + 1) + 2)(\eta s(\tau_2 s + 1) + 2) - (\eta s + 1))$$

$$D_{ad}(s) = \beta \left((\eta s + 1) \left(s + \frac{1}{\tau_1} \right) + (\eta s(\tau_1 s + 1) + 2) \left(s + \frac{1}{\tau_2} - \frac{1}{\tau_1} \right) \right)$$

where $\eta = Jv_r/EAR^2$, $\tau_1 = \frac{L_1}{v_r}$, and $\tau_2 = \frac{L_2}{v_r}$.

Expansion of the numerator, $D_{ad}(s)$, and the denominator, $C_{ad}(s)$, of the plant transfer function gives

$$C_{ad} = \eta^2 \tau_1 \tau_2 s^4 + \eta^2 (\tau_1 + \tau_2) s^3 + \eta(\eta + 2\tau_1 + 2\tau_2) s^2 + 3\eta s + 3 \quad (\text{A.7})$$

$$D_{ad} = \beta \eta \tau_1 s^3 + \beta \eta \left(1 + \frac{\tau_1}{\tau_2}\right) s^2 + \beta \left(3 + \frac{\eta}{\tau_2}\right) s + \beta \left(\frac{2}{\tau_2} - \frac{1}{\tau_1}\right) \quad (\text{A.8})$$

A.3 Structural Restrictions Based on the Upstream and Downstream Lengths

Proportional control was used to analyze the structural limitation on the experimental platform as given by [27]. The closed-loop characteristic equation with proportional feedback control, i.e., $U(s) = -K_p T_2(s)$, is

$$1 + K_p \frac{D_{ad}(s)}{C_{ad}(s)} = 0, \quad (\text{A.9})$$

where K_p is the proportional gain. The root-locus method was used to investigate the effect of $\tau_1 = \frac{L_1}{v_r}$ and $\tau_2 = \frac{L_2}{v_r}$ on the choice of the proportional gain.

The effects of the upstream and downstream lengths are shown in figures A.1 to A.3.¹ Figure A.1 shows that the control gain could be chosen as large as possible, but the choice of the gains should also move the closed-loop poles away from the imaginary axis. Figure A.2 shows a pair of complex conjugate open-loop poles very close to a pair of complex conjugate zeros. The proximity of the poles to the zeros reduce the flexibility and effectiveness of the control when the span lengths are equalled. Figure A.3 shows a pole in the right-half plane. Thus if the gain exceeds a certain value, the system becomes unstable when the upstream span length is less than the downstream span length.

¹Figures given in [32].

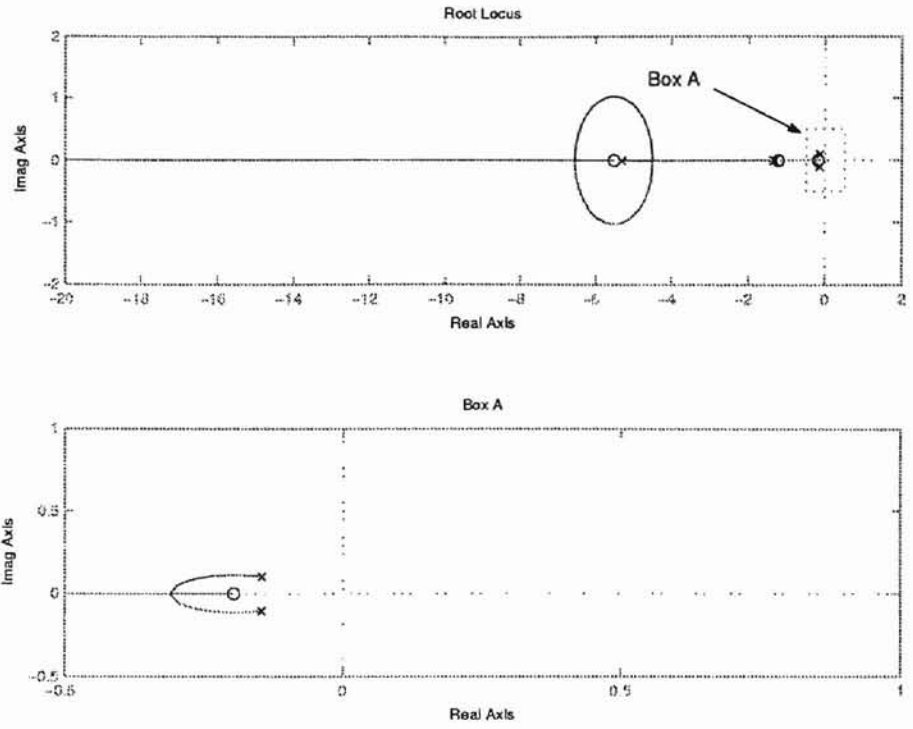


Figure A.1: Root locus plot for $L_1 > L_2$.

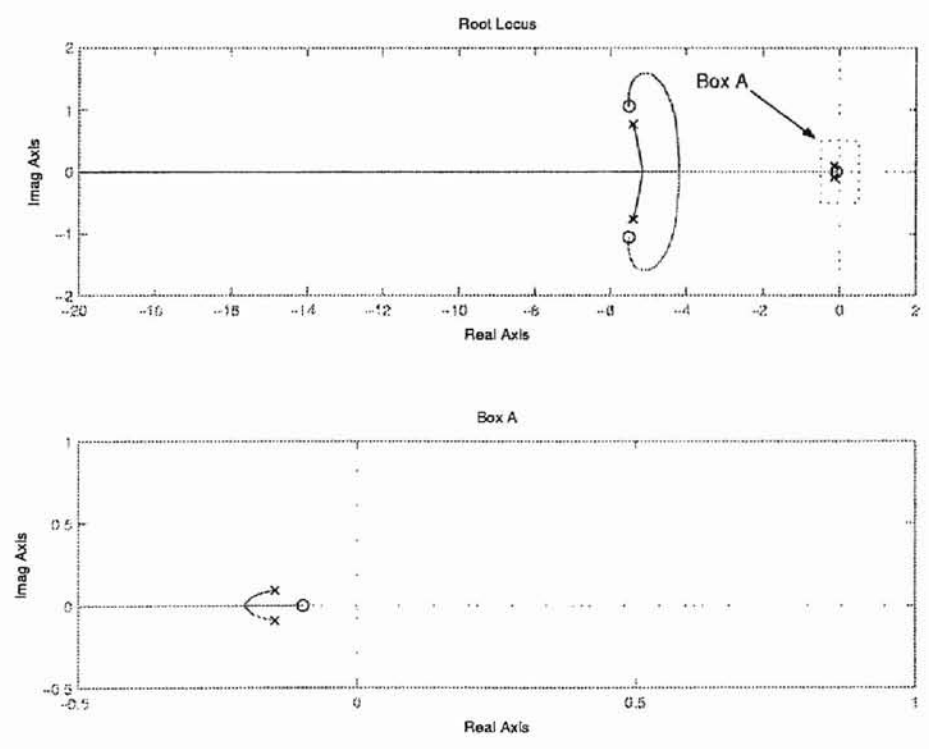


Figure A.2: Root locus plot for $L_1 = L_2$.

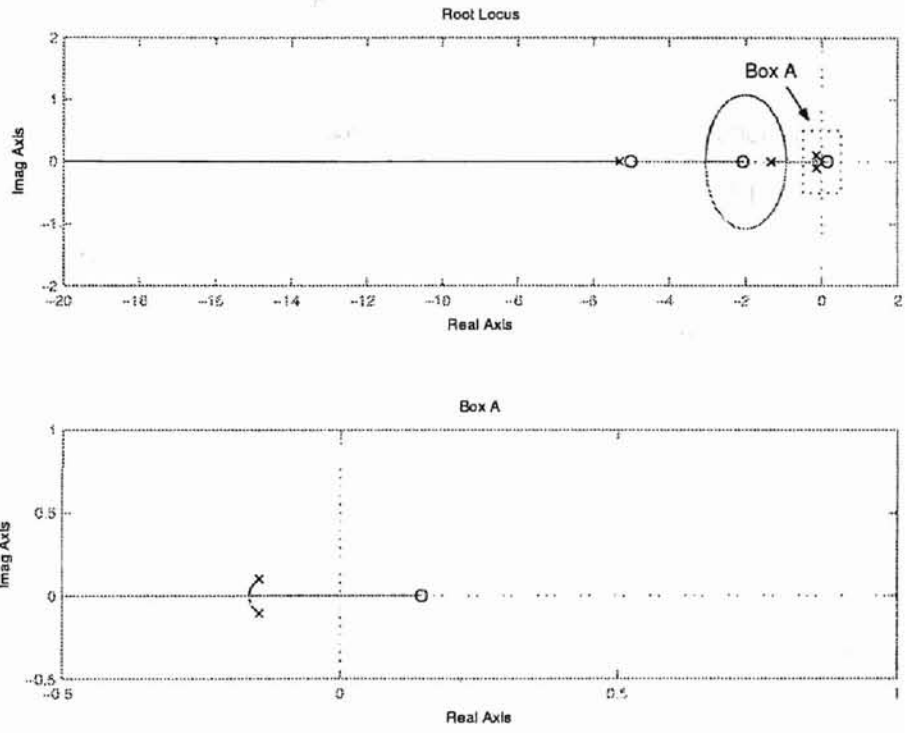


Figure A.3: Root locus plot for $L_1 < L_2/2$.

APPENDIX B

SENSOR CALIBRATION

The signals coming from the sensors are in voltages. The voltages from the load cells are converted to pound force to be used for feedback. The load cell calibrations are done by running the web process and setting the reference tension on the Digitrac and Versatec. Four different 20 seconds samples were taken with different reference tension. These four values were averaged. The upstream and downstream load cell calibrations are shown on figures B.1 and B.2, respectively.

In addition to the load cell calibrations, the speed indicator had to be calibrated as well. On the experimental platform, the speed of the web is changed by turning on a knob on the FIFE controller interface. The knob settings are numbered 1 to 10. The calibration is done by setting the knob to these numbers and then using a tachometer to measure the speed in feet per minute. The numbers given on the speed indicator are approximately equalled to 100 feet per minute. The plots of the relationship between the torque and the input current for the brake and clutch are also shown in figures B.4 and B.3, respectively.

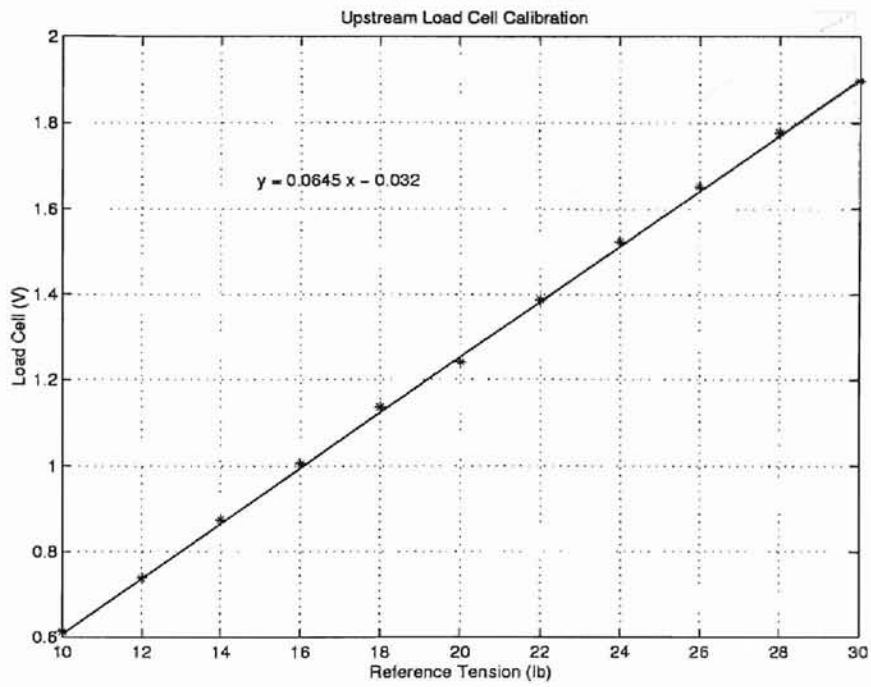


Figure B.1: Upstream load cell(near the brake) calibration.

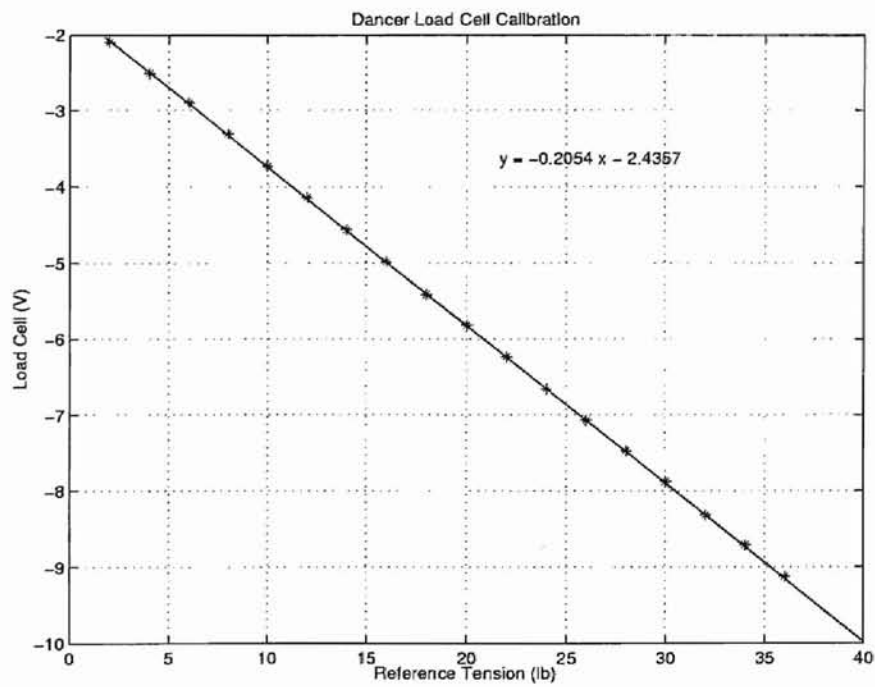


Figure B.2: Downstream load cell(near the dancer) calibration.

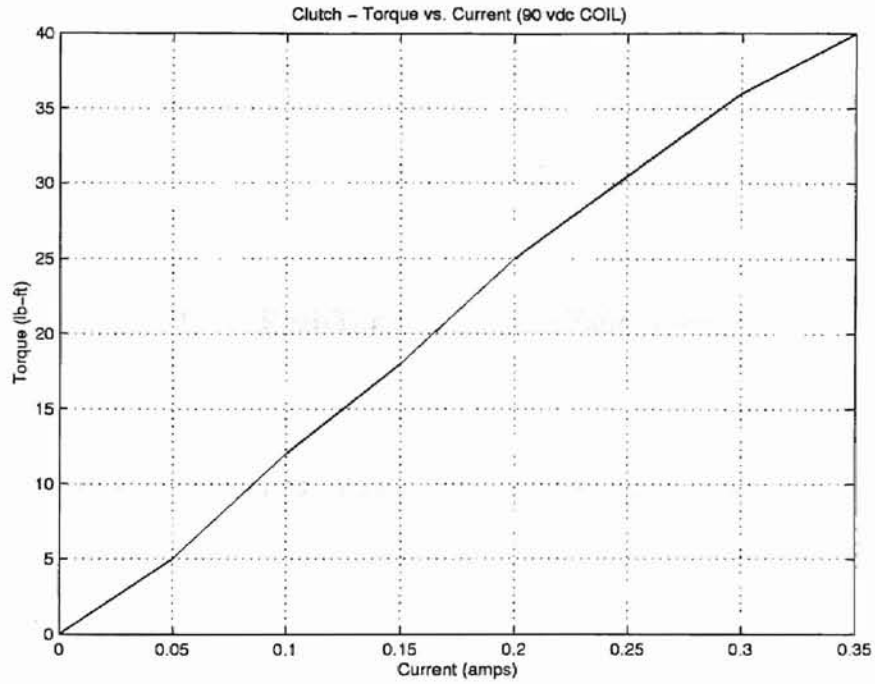


Figure B.3: The torque of the clutch in relationship to the current supplied with rated torque at 26 lb-ft.

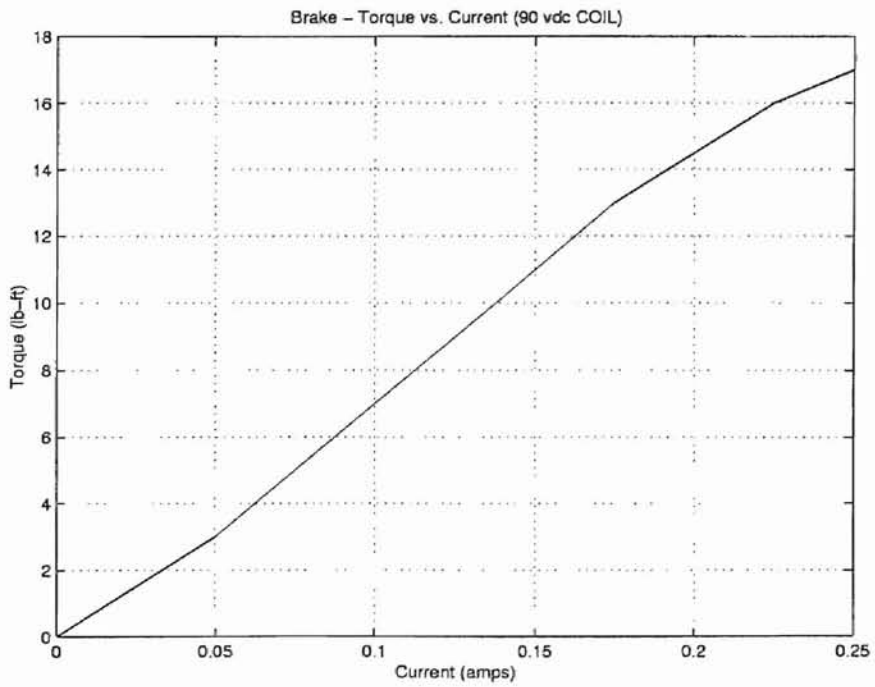


Figure B.4: The torque of the brake in relationship to the current supplied with rated torque at 11 lb-ft.

APPENDIX C

C.1 Real-Time Parameter Estimation

The least-squares method is a basic technique for parameter estimation. This method is particularly simple if the model has the property of being linear in the parameters.

Consider a dynamic system which is modeled by the transfer function relating the output y to the input u

$$\frac{y(z)}{u(z)} = \frac{b_m z^m + b_{m-1} z^{m-1} + \dots + b_1 z + b_0}{z^n + a_{n-1} z^{n-1} + \dots + a_1 z + a_0} = \frac{B(z)}{A(z)} \quad (\text{C.1})$$

Further, assume that the parameters a_i and b_i are constant but unknown. Equation (C.1) can be written in the form

$$y(k) = \begin{pmatrix} -a_{n-1}y(k-1) - \dots - a_0y(k-n) \\ + b_mu(k-d_0) + \dots + b_0u(k-d_0-m) \end{pmatrix} = \varphi^T(k)\theta \quad (\text{C.2})$$

where

$$\begin{aligned} \varphi^T(k) &= [-y(k-1), \dots, -y(k-n), u(k-d_0), \dots, u(k-d_0-m)] \\ \theta &= [a_{n-1}, \dots, a_0, b_m, \dots, b_0]^T \end{aligned} \quad (\text{C.3})$$

$d_0 = n - m$ is the relative degree of the transfer function. To implement the least squares parameter estimation algorithm, pairs of observations and regressors $(y(k), \varphi(k))$ are obtained from an experiment for $k = 1, 2, \dots, t$. The problem now is to determine the parameter θ , in such a way that the outputs computed from the model in equation (C.2) agree as closely as possible with the measured variables $y(k)$ in the sense of least squares.

The parameter θ should be chosen to minimize the least-square function

$$V(\theta, t) = \frac{1}{2} \sum_{k=1}^t (y(k) - \varphi^T(k)\theta)^2$$

The function $V(\theta, t)$ is shown in [31] to be minimum for parameters $\hat{\theta}$ such that

$$\Phi^T(t)\Phi(t)\hat{\theta} = \Phi^T(t)Y(t) \quad (C.4)$$

where

$$Y(t) = [y(1), y(2), \dots, y(t)]^T$$

$$\Phi^T(t) = [\varphi^T(1), \dots, \varphi^T(t)]$$

If the matrix $P^{-1} = \Phi^T(t)\Phi(t)$ in equation (C.4) is nonsingular, $\hat{\theta}$ can be uniquely determined.

$$\hat{\theta} = (\Phi^T(t)\Phi(t))^{-1}\Phi^T(t)Y = \left(\sum_{i=1}^t \varphi(i)\varphi^T(i) \right)^{-1} \left(\sum_{i=1}^t \varphi(i)y(i) \right). \quad (C.5)$$

The observations are obtained from the experiment in real time. Thus, the least-squares estimate can be arranged in such a way that the results obtained at time $(t-1)$ can be used to get the estimates at time t . Many variations of such algorithms are presented in [31]. One such algorithm, *Recursive least squares with exponential forgetting* is presented below:

$$\hat{\theta}(t) = \hat{\theta}(t-1) + K(t) \left(y(t) - \varphi^T(t)\hat{\theta}(t-1) \right)$$

$$K(t) = P(t)\varphi(t) = P(t-1)\varphi(t) \left(\lambda I + \varphi^T(t)P(t-1)\varphi(t) \right)^{-1} \quad (C.6)$$

$$P(t) = (I - K(t)\varphi^T(t)) P(t-1) / \lambda$$

The algorithm given in (C.6) lends itself conveniently in Pole Placement Design.

C.2 Derivation for Linearly Varying PID Controller

The Laplace transform is taken on equations 2.10, 2.14, and 2.15, which become the following equations.

$$J_u s V_u(s) = -R_u U(s)_u + R_u^2 T_1(s) \quad (C.7)$$

$$L_1 s T_1(s) = \frac{v_r}{R_u} U(s)_u + t_r V_u(s) + v_r T_1(s) - t_r V_1(s) + E A V_1(s) - E A V_u(s) \quad (C.8)$$

$$J_1 s V_1(s) = R_1^2 T_2(s) - R_1^2 T_1(s) \quad (C.9)$$

Solving equations C.7 and C.9 for $V_u(s)$ and $V_1(s)$, respectively, and substituting them into equation C.8 results in the following equation.

$$\begin{aligned} L_1 s T_1(s) = & \frac{v_r}{R_u} U(s)_u + t_r \left(-\frac{R_u}{s J_u} U_u + \frac{R_u^2}{s J_u} T_1(s) \right) - v_r T_1(s) \\ & - t_r \left(\frac{R_1^2}{s J_1} T_2(s) - \frac{R_1^2}{s J_1} T_1(s) \right) \\ & + E A \left(\frac{R_1^2}{s J_1} T_2(s) - \frac{R_1^2}{s J_1} T_1(s) \right) - E A \left(-\frac{R_u}{s J_u} U(s)_u + \frac{R_u^2}{s J_u} T_1(s) \right) \end{aligned} \quad (C.10)$$

The transfer function is obtain with the input as the brake torque ($U(s)_u$) and the output as the tension in span one $T_1(s)$.

$$\frac{T_1(s)}{U_u(s)} = \frac{s J_u J_1 (J_u v_r s + C)}{s R_u J_u (L_1 J_1 J_u s^2 + v_r J_1 J_u s + B)} \quad (C.11)$$

where $C = E A R_u^2 - t_r R_u^2$ and $B = E A R_1^2 J_u + E A R R_u^2 J_1 - t_r R_u^2 J_1 - t_r R_1^2 J_u$.

Equation is further simplified into the following

$$\frac{T_1(s)}{U_u(s)} = G_P = \frac{\alpha(s + \beta)}{s^2 + \theta s + \gamma} \quad (C.12)$$

where

$$\begin{aligned} \alpha &= \frac{v_r}{R_u L_1} \\ \beta &= \frac{C}{J_u v_r} \\ \theta &= \frac{v_r}{L_1} \\ \gamma &= \frac{B}{L_1 J_1 J_u} \end{aligned}$$

The PID controller is implemented to the system. The Laplace transform equation of the PID controller is defined as:

$$G_c = \frac{K_i + K_p s + K_d s^2}{s} e \quad (C.13)$$

where $e = t_r - T_1$

The transfer function with respect to a reference is defined as:

$$\frac{T_1(s)}{R(s)} = \frac{G_p G_c}{1 + G_p G_c} \quad (C.14)$$

After substituting the values into equation C.14 and simplifying,

$$\frac{T_1(s)}{R(s)} = \frac{a(s^3 + bs^2 + cs + d)}{s^3 + es^2 + fs + g} \quad (C.15)$$

where

$$\begin{aligned} a &= \frac{\alpha K_d}{1 - \alpha K_d} \\ b &= \frac{K_p + K_d \beta}{K_d} \\ c &= \frac{K_i + K_p \beta}{K_d} \\ d &= \frac{\beta K_i}{K_d} \\ e &= \frac{\theta + K_p \alpha + \alpha K_d \beta}{1 + \alpha K_d} \\ f &= \frac{\gamma + \alpha K_i + \alpha \beta K_p}{1 + \alpha K_d} \\ g &= \frac{\alpha \beta K_i}{1 + \alpha K_d} \end{aligned} \quad (C.16)$$

The characteristic equation in equation C.15 is a third order equation, which has three poles. The desired three poles are designed based on the percentage overshoot and the settling time. To reduce the third order system to a second order system, one pole is chosen to be at least ten times greater than the other two poles. The three roots of the desired characteristic equation are

$$p_{1,2} = -\zeta\omega_n \pm j\omega\sqrt{1 - \zeta^2} \quad (\text{C.17})$$

$$p_3 = -10\omega_n\zeta$$

With the desire roots given in equation C.17, the desire characteristic equation becomes

$$s^3 + xs^2 + ys + z \quad (\text{C.18})$$

where

$$x = 2\zeta\omega_n + 10\zeta\omega_n$$

$$y = 21\zeta^2\omega_n^2 + \omega_n^2(1 - \zeta^2)$$

$$z = 10\zeta\omega_n(\zeta^2\omega_n^2 + \omega_n^2(1 - \zeta^2))$$

The gains for the controllers are obtain by equating the coefficients from equation C.18 and the coefficients from the denominator of equation C.15.

$$K_d = \frac{\gamma - \frac{z}{\beta} + \beta x - y - \theta\beta}{\alpha y + \alpha\beta^2 - \frac{z\alpha}{\beta} - \alpha\beta x} \quad (\text{C.19})$$

$$K_p = \frac{x + x\alpha K_d - \theta - \alpha\beta K_d}{\alpha}$$

$$K_i = \frac{z + z\alpha K_d}{\alpha\beta}$$

APPENDIX D

EXPERIMENTAL DATA

D.1 Tension Attenuation Downstream Load Cell Signal

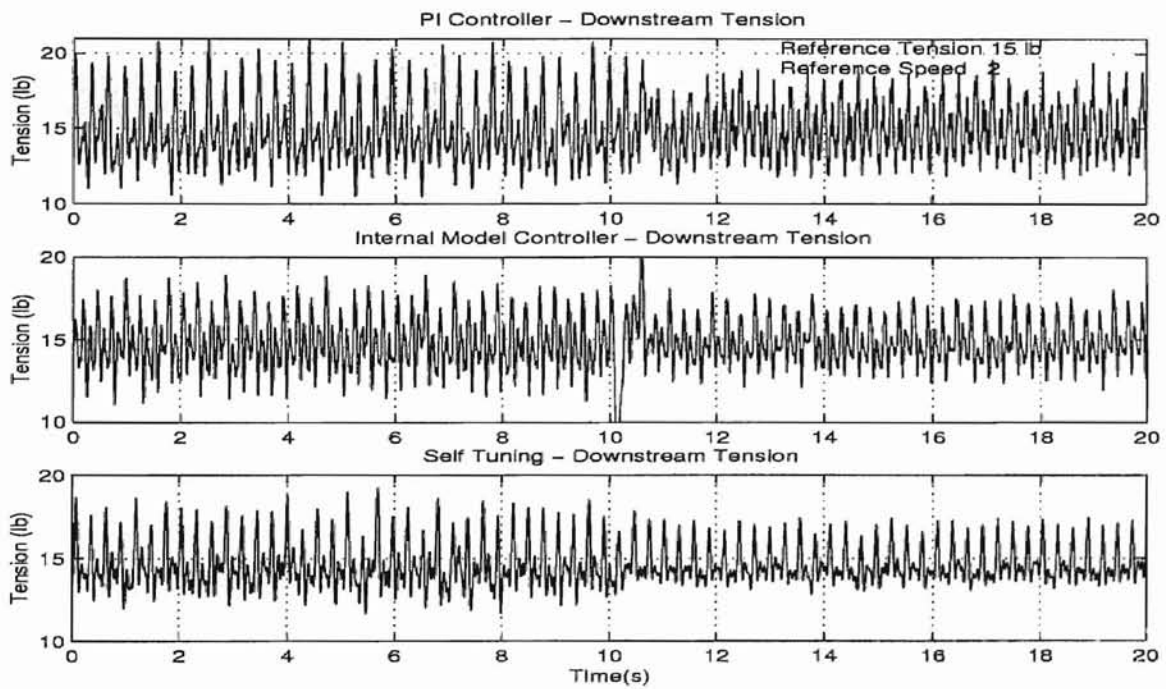


Figure D.1: Tension disturbance attenuation with downstream load cell as feedback.

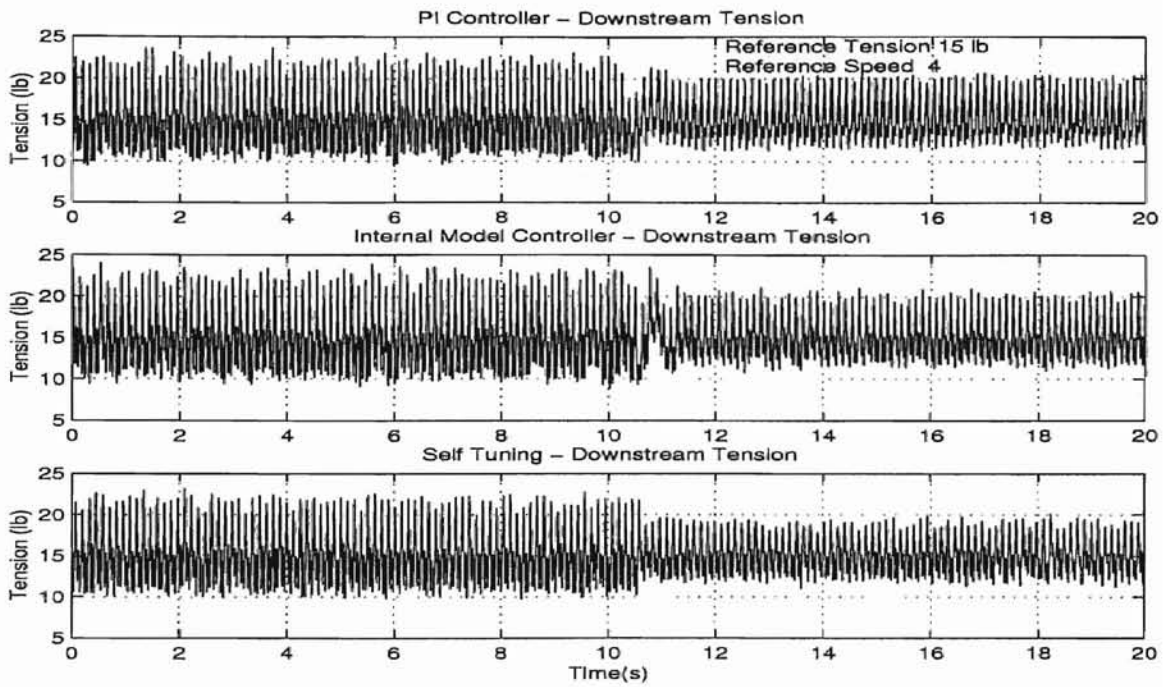


Figure D.2: Tension disturbance attenuation with downstream load cell as feedback.

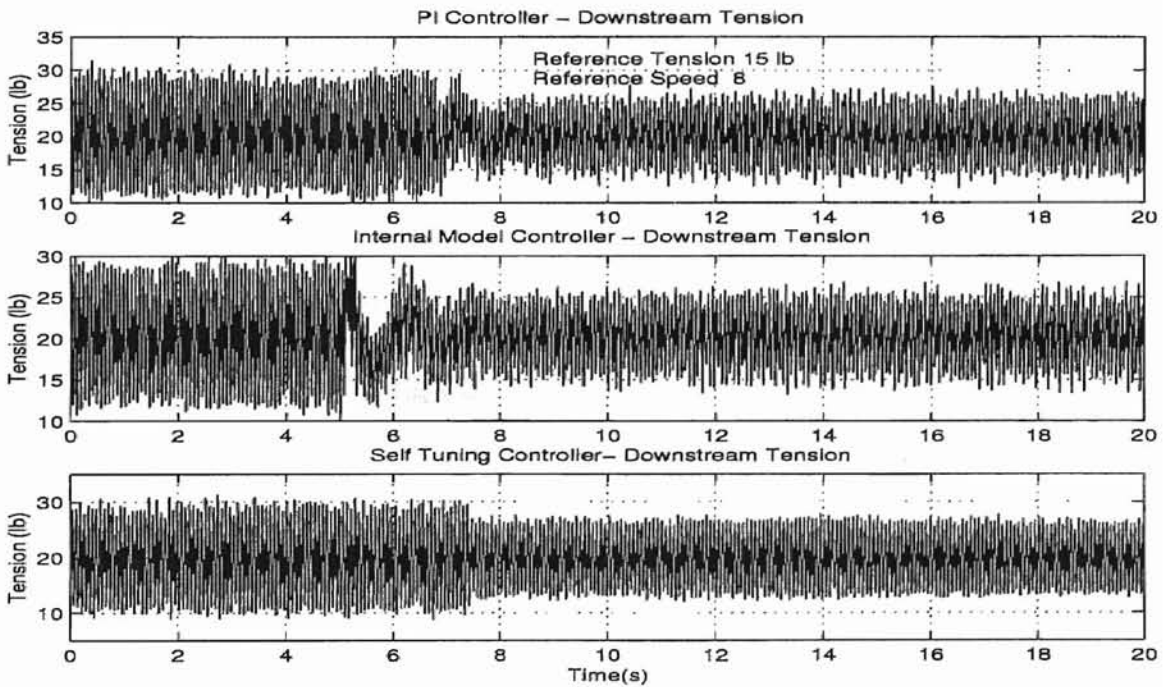


Figure D.3: Tension disturbance attenuation with downstream load cell as feedback.

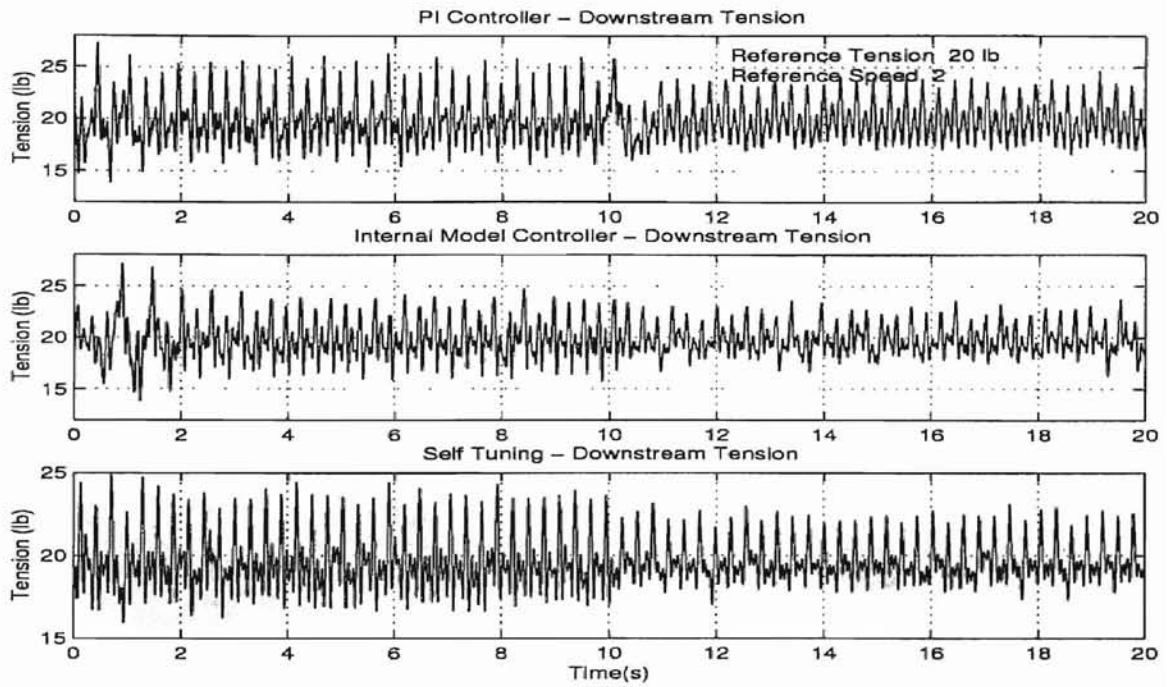


Figure D.4: Tension disturbance attenuation with downstream load cell as feedback.

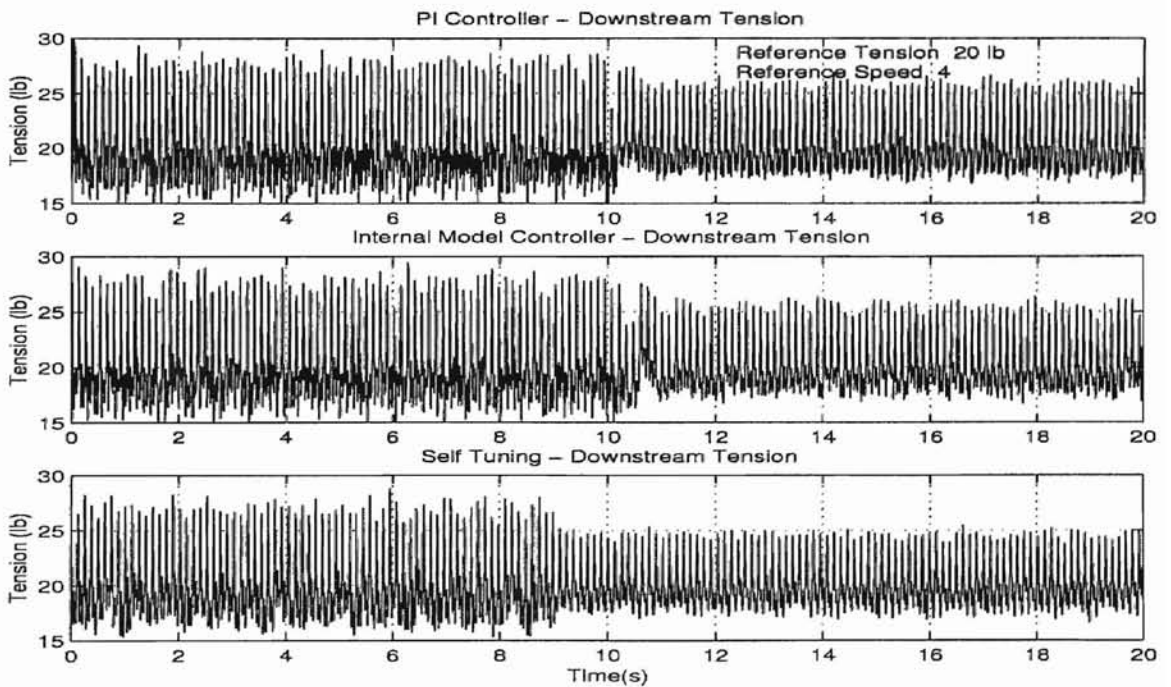


Figure D.5: Tension disturbance attenuation with downstream load cell as feedback.

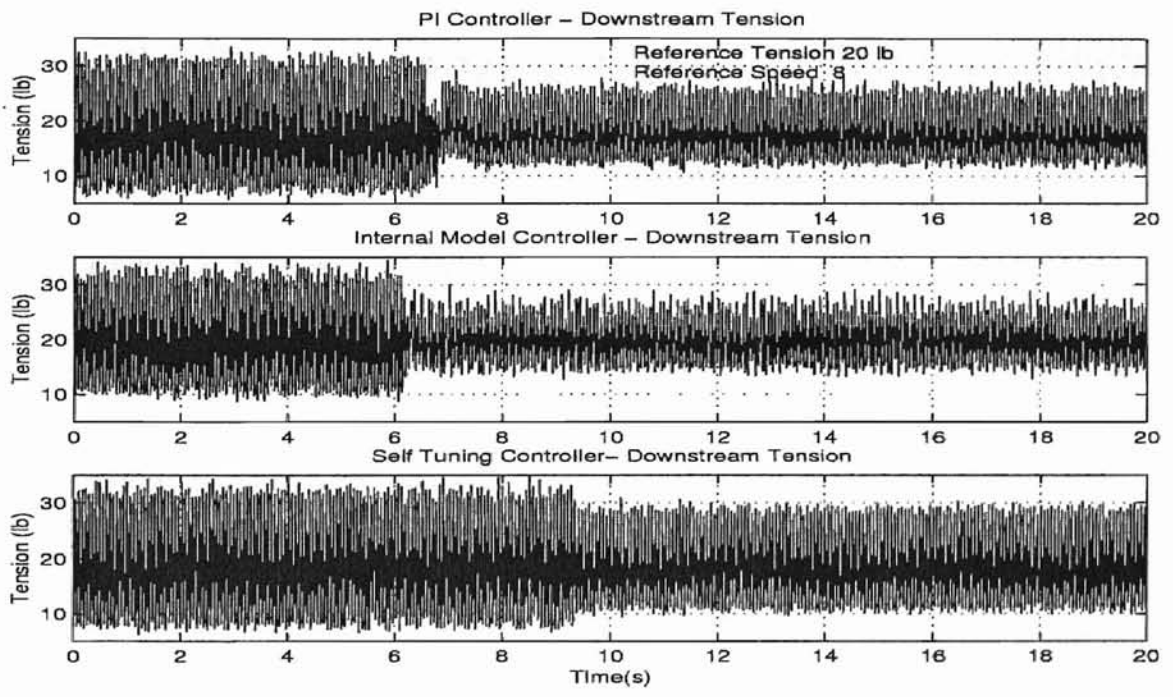


Figure D.6: Tension disturbance attenuation with downstream load cell as feedback.

D.2 Tension Attenuation Using Upstream Load Cell Signal

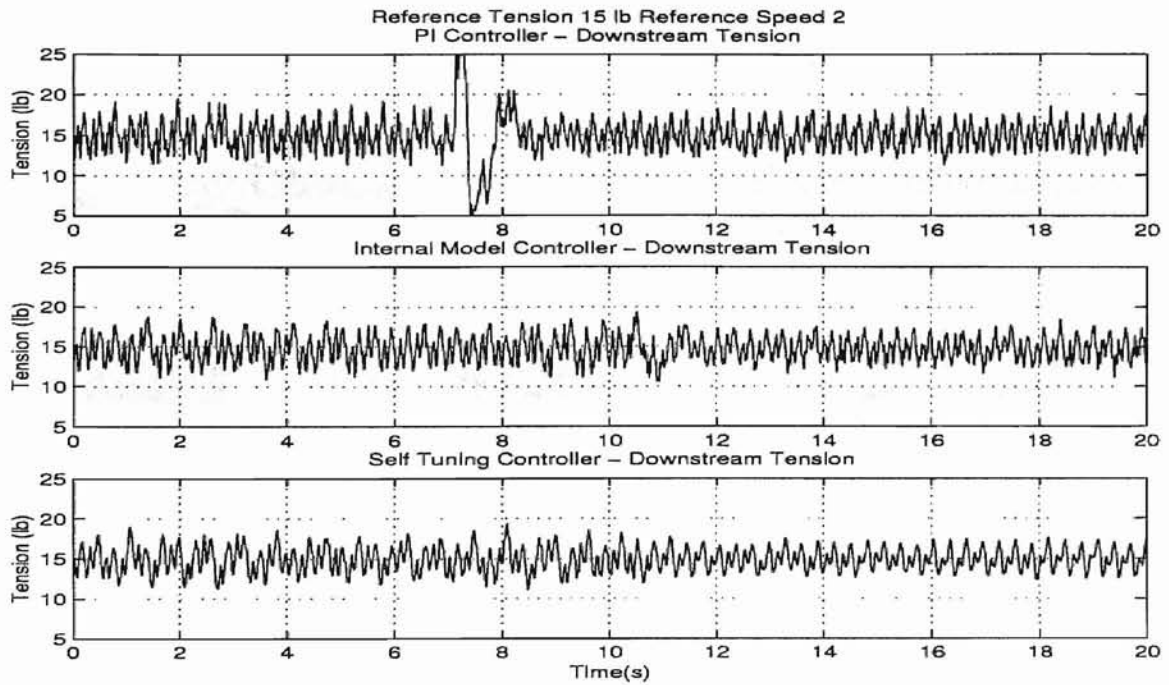


Figure D.7: Tension disturbance attenuation with upstream load cell as feedback.

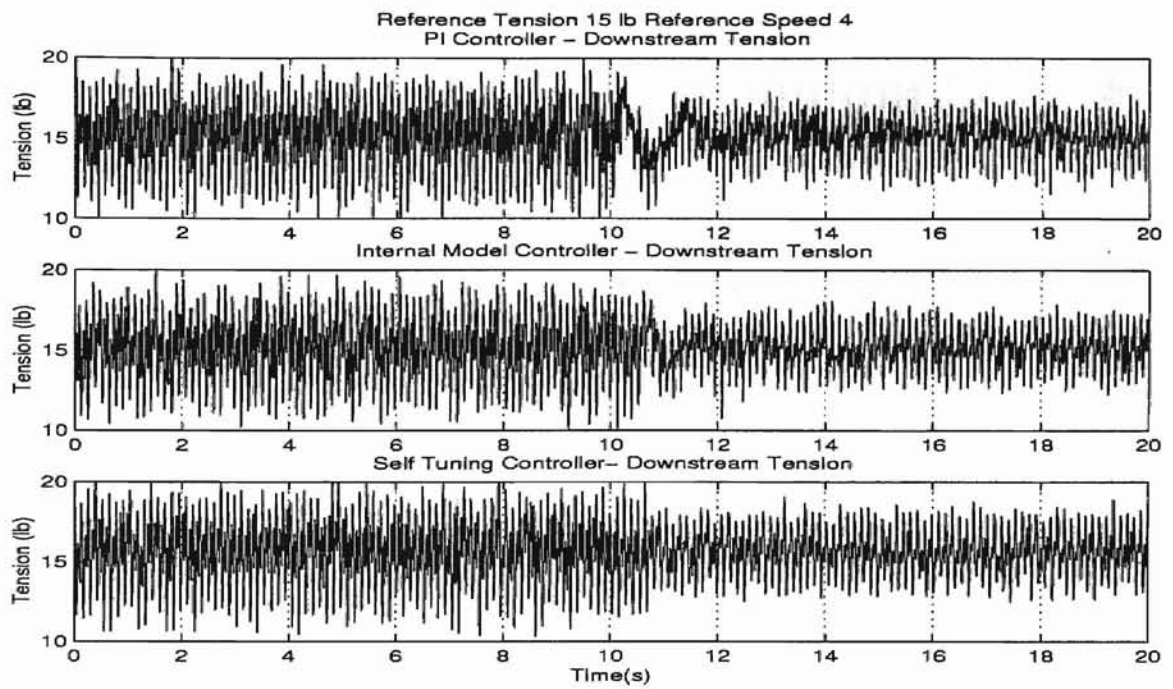


Figure D.8: Tension disturbance attenuation with upstream load cell as feedback.

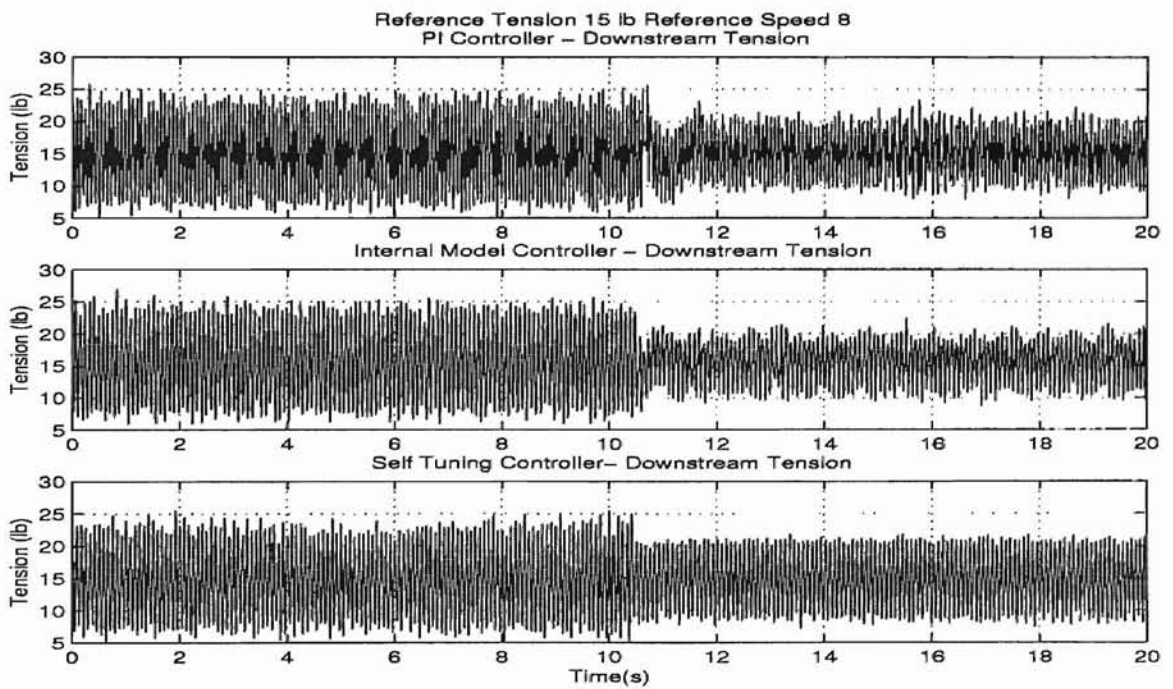


Figure D.9: Tension disturbance attenuation with upstream load cell as feedback.

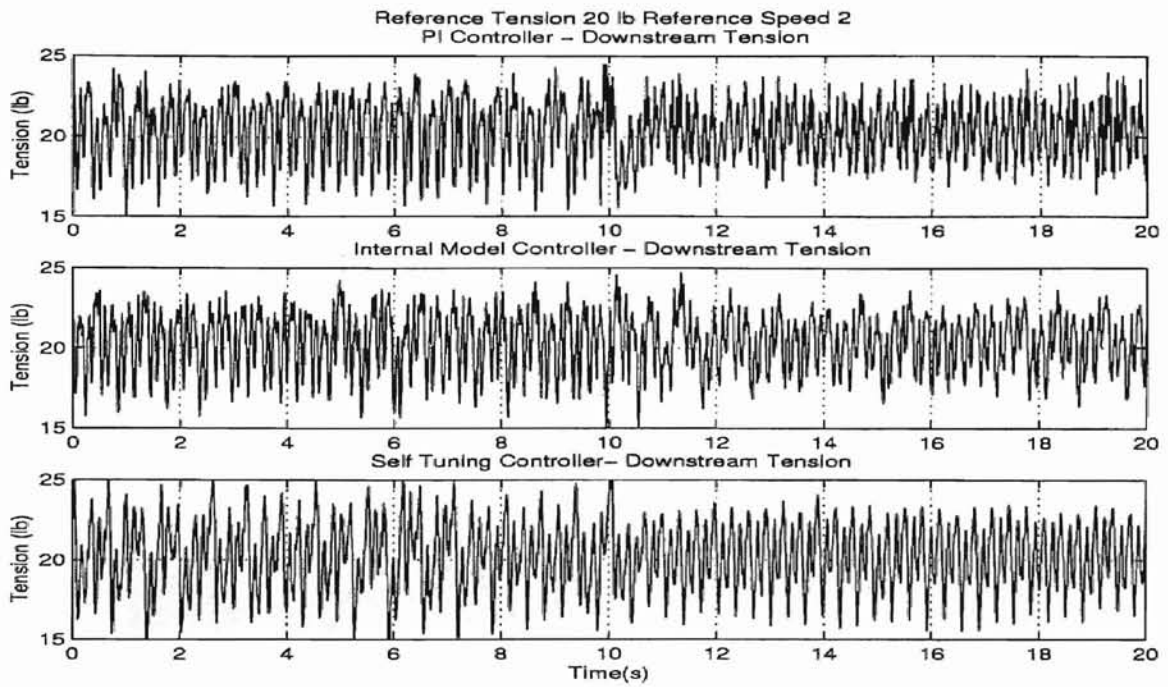


Figure D.10: Tension disturbance attenuation with upstream load cell as feedback.

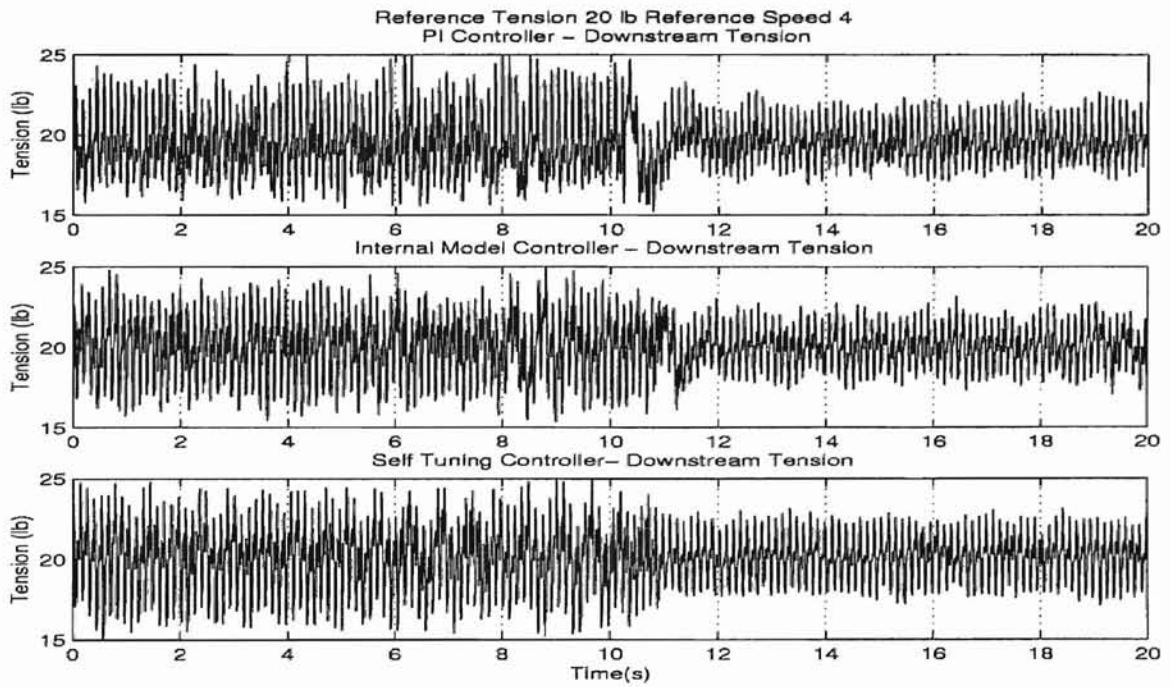


Figure D.11: Tension disturbance attenuation with upstream load cell as feedback.

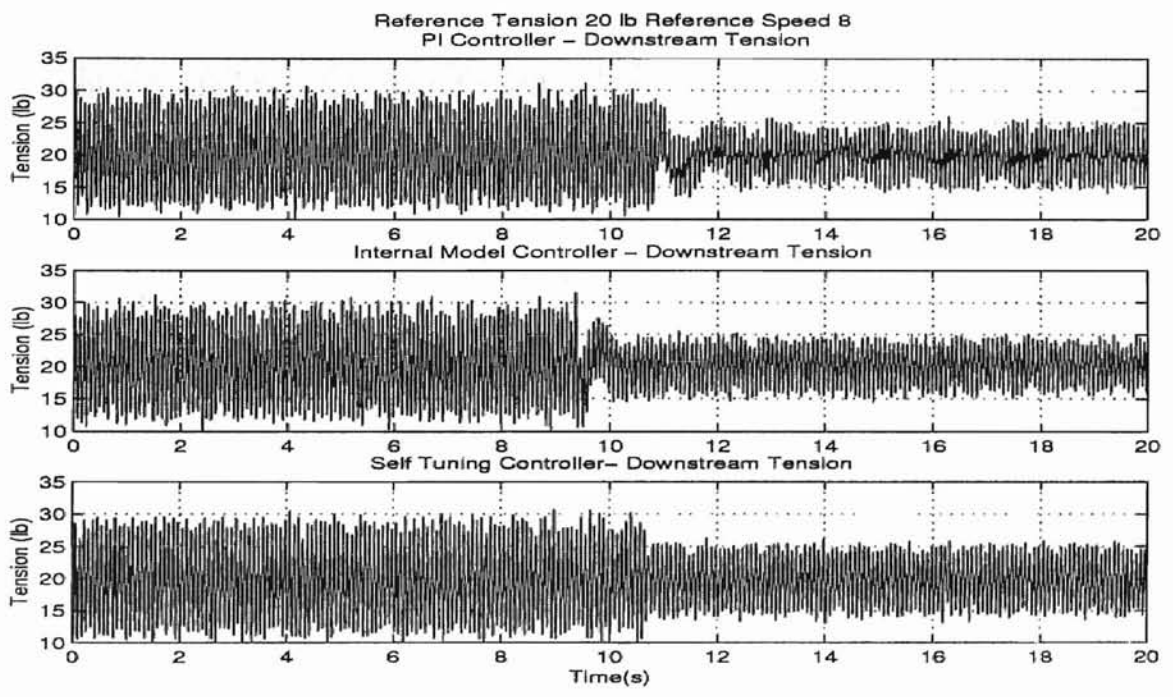


Figure D.12: Tension disturbance attenuation with upstream load cell as feedback.

D.3 Back Propagation

Initially, the graphs show the active dancer turned off displaying the effect of the disturbances. Then the dancer is turned on. The movement of the dancer changes the tension in the web. This change in the tension as detected by the upstream load cell indicates back propagation.

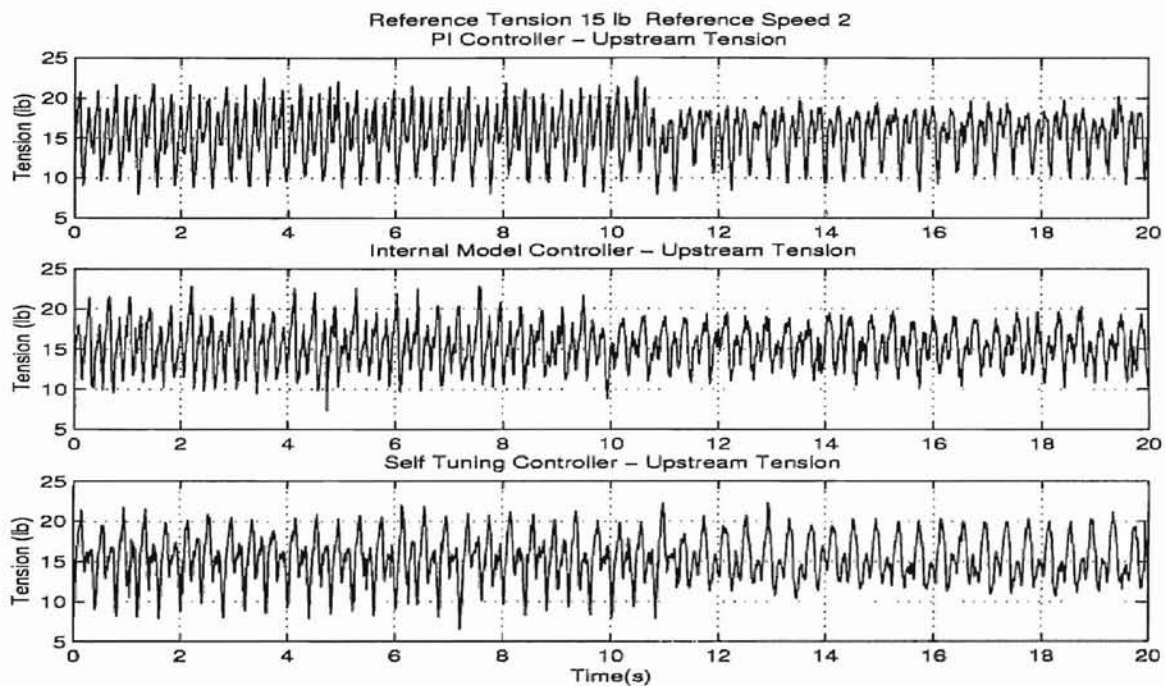


Figure D.13: Back propagation of tension disturbances.

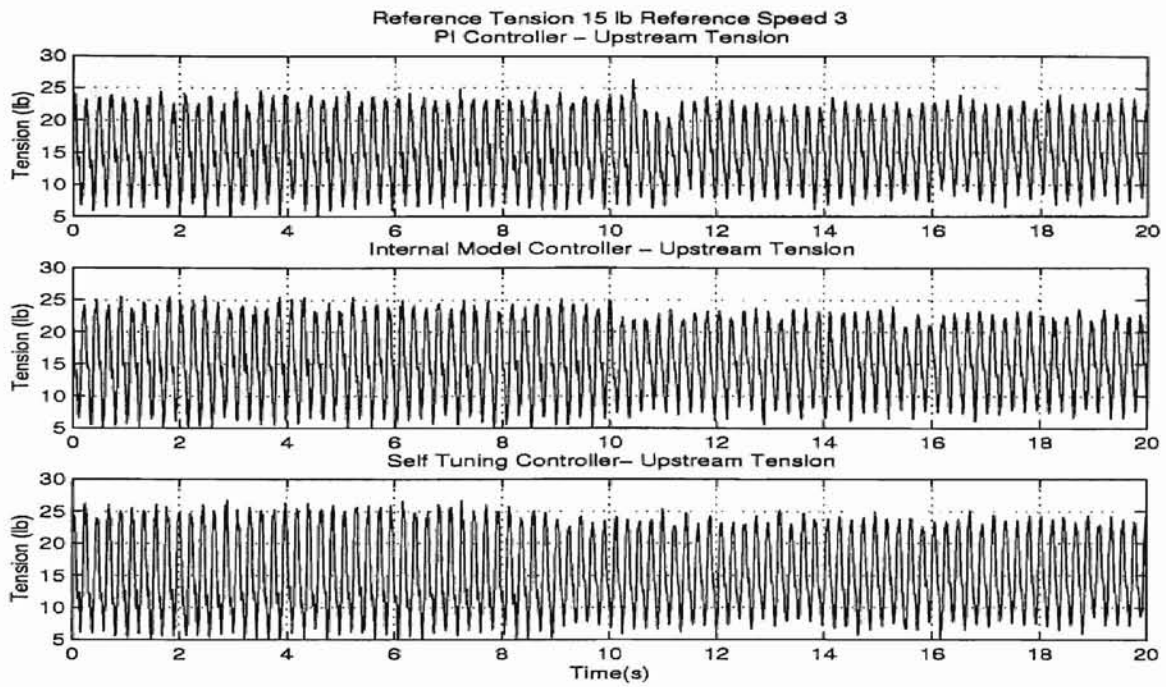


Figure D.14: Back propagation of tension disturbances.

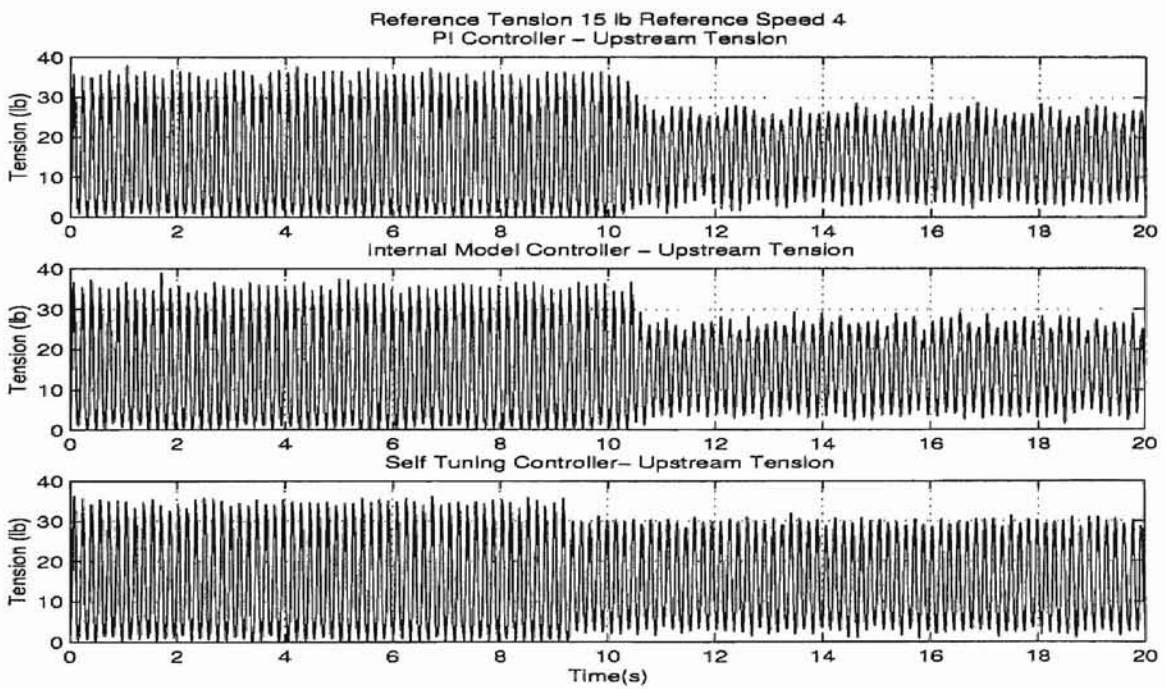


Figure D.15: Back propagation of tension disturbances.

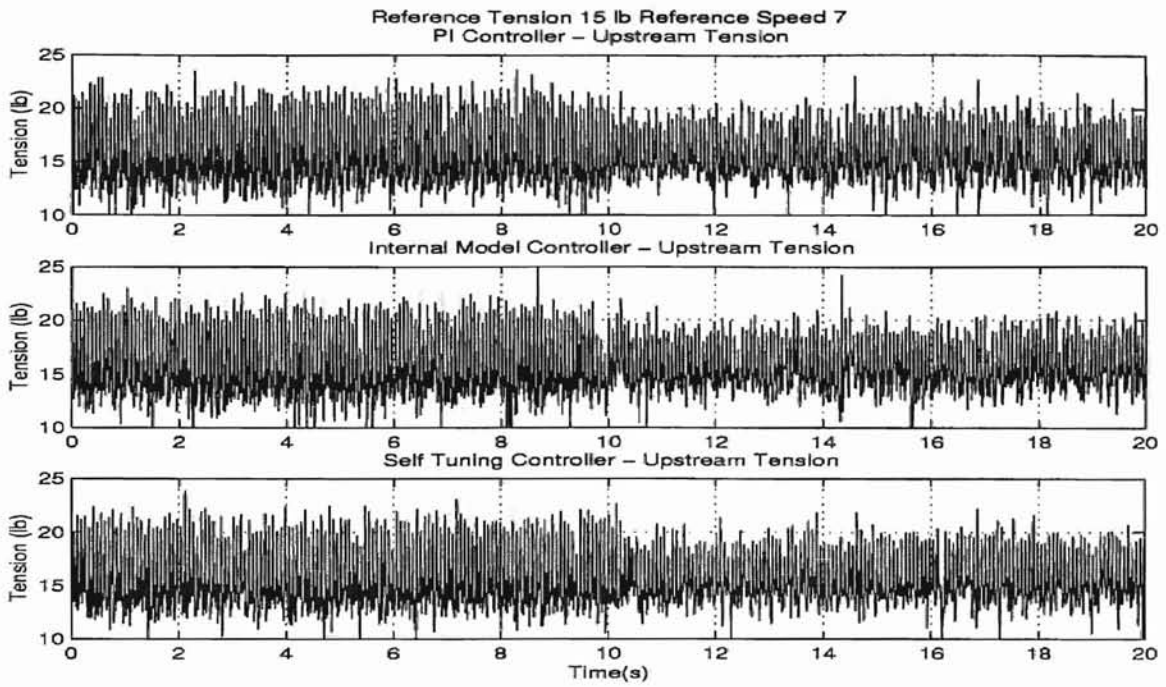


Figure D.16: Back propagation of tension disturbances.

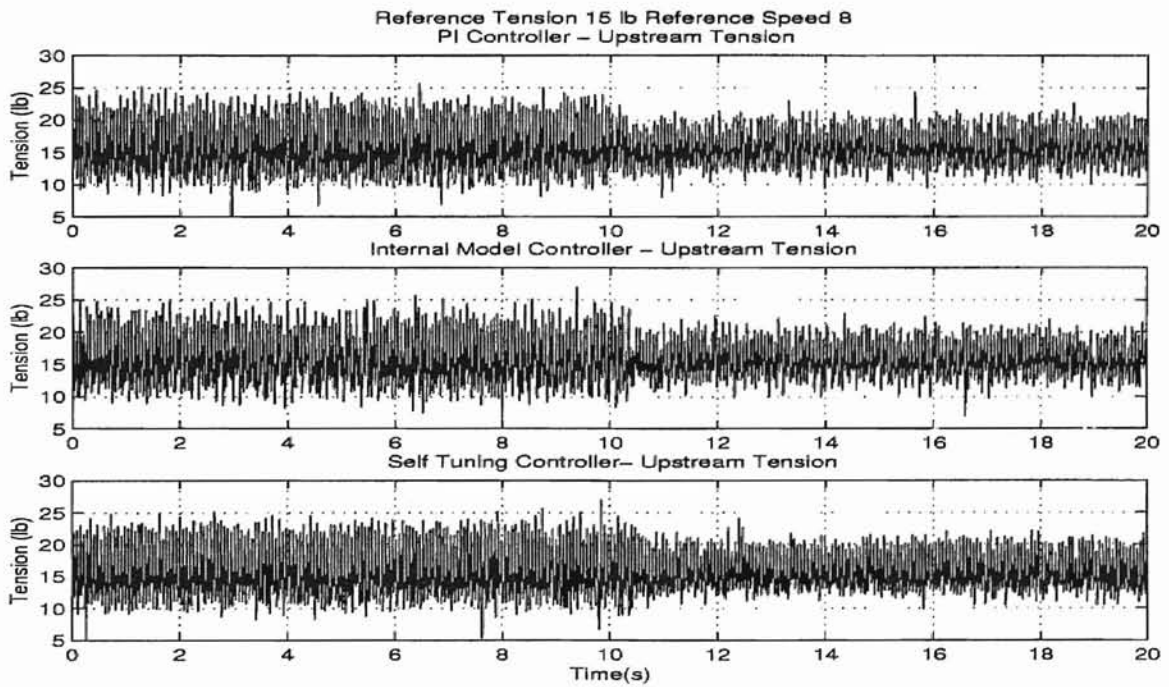


Figure D.17: Back propagation of tension disturbances.

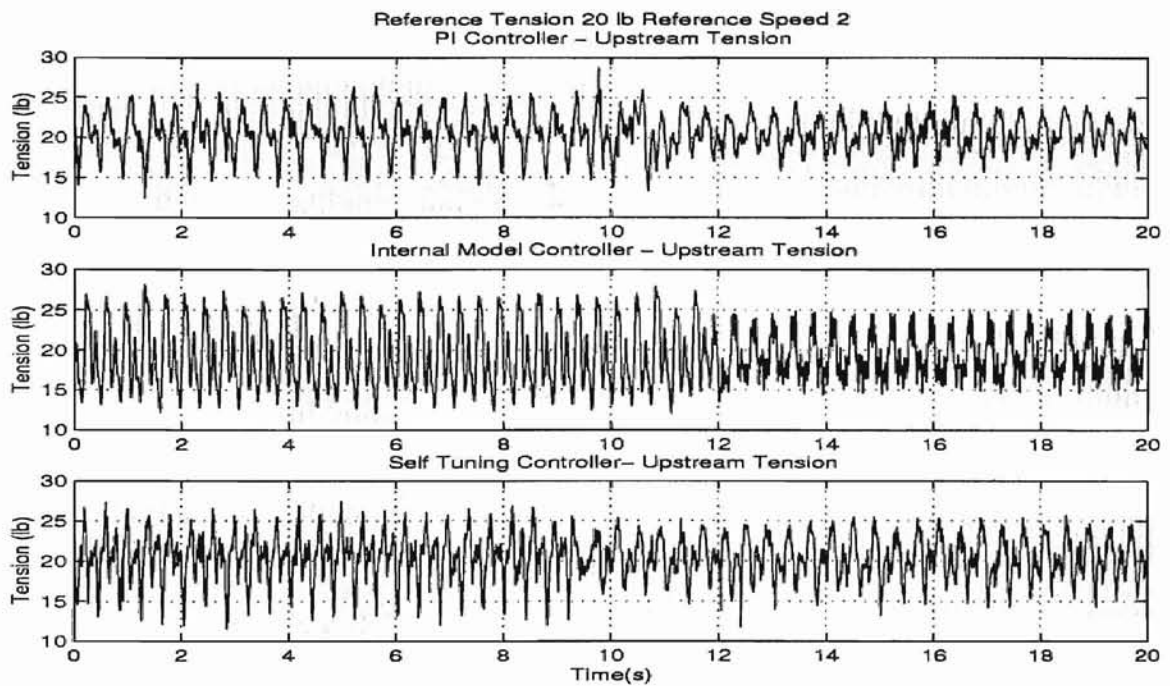


Figure D.18: Back propagation of tension disturbances.

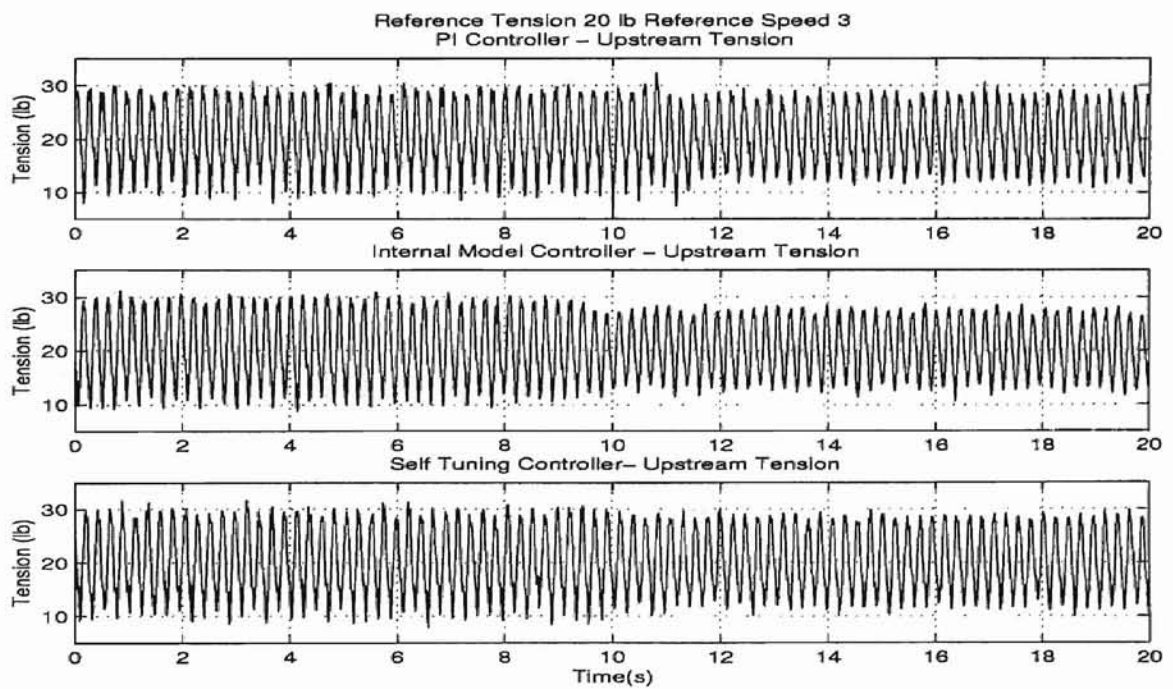


Figure D.19: Back propagation of tension disturbances.

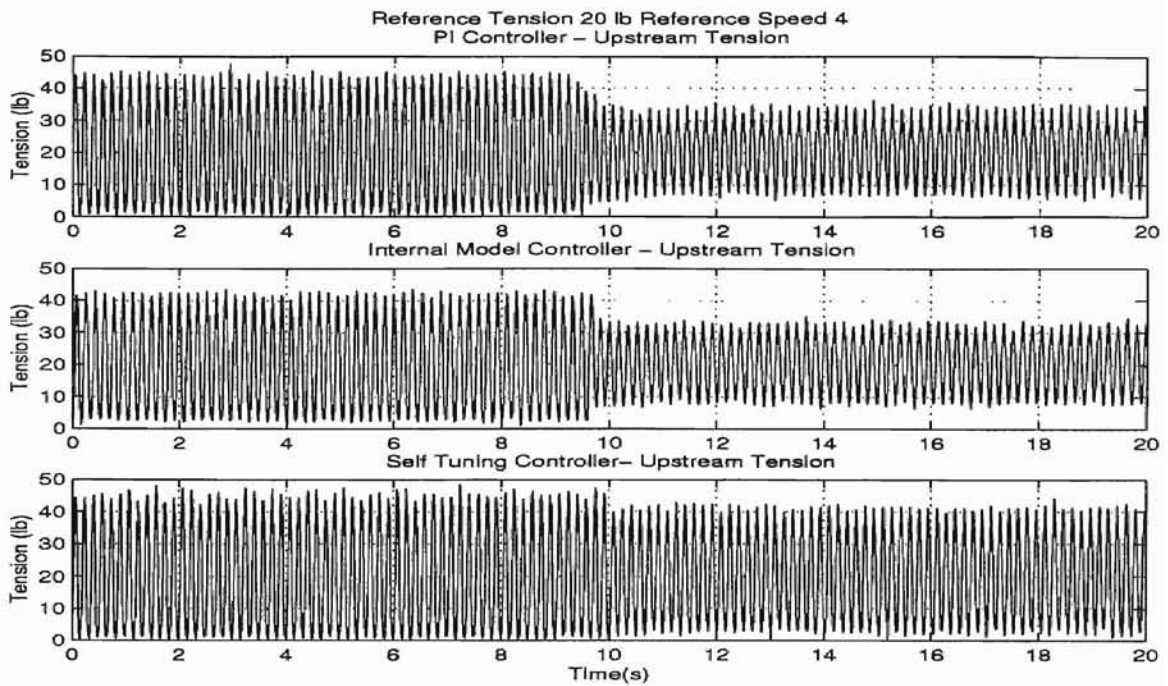


Figure D.20: Back propagation of tension disturbances.

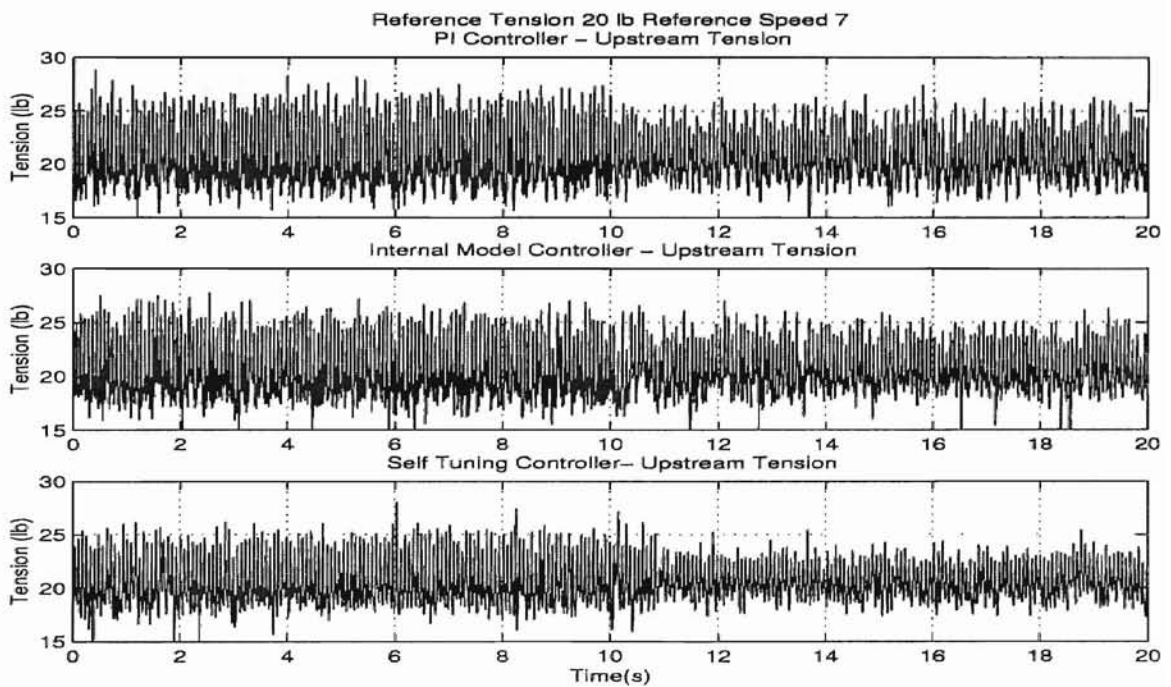


Figure D.21: Back propagation of tension disturbances.

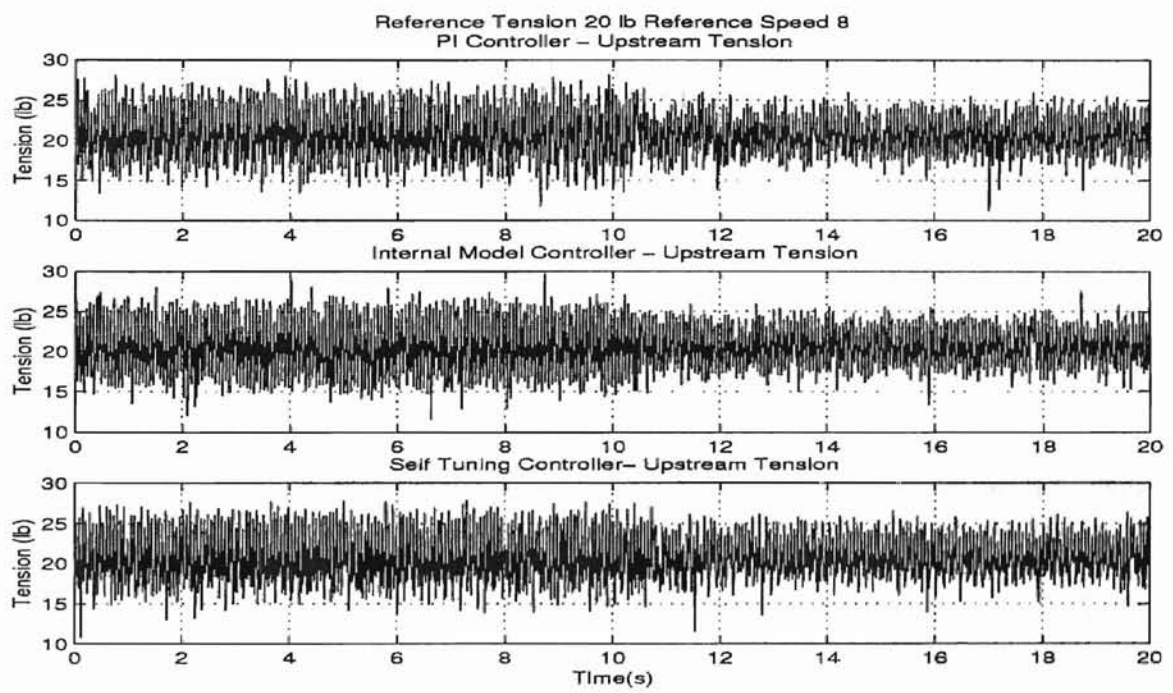


Figure D.22: Back propagation of tension disturbances.

VITA 2

Fu Pei Yuet

Candidate for the Degree of
Master of Science

Thesis: PERIODIC TENSION DISTURBANCE ATTENUATION
IN WEB PROCESS LINES USING
ACTIVE DANCERS

Major Field: Mechanical Engineering

Biographical:

Personal Data: Guangzhou, Guangdong, P.R. China on August 1975, the son of Pak Ying Yuet and Gui Zhen Cao.

Education: Graduated from Enid High School in 1995; received the B.S. degree from Oklahoma State University, Stillwater, Oklahoma, in 1999, in Mechanical Engineering. Completed the requirements for the Master of Science degree with a major in Mechanical Engineering at Oklahoma State University in August, 2002.

Experience: Research Assistant at Oklahoma State University from January 2000 to December 2002; Internship for Oklahoma Gas & Electric from July 1999 to October 1999; Research Engineer in Systems and Controls with Caterpillar Inc from February 2002 to present.

Professional Memberships: American Society of Mechanical Engineers, Mechanical Engineering Society (Pi Tau Sigma), Golden Key National Honor Society, Engineering Honor Society (Tau Beta Pi) .